

Aus der Medizinischen Poliklinik – Innenstadt
der Ludwig-Maximilians-Universität München
Komm. Direktor: Prof. Dr. med. Martin Reincke

The role of cytosolic RNA and DNA recognition in systemic autoimmunity and immune complex glomerulonephritis

Dissertation
zum Erwerb des Doktorgrades der Humanbiologie
an der Medizinischen Fakultät der
Ludwig-Maximilians-Universität zu München

vorgelegt von
Ramanjaneyulu Allam
Vempalli, India
2010

Mit Genehmigung der Medizinischen Fakultät
der Universität München

1.Berichterstatter: Prof. Dr. med. Hans- Joachim. Anders

2.Berichterstatter: Prof. Dr. Ludger Klein

1.Mitberichterstatter: Priv. Doz. Dr. Lutz T. Weber

2.Mitberichterstatter: Prof. Dr. W Lange

Dekan: Prof. Dr. med. Dr. h.c. M. Reiser, FACR, FRCR

Tag der mündlichen Prüfung: 20.05.2010

Ramanjaneyulu Allam M. Sc.
Med. Poliklinik, Klinische Biochemie,
Ludwig-Maximilians University (LMU),
Schillerstraße-42, Munich- 80336,
Germany
anji_rama@yahoo.com

DECLARATION

I here by declare that the present work embodied in this thesis was carried out by me under the supervision of Prof. Dr. Hans Joachim Anders, Internist-Nephrologe-Rheumatologie, Medizinische Poliklinik-Innenstadt Klinikum der Universität München. This work has not been submitted in part or full to any other university or institute for any degree or diploma.

This work has been published in two journals.

- 1) Allam R et. al. Viral RNA and DNA Trigger Common Antiviral Responses in Mesangial Cells. *J Am Soc Nephrol.* 2009; 20(9):1986-96.
- 2) Allam R et. al. Viral 5'-triphosphate RNA and non-CpG DNA aggravate autoimmunity and lupus nephritis via distinct TLR-independent immune responses. *Eur J Immunol.* 2008; 38(12):3487-98.

Ramanjaneyulu Allam

Date: 20-05-2010

ACKNOWLEDGEMENTS

I would like to sincerely thank my supervisor Prof. Dr. Hans-Joachim Anders for his support and guidance during my work in the laboratory. I am indebted to him for giving me scientific freedom and formulating my ideas in right direction.

It is my pleasure to thank Prof. Dr. Stefan Endres, Leader of GRAKO1202, LMU, for allowing me to become a member of graduate students network during my Ph.D. tenure, and Deutsche Forschungsgemeinschaft (DFG) for the grant that supported me during the course of my research term (2006-2009).

I wish to thank all the staff members, and colleagues of the Department of Klinische Biochemie, Nephrologisches Zentrum, Medical Policlinic, for their help, co-operation and for providing a friendly environment.

I wish to thank all researchers and their encouraging discussions during meetings and seminars of GRAKO1202.

I wish to express my profound gratitude to, Dan Draganovici, Ewa Radomska and Jana Mandelbaum for providing skillful technical assistance to carry out the research work successfully.

I would like to thank my past and current colleagues of this institute: Rahul, Onkar, Julia, Sufyan, Anela, Nuru, Mi, Maciej, Olga, Dilip, Veronika, Stephanie, Robert, Anil, Murthy, Peter, Kathi, Lilli, Henny, Holger, Ali, Anne, Christian, christoph, Pati, Sara, Liliana, Ilka, Farha and Khader.

I would like to take this opportunity to mention here few of the best pals during my stay in Munich: Nagendran, Rajesh, Pandu, Ravi, Pallavi, Praveen, Vishal, Arun, Tarun, Shiva, Johny.

I would like thank my childhood friends Amarnath, Nageswara Rao, Dakka sreenu, Ramchand, Hari, Sunil and Sagar

Many thanks to my brother Siva sankar, my uncle Venu Gopal, Annapurna, Manisha and other family members.

Dedicated to

My loving parents

CONTENTS

PAGE

1.	Introduction	
1.1	Systemic lupus erythematosus	1
1.2	Pathogenesis of lupus	3
1.2.1	Cell death	3
1.2.2	Nucleosomes	4
1.2.3	T and B lymphocytes	5
1.2.4	Autoantibodies	7
1.2.5	Type 1 interferons and other proinflammatory cytokines	9
1.3	Pattern recognition receptors	12
1.3.1	Toll like receptors	12
1.3.2	Cytosolic nucleic acid pattern recognition receptors	17
1.3.3	The inflammasome	22
1.4	Potential role of pattern recognition receptors in autoimmunity	23
1.5	MRLlpr/lpr mice- experimental mouse model of lupus	27
2.	Hypothesis/objectives	29
3.	Materials and methods	30
3.1	Materials	30
3.2	Methods	34
3.2.1	Cell culture and stimulation experiments	
3.2.2	RNA isolation, cDNA synthesis and real-time –PCR	35
3.2.3	Microarray studies	40
3.2.4	RNA silencing studies	41
3.2.5	Western blotting	41
3.2.6	Animals and experimental protocol	43
3.2.7	Morphological and histological analysis	44
3.2.8	Evaluation of serum autoantibodies	46
3.2.9	Flow cytometry	48
3.2.10	Other methods	49
3.2.11	Statistical analysis	50
4.	Results	51
4.1	Results part-I	51
4.1.1	TLR-independent IL-6 induction by 3P-RNA and non-CpG-DNA <i>in vivo</i>	51
4.1.2	3P-RNA and non-CpG-DNA dose dependent studies in MRLlpr/lpr mice	51
4.1.3	Non-CpG-DNA induces serum cytokines in MRLlpr/lpr mice	53
4.1.4	Non-CpG-DNA induces lymphoproliferation and splenomegaly	53
4.1.5	Non-CpG-DNA increased negative T cells and plasma cells	55
4.1.6	Dendritic cell activation	56
4.1.7	Expression of inflammatory mediators and transcription factors in spleen	57
4.1.8	Hypergammaglobulinemia and DNA autoantibodies	59

4.1.9	Renal inflammatory mediator mRNA expression	61
4.1.10	Glomerular IgG and complement deposits	61
4.1.11	Kidney histopathology	63
4.1.12	Localization of 3P-RNA and non-CpG-DNA in mice kidneys	65
4.1.13	3P-RNA and non-CpG-DNA induce interferon-related mediators in kidney glomeruli of C57BL/6 mice	66
4.1.14	Backbone chemistry of DNA affects their affinity to lupus Autoantibodies	68
4.2	Results part-II	69
4.2.1	Characterization of mesangial cells	69
4.2.2	Mesangial cells express nucleic acid-specific pattern recognition molecules	69
4.2.3	Cationic lipids enhance the uptake of non-CpG-DNA and 3P-RNA in mesangial cells	70
4.2.4	3P-RNA and non-CpG-DNA activate pMC to produce IL-6	71
4.2.5	3P-RNA and non-CpG-DNA activate pMC through a TLR-independent pathway	73
4.2.6	Rig-1 mediates 3P-RNA but not non-CpG-DNA induced activation of mesangial cells	74
4.2.7	Dai contributes to 3P-RNA but not non-CpG-DNA induced activation of mesangial cells	74
4.2.8	3P-RNA and non-CpG-DNA both activates interferon-regulated factor-3 in mesangial cells	77
4.2.9	Unique but overlapping gene expression program triggered by 3P-RNA and non-CpG-DNA in MC	77
4.2.10	3P-RNA and non-CpG-DNA trigger proinflammatory cytokines in mesangial cells	80
4.2.11	3P-RNA and non-CpG-DNA trigger type 1 interferon and interferon-related mediators in mesangial cells	81
4.2.12	3P-RNA and non-CpG-DNA both trigger apoptosis in MC	83
5.	Discussion	85
6.	Summary	93
7.	Zusammenfassung	94
8.	References	95
9.	Abbreviations	104
	Appendix	106
	Curriculum Vitae	108

1. Introduction

1.1 Systemic lupus erythematosus

Systemic lupus erythematosus (SLE) is a chronic immune disorder, classically depicted as a systemic autoimmune disease caused by the production of pathogenic autoantibodies to a spectrum of nuclear antigens. The clinical manifestations include immune complex-mediated glomerulonephritis, arthritis, vasculitis, cerebritis, pericarditis, cytopenias and serositis [1]. SLE affects females more frequently than males, at a rate of almost 9 to 1; this would argue that female hormones might play a role in disease incidence. The prevalence of SLE ranges from approximately 40 cases per 100,000 persons among Northern Europeans to more than 200 per 100,000 persons among blacks [2]. However there is a wide variation in the prevalence of SLE worldwide, the highest prevalence was reported in Italy, Spain, Martinique, and the UK Afro-Caribbean population and shown in Figure 1. The recent advancements in understanding of molecular mechanisms involved in SLE pathogenesis have translated to development of new therapies [3]. These therapies have improved the life expectancy in lupus patients. However, there is a significant morbidity and mortality still remains in lupus patients.

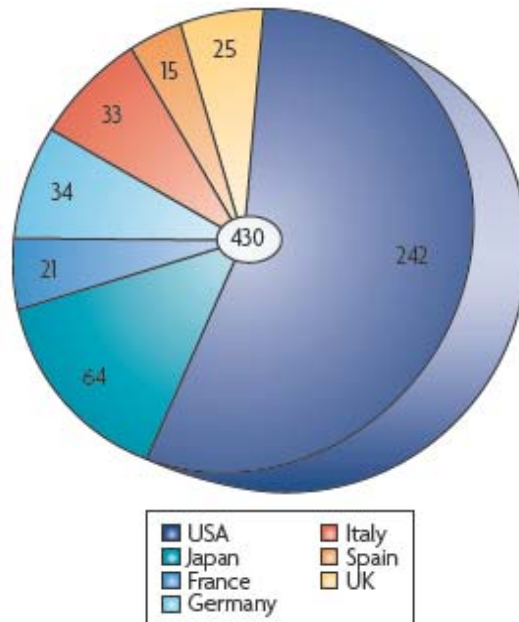


Figure 1. Prevalence of Systemic lupus erythematosus. Population shown in thousands
Taken From *Nature Reviews Drug Discovery*. 2008, 8: 103-104.

In SLE, nephritis is a leading cause of morbidity and mortality. It is referred as lupus nephritis (LN) and characterized serologically by a variety of autoantibodies to deoxyribonucleic acid (DNA), ribonucleic acid (RNA), other nuclear antigens (e.g. Smith, Ro, La) and cytoplasmic antigens. The presence of anti-dsDNA antibodies has been associated with disease activity [4, 5]. The clinical spectrum of LN ranges from mild urinary abnormalities to acute and chronic renal failure. Proteinuria present in almost every LN patient with nephritic syndrome [6]. Some of clinical features of lupus nephritis are mentioned in Table 1. Clinically, significant nephritis develops most commonly within three years after diagnosis. Mesangial and endocapillary hypercellularity, necrosis, crescent formation and granular deposition of immunoglobulin can observe in kidney biopsy sections of patients with lupus nephritis. The images of kidney sections were shown in Figure 2 [7].

Table 1. Clinical features of patients with lupus nephritis

Feature	% of nephritis
Proteinuria	100
Nephrotic syndrome	45 to 65
Granular casts	30
Red cell casts	10
Microscopic hematuria	80
Macroscopic hematuria	1 to 2
Reduced renal function	40 to 80
Rapidly declining renal function	30
Acute renal failure	1 to 2
Hypertension	15 to 50
Hyperkalemia	15
Tubular abnormalities	60 to 80

Adapted from *J Am Soc Nephrol* 1999, 10: 413–424.

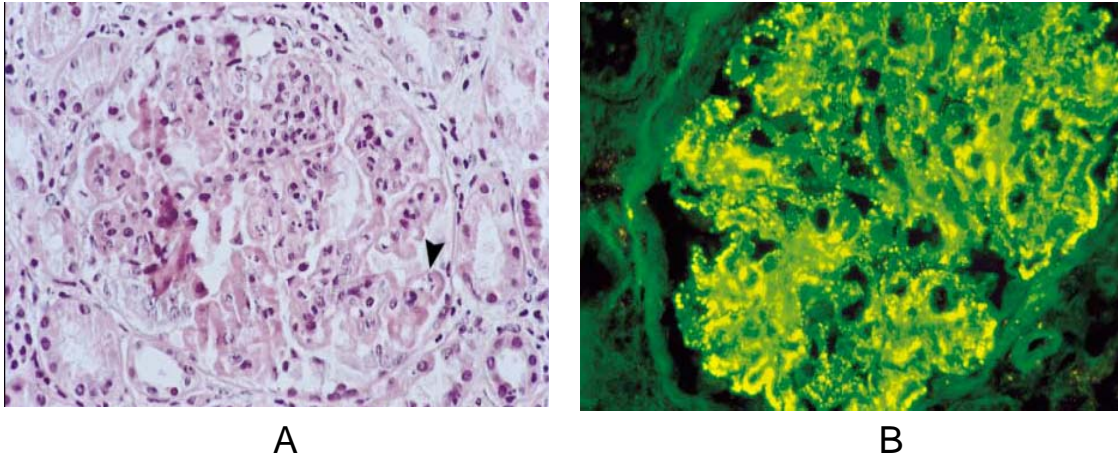


Figure 2. Histopathological staining of kidney sections from lupus nephritis patient
(A) PAS staining (B) IgG immunostaining
Adapted and modified from *N Engl J Med* 1998; 339: 888-99.

1.2 Pathogenesis of lupus

The pathogenesis of lupus remains unclear, although several studies reported that defects in immune tolerance mechanisms and apoptosis explain how the immune system might recognize predominantly intracellular antigens. Several predisposing factors like genetic, hormonal and environmental factors also contribute to the disease pathology. The main focus of the thesis is studying immunological and molecular aspects that are involved in lupus pathomechanism, therefore predisposing genetic factors are not reviewed in this thesis.

1.2.1 Cell death

Cell death plays an important role in pathogenesis of SLE because it is the primary source for autoantigens. Cells can die through a number of different mechanisms. Two of the major types of cell death are apoptosis and necrosis [8]. Whether cells die through apoptosis or necrosis is determined by the initial stimulus and the microenvironment. Apoptosis is an active, programmed and regulated cellular process, which appears under both physiological and pathological conditions in all tissues. Morphologically, apoptotic cells shrink and at least initially maintain integrity of their plasma membrane. In contrast, necrotic cell death occurs in response to many kinds of insults (e.g., trauma, infarction, toxins, etc.) and therefore is typically the result of a pathological process [9].

Morphologically, it is associated with cell swelling and the rapid loss of membrane integrity. The host responses to these two forms of cell death are different. Apoptotic cell death does not provoke inflammation [10], for example, there is continuous death of developing T cells in the thymus, and this occurs without inducing an inflammatory response. In contrast, necrotic cell death stimulates a host inflammatory response. Morphological and biochemical changes of dying cells are extremely important for their clearance from tissues by the scavenger system. Disordered regulation of both apoptosis and the clearance of apoptotic products have been implicated in the pathogenesis of SLE [11]. Under normal circumstances, activity against self antigens is prevented by several mechanisms, including the Apo-1/Fas pathway of apoptosis, which maintain immune tolerance by deleting unwanted autoreactive T cells and B cells [12]. Defect in this Fas pathway lead to accumulation of lymphocytes, particularly autoreactive lymphocytes. This is the basic mechanism by which Fas-deficient MRLlpr/lpr mice develop an autoimmune syndrome.

There is growing evidence for the concept that a clearance deficiency of apoptotic cells can lead to lupus in mouse models [13, 14] and in humans [15, 16]. Primary necrotic cells and secondary necrotic cells (cells that can't undergo apoptosis) release molecules for example DNA-containing nucleosomes, high mobility group B1 (HMB1) protein, heat shock proteins and uric acid. Collectively these self derived antigen molecules are termed as damage-associated molecular patterns (DAMPs). Among these nucleosomes are best studied in pathology of SLE. SLE patients have greater levels of circulating nucleosomes than the healthy individuals.

1.2.2 Nucleosomes

Nucleosomes are complexes of DNA and histones around which double stranded DNA (dsDNA) was wrapped twice. Several studies suggest that autoantibody interactions occur with nucleosomes. Antibodies reactive to nucleosomes have been detected both in SLE patients and in murine lupus models, even prior to the development of anti-dsDNA and antihistone antibodies [17]. These antibodies can bind to the glomerular basement membrane via nucleosomes [18], [19]. Nucleosomes and intracellular debris appear as

blebs on apoptotic cell surfaces, and might incite T cell-driven stimulation of B cells. The injection of syngeneic apoptotic cells into normal mice trigger the antinuclear antibodies and immune deposition in kidneys [20]. Nephritogenic lupus antibodies directly bind to glomerular basement membrane-associated chromatin fragments released from apoptotic intra glomerular cells [21, 22]. Furthermore, terminal deoxynucleotidyl-transferase (TdT)-mediated dUTP nick end-labeling (TUNEL) assay and activated caspase 3 staining demonstrated the accumulation of apoptotic cells in glomeruli and chromatin in glomerular capillary membranes and in the mesangial matrix. These data suggest that apoptotic nucleosomes can be released and bound to glomerular membranes. Later pathogenic anti-nucleosome antibodies bind to these glomerular membranes and initiate pathological events such as induction of inflammatory cytokines and mesangial cell proliferation. Finally, this leads to kidney damage.

Nucleosomes and other self antigens are internalized by antigen presenting cells (APC), such as, dendritic cells (DCs), macrophages and B cells. After internalization, APC present self antigens to CD4⁺ T cells via MHC class II molecule. This is the mechanism how self antigens activate the adaptive immune system in lupus. In adaptive immunity T and B cell are involved. However, self antigens can directly activate APC to release inflammatory cytokines via pattern recognition receptors. All these events are discussed in the following sections.

1.2.3 T and B lymphocytes

In lupus dsDNA-IgG high-affinity antibodies are strongly associated with tissue damage [5]. Production of these high-affinity IgG antibodies is driven by antigen, a process in which antigen binds to B lymphocytes, thereby stimulating the cells to proliferate. This antigen-driven process can occur only in B lymphocytes that are being stimulated by T helper lymphocytes as well as by antigen. This process is known as T lymphocyte help. Each T cell carries a surface-receptor molecule; it interacts with one particular antigen, generally complexed with an MHC molecule on the surface of an APC. Along with presentation of the antigen–MHC complex to T cell, APC also make another costimulatory signal to fully activate T cells. There are different costimulatory molecular pairs, including

the CD40–CD40 ligand and CD28–B7, which can activate T cells. Agents that block costimulation, for example anti- CD40 ligand [23] and cytotoxic T-lymphocyte–associated protein 4 IgG1 (CTLA-4–Ig) [24], a molecule that blocks the CD28–B7 interaction, are potential treatments for lupus. B cell and T cell interact and stimulate each other. T-cell cytokines can stimulate cell division of B cells, switching antibody production from IgM to IgG [25], so that it binds more strongly to the antigen [26]. Thus, T-cell help fosters the production of high-affinity IgG autoantibodies. These kinds of antibodies are closely linked to tissue damage in lupus. One study documented the significance of nephritogenic T cells in renal disease [27]. They generated MRL/lpr mice deficient in serum immunoglobulin but expressing a membrane bound anti-(4-hydroxy-3-nitrophenyl) acetyl transgenic antibody. These mice developed glomerulosclerosis and interstitial nephritis, showing that renal immune complexes were not required for chronic renal disease. T cell infiltration in kidneys is seen with increasing severity of glomerulonephritis in mouse models [28]. Regulatory T cells, one type of T cells suppress the activation of helper T cells and B cells in humans and mice. Some studies have reported a reduction in the number or function of regulatory T cells in patients with lupus and in lupus prone mice [29, 30]. Regulatory T cells from patients with active lupus have a reduced ability to suppress the proliferation of helper T cells, as compared with regulatory T cells from patients with inactive lupus or healthy controls [30]. All these data support the hypothesis that kidney reactive T cells play a direct role in pathogenesis of glomerulonephritis.

That B cells contribute to the pathogenesis of lupus nephritis is increasingly appreciated in many other ways. They function as potent antigen-presenting cells, this role and their ability to clonally expand makes them highly efficient activators of antigen-specific T cells. More recent evidences suggest that B cells also play a role in the production of lymphangiogenic factors; thus, the B cell may orchestrate the local expansion of lymphatics required to support a florid immune response. Furthermore, B cells regulate T cells and DCs through the production of cytokines or regulatory antibodies. B cells producing autoantibodies in SLE have undergone extensive clonal expansion, suggesting that these antibodies are produced in response to chronic stimulation of B cells by antigen and costimulatory autoreactive CD4 T cells. Another B-cell-related functions likely to be

important in the pathogenesis of SLE is cytokine release, particularly proinflammatory cytokines IL-12, tumor necrosis factor (TNF)- α , and IL-6, all of which are produced in high levels in SLE. BlyS/BAFF (B lymphocyte stimulator/B-cell activating factor), a TNF-family cytokine that promotes B-cell maturation, survival and plasma cell differentiation also produced high levels in SLE. [31]. The role of the B lymphocyte as an APC is also likely to be essential in the development of autoimmunity. In experimental models of autoimmune arthritis, the APC function of B cells is essential for the development of disease, while the antibody-secreting function is not [27, 32].

1.2.4 Autoantibodies

Kidneys from patients with lupus nephritis were shown to contain antibodies that bind native, dsDNA [33]. The importance of anti-dsDNA antibodies in the pathogenesis of lupus has been confirmed [34]. Anti-dsDNA antibodies are hallmark for lupus, 70% of lupus patients are positive for these antibodies. In many patients with SLE, increased renal disease activity is associated with rising titres of anti-DNA antibodies. Antibodies to single stranded DNA (ssDNA) and dsDNA are part of the normal repertoire of natural autoantibodies; most of these are low-affinity IgM antibodies that react weakly with several self-antigens. However, these natural antibodies can undergo an isotype switch (from IgM to IgG) that increases their pathogenic potential. In addition, somatic mutations in the encoding immunoglobulin genes can result in the production of high-affinity IgG antibodies to DNA. Several other autoantibodies are also present in SLE for example anti-Sm, anti-RNP, anti-Ro and anti-La etc. However the role of these antibodies in disease progression is uncertain [6]. Different types of autoantibodies present in lupus patients are shown in table 2.

Table 2. Autoantibodies present in lupus patients

Autoantibody	Frequency (%) in Untreated Patients with Lupus	Diagnostic Specificity	Association with Disease Activity
Anti-DNA antibodies			
anti-ds (native)DNA	40 to 90	High	Yes
anti-ss(denatured)DNA	70	Low	No
anti-histone	70	Low	No
anti-nucleosome	80	Low	No
Anti-ribonucleoprotein antibodies			
anti-Sm	5 to 30	High	No
anti-U1-RNP	25 to 35	Low	No
anti-SSA/Ro	35	Low	No
anti-SSB/La	15	Low	No
antiribosomal P protein	25 to 35	Low	No
Other antibodies			
anti-C1q	80 to 100	High	Yes
anti-hsp90	25	Low	No
antiphospholipidd	25 to 50	Low	No
anti-RA33	20 to 40	Low	No

Adapted from *J Am Soc Nephrol* 1999; 10: 413–424.

Anti-dsDNA antibodies can mediate tissue damage in lupus patients. There are two models proposed; both models state that, the binding of antibodies to dsDNA itself is not the most critical determinant of tissue damage. When cells undergo apoptosis, they release chromatin fragments, which are the main source for extracellular dsDNA and nucleosomes. In one study it was proposed that pathogenic anti-dsDNA autoantibodies in patients with lupus bind to nucleosomes that have entered the bloodstream, then these antibody-nucleosome complexes settle in the renal glomerular basement membrane [35]. These

immune complexes activate complement, which initiates the glomerulonephritis. This was demonstrated in animal models [36, 37]. Supporting this anti-nucleosome antibodies found in the blood and inflamed tissues of patients with lupus [38]. In second model anti-dsDNA, anti-nucleosome antibodies, or both cross-react with proteins in the kidney; thus, they have a direct pathogenic effect on renal cells. This is an example of polyreactivity, whereby the same antibody can bind to antigens with different structures because they have similar shared epitopes. Finally in lupus the deposition of immunoglobulins within the glomerular and tubular basement membranes leads to local inflammatory responses that ultimately cause renal fibrosis.

1.2.5 Type 1 interferons and other proinflammatory cytokines

Interferons (IFNs) and proinflammatory cytokines play an active role in the pathogenesis of SLE and can contribute significantly to the immune imbalance in the disease. The type I IFN family consists subtypes of α -IFN and the single β -IFN [39]. Increased levels of IFN- α in the serum of lupus patients were first noted over 30 years ago [40] and subsequently confirmed in several studies [41]. Surprisingly, an increase in IFN- α is not associated with a consistent increase in IFN- β , because of their independent regulation. Although other cytokines are also increased in lupus sera, IFN- α levels best coincide with disease exacerbations [42]. Sometimes IFN- α treatment (for viral infections, tumours) also exacerbates or even induces a wide spectrum of autoimmune manifestations, including lupus [43]. The role of IFN- α in pathogenesis of lupus was substantiated by the recent finding that sera from lupus patients induced maturation of normal blood monocytes into efficient antigen-presenting DCs, and the active factor for this effect was IFN- α [44]. In addition to that, microarray studies with peripheral blood mononuclear cells of lupus patients showed increased signatures of IFN- α - and IFN- γ [39]. Recent microarray analysis of laser-captured glomeruli from lupus patients showed type I IFN response elements among the four dominant clusters of over expressed genes, whereas IFN- γ -induced transcripts were less prominent [45].

Why lupus patients have higher levels of IFN- α has not been fully explained, but both exogenous and endogenous inducers may play a role (Figure 3). As exogenous inducers,

viral components may be the culprits, IFN- α/β production may be a common pathway by which infection by a variety of pathogens can induce or exacerbate systemic autoimmunity in susceptible individuals, as often seen in SLE following infection. However, there is also evidence for endogenous IFN- α/β inducers, such as products of apoptotic or necrotic cells combined with lupus serum autoantibodies [46]. Anti-DNA and anti-ribonucleoprotein (anti-RNP) complexes with DNA or RNA, respectively can stimulate IFN- α/β production through Fc γ RIIa binding and internalization [47]. This finding is consistent with the recent suggestion that mammalian RNA and DNA, which is capable of binding to IFN- α/β -inducing endosomal TLRs. Thus, only the anti-RNP/RNP complexes, taken up in the endosomes, could result in activation of the relevant TLRs and production of IFN- α/β . IFNAR1-deficient NZB lupus mice showed significant reduced disease pathology [48]. In addition to NZB mice, disease reduction was reported in IFNAR1-deleted B6.Fas lpr mice [49] but, surprisingly, not in similarly deleted MRL lpr/lpr mice [50]. No clear reason was reported for these opposite responses. Because IFNs exert potent pleiotropic effects, their role as pathogenic effectors in this disease is likely to be mediated by multiple mechanisms (Figure 3), including enhanced DC maturation and self-Ag presentation; promotion of T and B cell differentiation, proliferation, and survival Disturbances in the balance of anti- and proinflammatory cytokines; and induction of chemokines and their receptors promote homing of inflammatory cells in tissues. Overall, IFN- α/β signaling appears to be a master switch that activates all or most of the above pathways, leading to pathogenicity in lupus-predisposed backgrounds.

Other cytokines are also involved in pathogenesis of lupus. The role of TNF- α in lupus is controversial. This cytokine may be protective in patients with lupus, since giving TNF- α to lupus-prone NZB/W F1 mice delayed the development of lupus [51]. The protective effect is specific to that mouse strain, and the mechanism is unknown. In some patients with rheumatoid arthritis who were treated with anti-TNF- α developed anti-dsDNA antibodies [52], and lupus erythematosus in a few of these patients [53]. IL-6 is yet another important cytokine, which induces the expression of acute phase proteins and also leads to

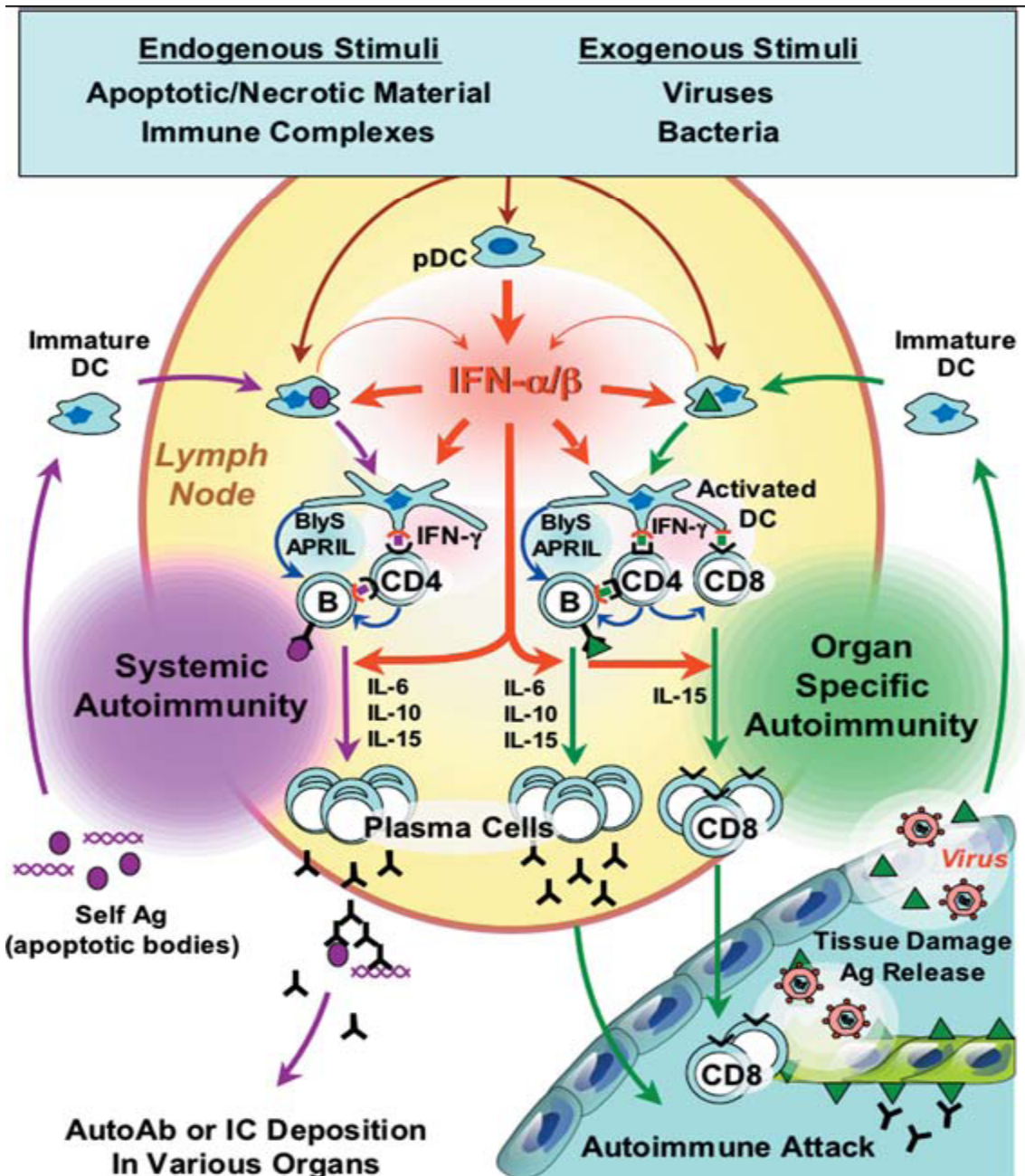


Figure 3. Mechanisms by which IFN- α/β may contribute to the pathogenesis of systemic and organ-specific autoimmune diseases in predisposed backgrounds. Taken from *Annu Rev Immunol* 2005, 23: 307-36.

increased antibody secretion by B-lineage cells [54]. TGF β could exert a bi-directional effect similar to the effects of the classical Th2 cytokines, with less inflammation on the one hand, but more fibrosis on the other hand. TGF β may also play a role for regulatory T cell action. Increased glomerular TGF β was found in samples of adults as well as children

with lupus nephritis [55]. In MRLlpr/lpr mice, TGF β is over expressed, additional TGF β is beneficial with regard to autoantibody formation, kidney disease and survival [56], but its role in fibrosis has been suggested to be critical.

1.3 Pattern recognition receptors

The mammalian immune system is divided into innate and adaptive immunity, and cooperative interactions of both are required for elimination of infective pathogens with the highest efficiency. The innate immune system is an evolutionarily conserved system that provides the first line of protection against invading microbial pathogens and is mediated by macrophages, dendritic cells, neutrophils, natural killer cells, basophils, mast cells and eosinophils [57-60]. These cells sense microbial infection and induce inflammatory responses. Innate immune system senses microbial infection using ‘pattern recognition receptors (PRRs)’ that recognize ‘pathogen-associated molecular patterns (PAMPs) [61]. Because PAMPs are broadly expressed in pathogens but not in host cells, PRRs discriminate between self and non-self. PRR activation can differentially modulate immune responses in cases of infection and autoimmune disorders. Among these receptors are Toll like receptors (TLR), nucleic acid specific-cytosolic receptors (RIG like helicases) and NOD like receptors [58].

1.3.1 Toll like receptors

TLRs are type I membrane-spanning non catalytic receptors and consist of an extracellular LRR (leucine-rich repeat) domain, a transmembrane domain and a cytoplasmic TIR (Toll/interleukin-1 receptor) domain [62]. The LRR domain of TLRs consists of 16–28 tandem repeats of the LRR motif [63] and mediates the recognition of ligands. The TIR domain of TLRs consists of approx. 150 amino acids and shows homology with the cytoplasmic region of the IL-1 receptor [64]. The TIR domain interacts with TIR-domain-containing adaptors such as MyD88 (myeloid differentiation primary response gene 88), TIRAP (TIR-containing adaptor protein), also known as MAL (MyD88-adaptor-like), TRIF (TIR-containing adaptor-inducing IFN interferon- β), also known as TICAM1 (TIR-domain containing adaptor molecule 1) and TRAM (TRIF-related adaptor molecule), also known as TICAM2. The cellular localization of the TLRs has important consequences for

ligand accessibility and can also affect downstream signaling events. The TLRs involved in the recognition of nucleic acids (TLR3, TLR7, TLR8 and TLR9) are localized within endolysosomal compartments, whereas other TLR family members (TLR1, TLR2, TLR4, TLR5 and TLR6) are found at the cell surface [65]. TLRs, their recognition molecules and their adaptor molecules are mentioned in Table 3 and signaling pathways shown in Figure 4. The thesis main focus is nucleic acid recognition receptors so TLRs which recognize non nucleic acid molecules are not reviewed here.

TLR3

TLR3 recognizes viral dsRNA from dsRNA viruses such as reovirus and dsRNA produced during replication of ssRNA viruses, such as West Nile virus and RSV [66, 67]. In addition, poly (I:C) a synthetic analogue of dsRNA can also be recognized by TLR3 (Table 3). TLR3 is expressed in the endosomal compartments of immune cells, including cDCs (conventional DCs), macrophages, B-cells, NK cells and non-immune cells, including epithelial cells. However pDCs (plasmacytoid DCs) don't express TLR3. TLR3 is dispensable for protection against various RNA viruses such as murine cytomegalovirus, vesicular-stomatitis virus, lymphocytic choriomeningitis virus, RSV and reovirus [68]. Therefore, the role of TLR3 in viral infection is unclear.

TLR7/8

TLR7 is responsible for the imidazoquinoline-induced immune responses [69]. TLR7 also recognizes guanosine- or uridine-rich ssRNA from viruses such as human immunodeficiency virus, vesicular stomatitis virus, and influenza virus (Table 3). The ssRNA is also produced within the host, but it is not recognized by TLR7 under normal conditions, may be this is explained by the unique distribution of TLRs. TLR7 is expressed in the endosomal membrane and self-derived ssRNA cannot reach to this compartment. TLR8 is homologous to the TLR7. Human TLR8 has been shown to recognize the imidazoquinolines and ssRNA, which are the ligands for TLR7. In contrast, mouse TLR8 expressed in different cells but does not recognize these TLR7 ligands, it indicates that mouse TLR8 is nonfunctional. Human TLR8 is expressed in regulatory T cells (Treg), and activation of TLR8 inhibits Treg function [70].

Table 3. PRRs and PAMPs

	PRRs	Adapters	PAMPs/Activators	Species	
TLR	TLR1–TLR2 (LRR–TIR)	MyD88 (TIR–DD), TIRAP (TIR)	Triacyl lipopeptides	Bacteria	
	TLR2–TLR6 (LRR–TIR)	MyD88 TIRAP	Diacyl lipopeptides LTA Zymosan	Mycoplasma Bacteria Fungus	
	TLR2 (LRR–TIR)	MyD88, TIRAP	PGN Lipoarabinomannan Porins tGPI-mucin HA protein	Bacteria Mycobacteria Bacteria Parasites Virus	
	TLR3 (LRR–TIR)	TRIF (TIR)	dsRNA	Virus	
	TLR4 (LRR–TIR)	MyD88, TIRAP, TRIF, TRAM (TIR)	LPS Envelope proteins	Bacteria Virus	
	TLR5 (LRR–TIR)	MyD88	flagellin	Bacteria	
	TLR7 (LRR–TIR)	MyD88	ssRNA	RNA virus	
	hTLR8 (LRR–TIR)	MyD88	ssRNA	RNA virus	
	TLR9 (LRR–TIR)	MyD88	CpG DNA DNA Malaria hemozoin	Bacteria DNA virus Parasites	
	mTLR11 (LRR–TIR)	MyD88	Not determined Profilin-like molecule	Bacteria Parasites	
	RLR	RIG-I (CARDx2–helicase)	IPS-1 (CARD)	RNA (5'–PPP ssRNA, short dsRNA)	Virus
		MDA5 (CARDx2–helicase)	IPS-1	RNA (poly IC)	Virus
		LGP2 (helicase)		RNA	Virus
NLR NOD1/NLRC1		RICK (CARD), CARD9 (CARD)	iE-DAP	Bacteria	
NOD2/NLRC2		RICK, CARD9	MDP	Bacteria	
NALP3/NLRP3		ASC (PYD–CARD) CARDINAL (PYD–FIND)	MDP RNA	Bacteria Bacteria, Virus	
			ATP Toxins Uric acid, CPPD, amyloid-b	Bacteria? Host? Bacteria Host	
NALP1/NLRP1 (CARD–FIND–NBD–LRR–PYD)		ASC	Anthrax lethal toxin	Bacteria	
IPAF/NLRC4 (CARD–NBD–LRR)			Flagellin	Bacteria	
NAIP5 (BIRx3–NBD–LRR)			Flagellin	Bacteria	

Taken from *International Immunology* 2009, 21: 317–337.

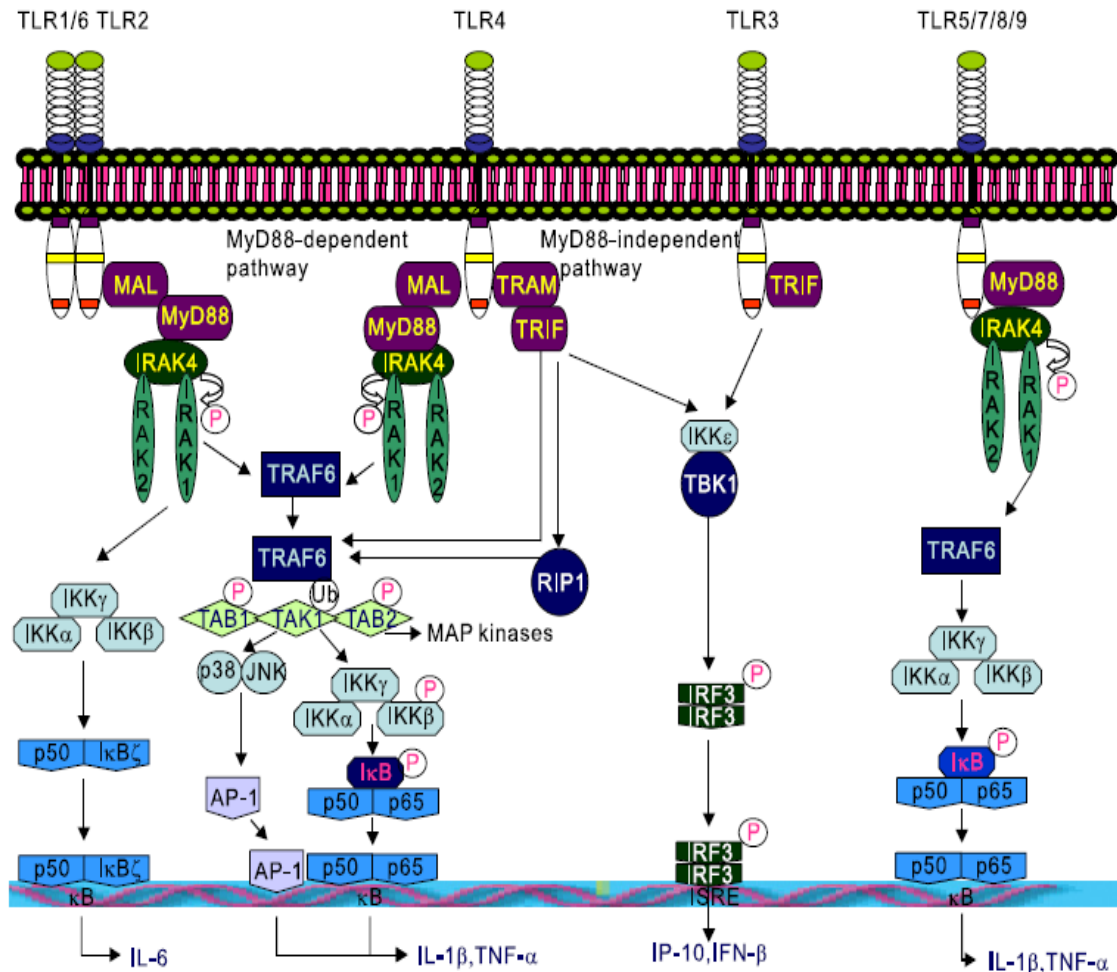


Figure 4. Signaling mediated by TLR is broadly classified as MyD88-dependent and independent pathways. See the text for detailed description.

Taken from *Experimental and molecular medicine* 2007, 39: 421-438.

TLR9

TLR9 recognize CpG motif of bacterial and viral DNA (Table 3). TLR9 knockout mice does not show any response to CpG DNA [71]. In vertebrates, the frequency of CpG motifs are less and the cysteine residues of the CpG motifs are highly methylated, because of this vertebrates DNA loss the immunostimulatory activity. There are two types of CpG DNA, CpG-A and CpG-B, both of which are recognized by TLR9. CpG-B is the conventional type, and it is a potent inducer of inflammatory cytokines such as IL-12 and TNF- α . CpG-A is structurally different from CpG-B and has a greater ability to induce IFN- α production from pDCs, but a lesser ability to induce IL-12 [72]. Differential patterns of cytokine

induction by both CpG DNAs are now explained by the retention of CpG-A in the endosome of pDCs that induce activation of the MyD88-IRF7 pathway essential for IFN- α induction [73].

TLR signaling

Signaling through TLR recruits various TIR-domain-containing adaptors to the TIR domain of TLRs. TLR7, TLR8 and TLR9 use only MyD88. TLR3 only uses TRIF (Figure 4) [58, 64, 74]. In the MyD88-dependent signaling pathway, the IRAK (IL-1 receptor-associated kinase) family members, such as IRAK4, IRAK1 and IRAK2 are recruited to the MyD88. IRAK4 is initially activated and IRAK1 and IRAK2 are sequentially activated [75]. The activated IRAK family proteins associate with TRAF6 (TNF receptor-associated factor 6). This complex polyubiquitinates TRAF6 itself and IKK γ (I κ B kinase γ), also known as NEMO (NF- κ B essential modifier) through K63 (Lys63) linkage. The polyubiquitinated TRAF6 activates the protein kinase TAK (transforming growth factor- β -activated kinase 1) and TABs (TAK1-binding proteins) such as TAB1, TAB2 and TAB3, which subsequently activate transcription factors such as NF- κ B and AP-1 (activator protein-1) through the canonical IKK complex and the MAPK, ERK (extra cellular-signal-regulated kinase), JNK (c-jun N-terminal kinase) and p38 pathway respectively for the transcription of inflammatory cytokine genes [76].

Stimulation with TLR3 ligands activates the TRIF-dependent signaling pathway and induces inflammatory cytokines in addition to type I IFNs and IFN-inducible genes in DCs and macrophages, which depend on IRF3 and IRF7 [77]. IRF3 and IRF7 are activated by IKK-related kinase TBK1 (TANK binding kinase 1) [78, 79]. TBK1 and IKKi interact with TANK (TRAF family member-associated NF- κ B activator) which then phosphorylates IRF3 and IRF7. Phosphorylated IRF3 and IRF7 form a homodimer, which subsequently translocates into the nucleus and binds to the ISREs (IFN-stimulated response elements) to induce type I IFNs and IFN-inducible genes (Figure 4). In pDCs, TLR7 and TLR9 are highly expressed and induce a huge amount of type I IFNs, particularly IFN- α , after virus infection. Upon stimulation, MyD88 forms a complex with IRF7 [73, 80] (which is highly expressed in pDCs) and TRAF6 to induce the production of type I IFNs. IRAK1 interacts with MyD88 and can phosphorylate IRF7 [81]. IRAK1-deficient pDCs consistently have

defects in type I IFN production, but show intact inflammatory cytokine production. Taken together, these observations suggest that the TLR7 or TLR9 signaling pathway is active in pDCs for the robust production of type I IFNs after virus infection (Figure 4).

1.3.2 Cytosolic nucleic acid pattern recognition receptors

Rig-I-like receptors

There are three members of RLR family, Retinoic acid-inducible gene 1(RIG-1), melanoma differentiation associated gene 5 (MDA5) and laboratory of genetics and physiology 2 (LGP2)— These receptors recognize viral RNA in the cytoplasm (Figure 5) [82].

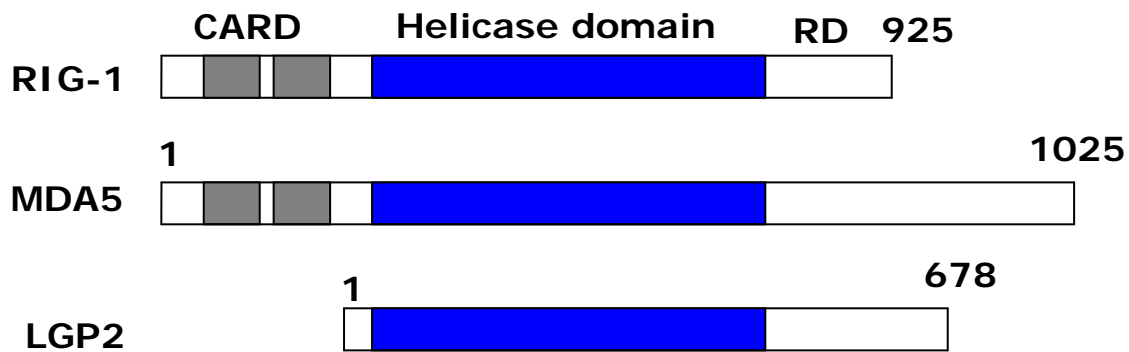


Figure 5. Structure of RIG-I family helicases. The RIG-I family consists of RIG-1, MDA5 and LGP2.

RIG-1, a prototypical member of the RLR family, contains tandem caspase recruitment domain (CARD)-like regions at its N-terminus that function as an interaction domain with other CARD-containing proteins, the central the DExD/H helicase domain, which has an ATP-binding motif (Figure 5). RIG-1 also has a C-terminal repressor domain (RD), which binds to RNA [83, 84]. Normally, RIG-1 is inactive as a monomer, but viral infection or RNA binding trigger conformational changes to facilitate self-association, which promotes CARD interaction with downstream signaling molecules. MDA5 contains tandem CARD-like regions and a DExD/H helicase domain, but it is unknown whether the C-terminal region of MDA5 really functions as an RD. LGP2 contains a DExD/H helicase domain and an RD, but lacks the CARD-like region (Figure 5). LGP2 is a negative regulator of RNA virus-induced responses, because the LGP2, RD binds to that of RIG-I and suppresses

signaling by interfering with the self-association of RIG-I. Knock out mice data showed that [85, 86]. RIG-I is essential for the recognition of various ssRNA viruses, which include paramyxoviruses, influenza A virus, VSV and Japanese encephalitis virus.

MDA5 is required for the recognition of other RNA viruses, including picornaviruses such as EMCV, Mengo virus and Theiler's virus; moreover, MDA5 is involved in the recognition of poly I:C. These findings suggest through recognition of distinct structures of viral RNA might be the reason that RIG-I and MDA5 can detect different RNA viruses. This is likely because RIG-1 is activated following transfection of in vitro transcribed RNA, whereas MDA5 is activated by poly I:C. RIG-1 recognize ssRNA bearing a 5'-triphosphate moiety [87, 88]. 5'-triphosphate structures are removed or masked by a cap structure in the case of self-RNA. This demonstrates a discrimination mechanism between self and non-self RNA; however, the 5'-triphosphate structure is necessary but not sufficient for RIG-1 recognition. Later it was shown that RIG-1 recognition is determined by a homopolymeric ribonucleotide composition such as the polyuridine motif of the hepatitis C virus (HCV) genome 3'non-translated region, by linear RNA structure and by RNA length [89] and also it was shown that RIG-1 recognizes small dsRNA species ranging from 21 to 27 nucleotides without a 3'-overhang [90]. RIG-1 and MDA5 distinguish dsRNA by size; RIG-1 binds short dsRNA, whereas MDA5 binds long dsRNA [91]. Initially LGP2 implicated as a negative regulator, but LGP2- deficient mice exhibit complicated phenotypes [92]. They show elevated levels of type I IFN in response to poly IC and VSV, but decreased type I IFN following EMCV infection, suggesting that LGP2 negatively or positively regulates RIG-I and MDA5 responses, depending on the type of RNA viruses.

In RLR signaling, after the ligand binding to the receptors, they activate NF- κ B, MAPK and IRFs for induction of type I IFN and inflammatory cytokines. IFN β promoter stimulator 1 (IPS-1), also known as mitochondrial anti-viral signaling (MAVS), CARD adapter inducing IFN β (Cardif) or virus-induced signaling adapter (VISA) is the adapter for RIG-I and MDA5 (Figure 6) [93-96]. IPS-1 contains an N-terminal CARD-like domain and a transmembrane domain at the C-terminal end. CARD like domain is responsible for the

interaction with RLRs and transmembrane domain is required for mitochondrial targeting as well as triggering anti-viral responses. NS3/4A serine protease in HCV cleaves IPS-1. It suggests that HCV utilizes NS3/4A as a strategy to evade host anti-viral responses. IPS-1 recruits TRADD, which in turn assembles with Fas-associated death domain protein (FADD) and RIP-1 [94, 97]. Caspase-8 and caspase-10 are then recruited to FADD, where they are processed and activate NF- κ B. TRADD forms a complex with TRAF3, then it induces TBK1–IKK α -dependent IRF3 activation. STING is also involved in RIG-I signaling (Figure 6). STING interacts with RIG-I but not MDA5, and cells lacking STING showed attenuated type I IFN induction following infection with VSV. TLR signaling was unimpaired by STING deficiency. Similar to STING, mediator of IRF3 activation (MITA) also participates in RLR signaling. TRIM25 is another protein, which directly binds to RIG-I and promotes Lys-63-linked ubiquitination of the CARD of RIG-I, which facilitates the recruitment of IPS-1 to activate signaling. TRIM25-null cells consistently display a loss of RIG-I ubiquitination as well as impaired anti-viral responses [98].

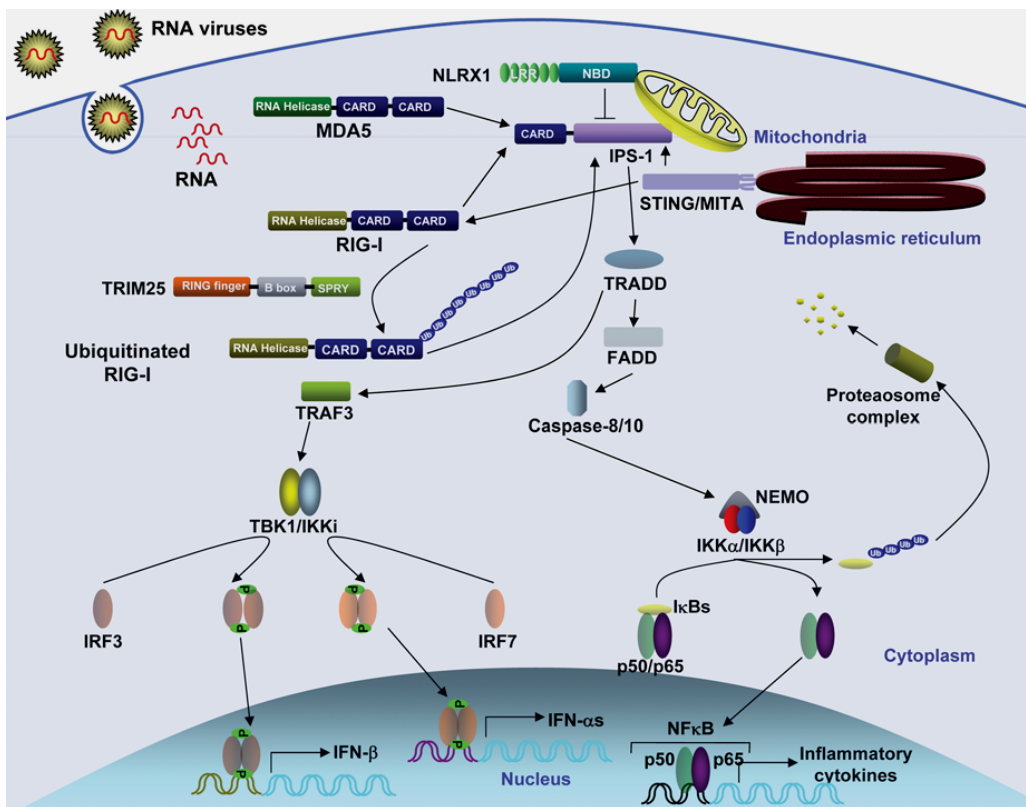


Figure 6. RLR signaling pathway. See the text for description

Taken from *Biochem. J* 2009, 420: 1–16.

DNA recognition by cytosolic receptors

TLR 9 recognizes CpG DNA, however dsDNA without CpG motifs derived from host or pathogens can initiate strong immune response, but ssDNA failed to activate immune responses [99-101]. This effect was observed when DNA transfected inside dendritic cells, macrophages and nonimmune cells such as epithelial cells, fibroblasts, and thyroid cells can induce production of type I IFNs through recognition pathways independent of TLR9 [101]. The dsDNA recognition occurs similar to RLRs via TBK1, a protein kinase that phosphorylates the transcription factor IFN regulatory factor (IRF) 3 (Figure 7), in contrast TLR9 triggers type I IFN without TBK1. Whereas right-hand B-form of dsDNA shows high immunostimulatory activity with regards to cytokine induction compare to the left-hand Z-form dsDNA or ssDNA has low or no activity [100]. RNA interference analysis clearly demonstrated that signaling adaptor IPS-1 and RIG-I were involved in B-DNA-mediated signaling in human cells [102]. However, IPS-1^{-/-} or RIG-I^{-/-} mouse embryonic fibroblasts (MEFs) responded similar to wildtype cells for B-DNA stimulation. The response was completely abrogated in TBK1^{-/-} MEFs, suggesting that species-specific signaling pathways exist [103, 104].

Several molecules were screened to identify cytoplasmic DNA receptors, among these DNA-dependent activator of IRF (DAI, also known as Z-DNA-binding protein 1 and DLM1) has been isolated as a DNA sensor with DNA-binding and TBK1-activating properties [105]. However, responses against dsDNA were unaffected by DAI deficiency in mice, suggesting a redundant or non-essential role of DAI [106]. Recently, stimulator of IFN genes (STING), a membrane protein predominantly expressed in the ER, has been identified [107]. STING-deficient cells showed diminished type I IFN induction following cytosolic dsDNA stimulation. Caspase-1 regulates the B-DNA-mediated production of IL-1 β , IL-18, and IL-33. PYHIN (pyrin and HIN domain-containing protein) family member absent in melanoma 2 (AIM2) was also identified as a receptor for cytosolic DNA, which regulates caspase-1 [108]. The HIN200 domain of AIM2 binds to DNA, whereas the pyrin domain (but not that of the other PYHIN family members) associates with the adaptor molecule ASC (apoptosis-associated speck-like protein containing a caspase activation and recruitment domain) to activate both NF-kappaB and caspase-1. But AIM2 is not

responsible for B-DNA induced interferon signaling [108-112]. Recently, it was shown that polymerase III plays a role in poly (dA:dT) signaling. AT-rich dsDNA served as a template for RNA polymerase III and it transcribed into dsRNA containing a 5'-triphosphate moiety. Then this dsRNA activate RIG-1 pathway for the production of type I interferon and activation of the transcription factor NF-kappaB. Other format of B-DNA are independent of polymerase III and this system exist in humans only [113].

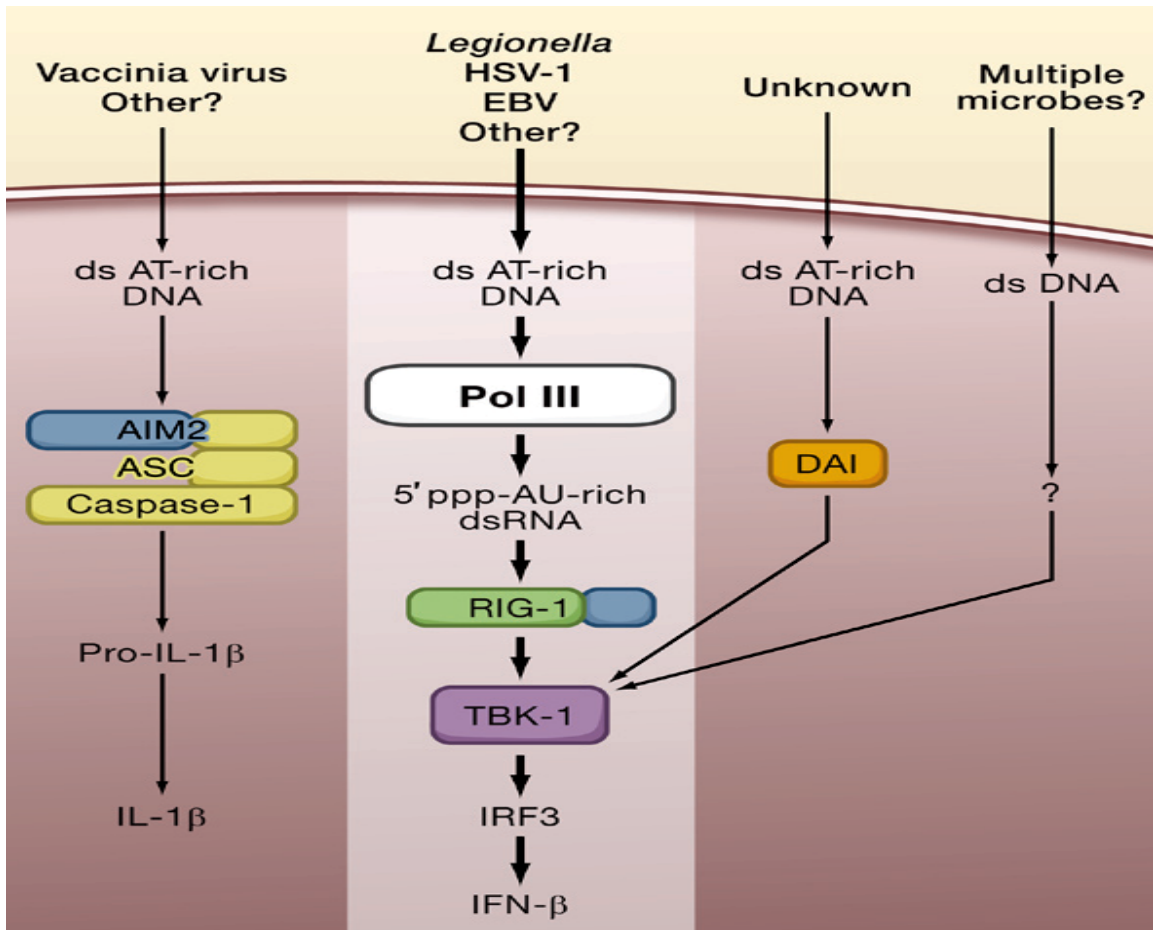


Figure 7. Cytosolic DNA signaling pathways

Taken from *Cell*, 2009, 138: 428-430

1.3.3 The inflammasome

The Inflammasome is one of the subgroup in NLR family proteins. It is involved in processing of cytokines belongs to IL-1 family. The IL-1 family of cytokines, includes IL-1 β , IL-18 and IL-33, which are key cytokines that regulate various components of innate and adaptive immunity. The production of these cytokines is regulated by two signals in innate immune cells (e.g. macrophages). The first signal comes from various TLR, NLR and RLR agonists and the second signal comes from the inflammasome. The type of inflammasomes are NALP3 (NACHT [NTPase-domain named after NAIP, CIITA, HETE and TP1]–LRR-PYD–containing protein 3), NALP1 (also known as NLRP1), or NLRC4 (also known IL-1 β -converting-enzyme protease-activating factor [IPAF]). Recently, the protein AIM2 was shown to assemble an inflammasome (Figure 8) [114]. The NALP3 inflammasome is activated by various exogenous and host endogenous ligands. Exogenous ligands include microbial ligands such as MDP, bacterial and viral RNA, toxins such as nigericin, maitotoxin, environmental pollutants such as asbestos and silica [115] and vaccine adjuvant alum (aluminium salts) [116]. Host endogenous ligands include MSU (monosodium urate), calcium pyrophosphate dehydrate, amyloid- β fibrillar peptide and ATP. AIM2 has been shown to recognize dsDNA. Phagocytosis of silica crystal and fibrous particles of amyloid- β induce lysosomal destabilization and permeabilization which leads to the release of cathepsin B into the cytosol. The released cathepsin B then activates the NALP3 inflammasome [117, 118].

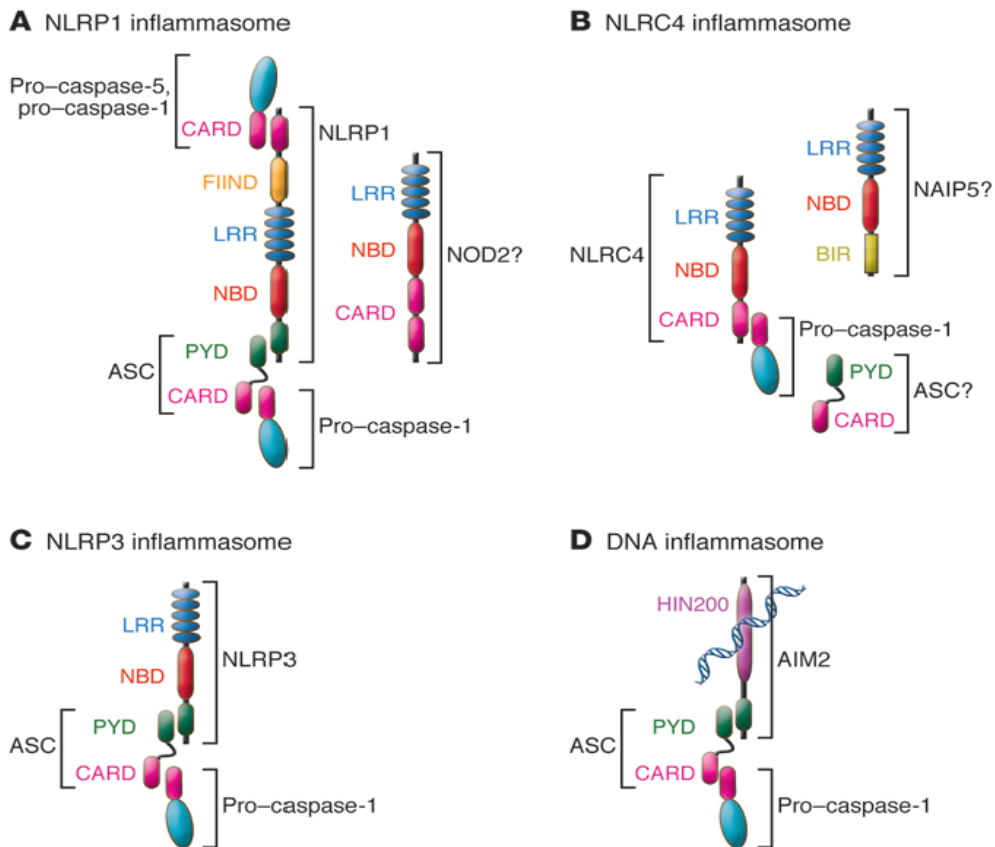


Figure 8. Type of inflammasomes

(A) NLRP1 contains, in addition to the NLR-typical LRR and NBD domains, a PYD, a FIIND, and a CARD. NLRP1 can recruit pro-caspase-1 and -5 and possibly forms a complex with NOD2. Recruitment of ASC enhances activation of pro-caspase-1. (B) NLRC4 contains a CARD that can directly recruit pro-caspase-1. (C) NLRP3 activates pro-caspase-1 via recruitment of ASC. (D) AIM2 is a bipartite protein consisting of a PYD and DNA-binding.

Taken from *J. Clin. Invest* 2009, 119: 3502–3511.

1.4 Potential role of pattern recognition receptors in autoimmunity

The role of pattern recognition receptors in autoimmunity is well documented. Signaling through these receptors may play an important role in the loss of self-tolerance and induction of autoimmunity. Several studies reflect the major role for nucleic acid specific TLRs in linking innate immunity to adaptive immunity [119, 120]. In one study it was reported that TLR 3 and 7 engagement can convert T-cell autoreactivity into autoimmune disease, through release of IFN α -mediated upregulation of MHC I on pancreatic tissue [121]. TLR7, TLR3, TLR8, and TLR9 all are expressed in the endosomal membrane.

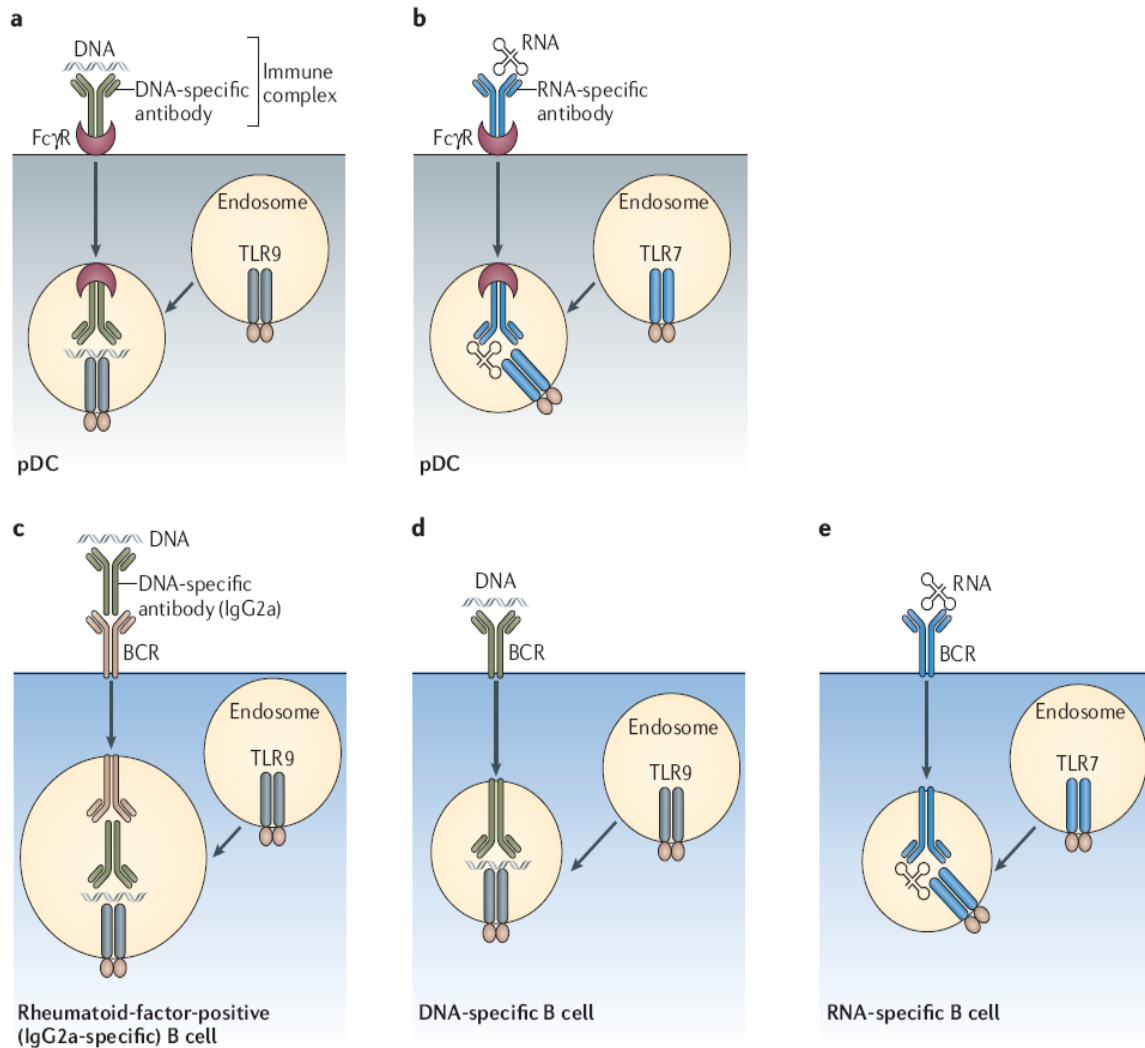


Figure 9. Receptor-mediated delivery of autoantigens to TLR7 or TLR9.

Fc γ Rs are present at the surface of pDCs bind immune complexes and transport both the autoantibody and the autoantigen to the cytoplasmic compartment that contains TLR9 (a) or TLR7 (b). The B-cell receptor (BCR) at the surface of AM14 B cells (which are specific for IgG2a) has the same function and can transport both DNA- and RNA-containing immune complexes (c). BCRs that directly bind autoantigen, either DNA (d) or RNA (e), provide the same delivery system.

Taken from *Nat Rev Immunol* 2006, 6: 823-35.

When self-derived ssRNA is conjugated with RNA-specific antibody, then ssRNA is recognized by TLR7, leading to production of IFN- α . Alternatively, ssRNA can engage the RNA-specific B cell receptor (BCR) of autoreactive B cells, thereby inducing autoantibody production (Figure 9) [122-124]. Both cases might cause autoimmune diseases. This concept was supported by TLR7 gene duplication studies [125, 126]. TLR9 is also involved in the pathogenesis of autoimmune disorders similar to TLR7 [127]. AM14 B cells express

a receptor specific for autologous IgG2a, a specificity that is commonly found in the B-cell repertoire of autoimmune-prone mice. This receptor binds monomeric IgG2a with relatively low affinity. As a result, in mice that are not prone to autoimmunity, AM14 B cells manage to evade the common mechanisms of tolerance induction and develop into relatively normal mature B cells. *In vitro*, AM14 B cells proliferate in response to immune complexes that contain IgG2a bound to DNA or DNA-associated proteins and RNA or RNA-associated proteins, but these B cells fail to respond to immune complexes of IgG2a bound to proteins (Figure 9) [128]. These data established a critical link between the innate and adaptive immune systems in the development of systemic autoimmune disease. Similarly, pDCs produce IFN α in response to immune complexes containing IgG and chromatin. B cell receptor or Fc receptor-mediated internalization of the immune complex is thought to result in TLR9-mediated recognition of host derived CpG-DNA within chromatin (Figure 9).

IFN α plays a crucial role in the induction of autoimmunity [39]. Activation of APCs by TLR9 engagement can break self-tolerance and trigger the development of autoimmunity even in a genetically resistant strain such as B10.S mice, transgenic for a T cell receptor specific for the encephalitogenic protein peptide, that normally are resistant to spontaneous experimental allergic encephalomyelitis (EAE) [129]. Experimental studies with rodents suggest that exposure to synthetic CpG-ODN can exacerbate underlying autoimmune tissue injury e.g. experimental encephalomyelitis, collagen-induced arthritis or SLE [130, 131]. TLR9 activation by CpG-ODN aggravate disease activity in spontaneous immune complex glomerulonephritis of MRLlpr/lpr mice [132, 133]. Furthermore, in vertebrates, inhibitory DNA sequence elements counterbalance the immunostimulatory effects of unmethylated CpG-DNA [134].

Certain synthetic ODNs with such inhibitory motifs can block CpG-DNA-induced effects [135]. In one study it was reported that inhibiting TLR 7 and 9 using inhibitory oligonucleotides ameliorate the disease in MRLlpr/lpr mice [136]. However, experimental evidence for a pathogenic role of CpG motifs in self-DNA for lupus is lacking. TLR9-deficient murine models of SLE showed increased production of anti-DNA autoantibody

formation and severe glomerulonephritis and early mortality compare to control mice [137-139]. *In vitro* studies in autoimmune-prone mice demonstrate that dual signaling via the B-cell receptor and non-CpG-DNA resulting in synergistic B-cell activation in a TLR9-independent manner. These results suggest that engagement of a TLR9-independent DNA activation pathway may promote autoimmunity, while TLR9 signaling can protect SLE-like immune pathology *in vivo* [139].

TLR-independent nucleic acid recognition receptors might also play a role in the pathogenesis of systemic autoimmunity, because activation of these receptors results in type I IFN and other inflammatory cytokine production (Figure 10). As mentioned earlier, one form of such induction is mediated by cytosolic RNA sensed by the RIG-1 or MDA5 helicases. Because most eukaryotic RNA species are known to lack 5'-triphosphate groups, which are required for sensing by RIG-1, this feature allows discrimination between self-RNA and viral RNA. However, RNA transcripts in the nucleus and some RNA species (for example, 7SL RNA) in the cytosol of eukaryotic cells display 5'-triphosphates, and therefore uptake of apoptotic materials containing such RNA species by conventional DCs or macrophages may lead to RIG-1 engagement and type I IFN production [140]. Intracellular administration of right-handed B-form dsDNA, the most common conformation of mammalian DNA, also triggers TLR-independent production of type I IFNs, and such DNA may be present in phagocytosed apoptotic debris. Purified nucleosomes have also been found to directly induce MyD88-independent DC maturation and production of inflammatory cytokines and chemokines [141]. Inadequate digestion of extracellular DNA in DNase I-deficient mice leads to a lupus-like disease [142], and function-impairing DNase I gene mutations have been found in a few individuals with lupus [143]. In addition, non degraded intracellular DNA in DNase II-deficient macrophages mediates TLR-independent induction of inflammatory cytokines, including IFN β , and causes severe anemia. Induction of type I IFNs and cytokines by uptake of mammalian nucleic acids derived from apoptotic materials may amplify immunologic responses not only against foreign pathogens, but also against self-antigens in predisposed individuals.

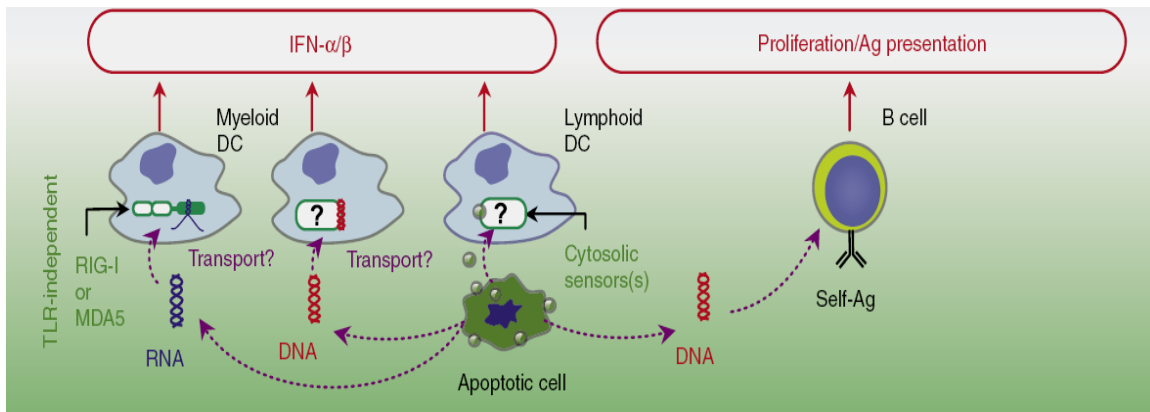


Figure 10. Endogenous stimuli promoting IFN- α/β production by pDCs and conventional DCs, and activation of B cells

Taken from *Nat Med* 2007, 13: 543-51

Finally, the role of nucleic acid recognition TLRs in lupus studied in great detail; however the role of TLR-independent nucleic acid recognition receptors in lupus not well studied. So it is interesting to study disease progression by activating TLR-independent nucleic acid receptors with their respective agonists and the role of intracellular TLR-independent nucleic acid receptors in lupus pathogenesis. In this study first we tested whether 3P-RNA and non-CpG-DNA can aggravate disease or not? 3P-RNA and non-CpG-DNA activate RIG-1 and cytosolic DNA pathways respectively. In second study we studied what is the impact of these agonists in local kidney cells. For that we stimulated mesangial cells with 3P-RNA and non-CpG-DNA and analysed signaling pathways and gene expression profiles.

1.5 MRLlpr/lpr mice- experimental mouse model of lupus nephritis

MRLlpr/lpr mice lack functional expression of the apoptosis-inducing receptor Fas, thereby accelerating the manifestation of the autoimmune disease. MRLlpr/lpr mice show systemic autoimmunity, massive lymphadenopathy associated with proliferation of aberrant CD3⁺CD4⁻CD8⁻ T cells and immune complex-derived glomerulonephritis. Starting at approximately 3 months of age, levels of circulating immune complexes, such as those from spontaneously generated anti-dsDNA antibodies, rise dramatically in MRLlpr/lpr but not in wild-type MRL controls. Lymph node weight of MRLlpr/lpr increases

approximately 75-fold over controls and renal pathology occurs extensively in MRLlpr/lpr at approximately 4 months of age. In MRLlpr/lpr mice, a proliferative glomerulonephritis is seen, with mononuclear cell infiltration, endothelial and mesangial cell proliferation, and crescent formation [144]. Finally, female MRLlpr/lpr mice die at an average of 17 weeks of age and males at 22 weeks.

2. Hypothesis/Objectives

Previous studies in our laboratory reported that, administration of TLR ligands in MRLlpr/lpr mice can aggravate the disease pathology. These results demonstrated that viral infections, which activate TLR signaling, play a significant role in aggravating disease pathology. This supports the idea that, viral infections in lupus patients can worsen the disease pathology. However, recent findings demonstrated that viral infections also activate TLR-independent nucleic acid recognition pathways. These findings prompt us to study the TLR-independent nucleic acid recognition pathways in the context of lupus.

- 1) My first objective was to characterise the effect of exogenous 3P-RNA and non-CpG-DNA on MRLlpr/lpr mouse model.
- 2) My second objective was to study the effect of 3P-RNA and non-CpG-DNA-induced glomerular inflammation.
- 3) My third objective was to study whether 3P-RNA and non-CpG-DNA activate inflammatory cytokines in mesangial cells and what are the gene expression profiles induced by 3P-RNA and non-CpG-DNA.

3. Materials and Methods

3.1 Materials

Equipments

Balances:

Analytic Balance, BP 110 S	Sartorius, Göttingen, Germany
Mettler PJ 3000	Mettler-Toledo, Greifensee, Switzerland

Cell Incubators:

Type B5060 EC-CO ₂	Heraeus Sepatech, München, Germany
-------------------------------	------------------------------------

Centrifuges:

Heraeus, Minifuge T	VWR International, Darmstadt, Germany
Heraeus, Biofuge primo	Kendro Laboratory Products, Hanau, Germany
Heraeus, Sepatech Biofuge A	Heraeus Sepatech, München, Germany

ELISA-Reader

Tecan, GENios Plus	Tecan, Crailsheim, Germany
--------------------	----------------------------

Fluorescence Microscope

Leica DC 300F	Leica Microsystems, Cambridge, UK
Olympus BX50	Olympus Microscopy, Hamburg, Germany
LSM510 laser scanning microscope	Carl Zeiss, Jena, Germany

Spectrophotometer

Beckman DU [®] 530	Beckman Coulter, Fullerton, CA, USA
-----------------------------	-------------------------------------

TaqMan Sequence Detection System

ABI prism [™] 7700 sequence detector	PE Biosystems, Weiterstadt, Germany
-----------------------------------------------	-------------------------------------

Other Equipments

Cryostat CM 3000	Leica Microsystems, Bensheim, Germany
Homogenizer T25	IKA GmbH, Staufen, Germany
Microtome HM 340E	Microm, Heidelberg, Germany
pH meter WTW	WTW GmbH, Weilheim, Germany
Thermomixer 5436	Eppendorf, Hamburg, Germany
Vortex Genie 2 [™]	Bender&Hobein AG, Zurich, Switzerland

Water bath HI 1210

Leica Microsystems, Bensheim, Germany

Chemicals and materials

Chemicals for the molecular biology techniques

RNeasy Mini Kit	Qiagen, Hilden, Germany
RT-PCR primers	PE Biosystems, Weiterstadt, Germany
dNTP mixture	Amersham Pharmacia Biotech, Freiburg, Germany
Pre-separation Filters	Miltenyi Biotec, Bergisch Gladbach, Germany
RNeasy Mini Kit	Qiagen, Hilden, Germany
DNase solution	Qiagen, Hilden, Germany
RNeasy Mini Kit	Qiagen, Hilden, Germany
5 x buffer	Invitrogen, Karlsruhe, Germany
DTT	Invitrogen, Karlsruhe, Germany
RNasin	Promega, Mannheim, Germany
Acrylamide	Ambion Ltd, 36 Cambridgeshire,
Hexanucleotide	Roche, Mannheim, Germany
JetPEI™	Polyplus-transfection, Illkirch, France
Lipofetamine2000	Invitrogen, Karlsruhe, Germany

Cell culture

DMEM-medium	Biochrom KG, Berlin, Germany
RPMI-1640 medium	GIBCO/Invitrogen, Paisley, Scotland, UK
FSC	Biochrom KG, Berlin, Germany
Dulbecco's PBS (1×)	PAA Laboratories, Cölbe, Germany
Trypsine/EDTA (1×)	PAA Laboratories, Cölbe, Germany
Penicillin/Streptomycin (100×)	PAA Laboratories, Cölbe, Germany

Antibodies

Anti-Mac2	Cederlane, Ontario, Canada
Anti-CD3	BD Pharmingen, Hamburg, Germany
Anti-CD4	BD Pharmingen, Hamburg, Germany

Anti-CD8	BD Pharmingen, Hamburg, Germany
Anti-CD25	BD Pharmingen, Hamburg, Germany
Anti-CD45	BD Pharmingen, Hamburg, Germany
Anti-7/4	Abd-Serotec, Kidlington, UK
Anti-Ly6G	BD Pharmingen, Hamburg, Germany
Anti-mouse IgG1	Caltag Laboratories, Burlingame, CA, USA
Anti mouse IgG2a	Caltag Laboratories, Burlingame, CA, USA
Anti-mouse C3	Nordic Immunological Laboratories, Tilburg, Netherlands
Mouse IgG	Rockland Immunochemicals Research, Gilbertsville, PA, USA
FITC-labelled phalloidin	Invivogen, San Diego, USA

Miscellaneous

Needles	BD Drogheda, Ireland
Pipette's tip 1-1000 μ L	Eppendorf, Hamburg, Germany
Plastic histosettes	NeoLab, Heidelberg, Germany
Preseparation filters	Miltenyi Biotec, Bergish Gladbach, Germany
Microscope slides	Menzel-Gläser, Braunschweig, Germany
Silver Impregnation Kit	Bio-Optica, Milano, Italy
Syringes	Becton Dickinson, Germany
PVDF membrane	Millipore Immobion, Schwalbach, Germany.
Hep-2 slides	Biosystems S.A. Costa Brava, Barcelona, Spain

Chemicals

Acetone	Merck, Darmstadt, Germany
AEC Substrat Packung	Biogenex, San Ramon, USA
Diethyl ether	Merck, Darmstadt, Germany
Bovine Serum Albumin	Roche Diagnostics, Mannheim, Germany
Cyclophosphamide	Sigma-Aldrich Chemicals, Steinheim, Germany
DEPC	Fluka, Buchs, Switzerland

DMSO	Merck, Darmstadt, Germany
EDTA	Calbiochem, SanDiego, USA
Ethanol	Merck, Darmstadt, Germany
Formalin	Merck, Darmstadt, Germany
Hydroxyethyl cellulose	Sigma-Aldrich, Steinheim, Germany
HCl (5N)	Merck, Darmstadt, Germany
Isopropanol	Merck, Darmstadt, Germany
Calcium chloride	Merck, Darmstadt, Germany
Calcium dihydrogen phosphate	Merck, Darmstadt, Germany
Potassium hydroxide	Merck, Darmstadt, Germany
MACS-Puffer	Miltenyi Biotec, Bergisch Gladbach, Germany
Mercaptoethanol	Roth, Karlsruhe, Germany
Sodium acetate	Merck, Darmstadt, Germany
Sodium chloride	Merck, Darmstadt, Germany
Sodium citrate	Merck, Darmstadt, Germany
Sodium dihydrogen phosphate	Merck, Darmstadt, Germany
Penicillin	Sigma, Deisenhofen, Germany
Roti-Aqua-Phenol	Carl Roth GmbH, Karlsruhe, Germany
SSC (Saline-sodium citrate Puffer)	Sigma, Deisenhofen, Germany
Tissue Freezing Medium	Leica, Nussloch, Germany
Trypan Blue	Sigma, Deisenhofen, Germany
Oxygenated water	DAKO, Hamburg, Germany
Xylol	Merck, Darmstadt, Germany
ABC reagent	Vector, Burlingame, CA USA
Histomount	Zymed Laboratories, San Francisco, USA
DAPI	Vector Laboratories Inc, Burlingame, USA

3.2 Methods

3.2.1 Cell culture and stimulation experiments

Cell line

A murine mesangial cell line (MMC) [145] was maintained under standard culture conditions (in an incubator at 37 °C temperature and supplied with 5% CO₂) in DMEM medium (Dulbecco's modified Eagle's medium), supplemented with 2.5% fetal calf serum (FCS), penicillin 100 U/ml and streptomycin 100 µg/ml (PS) and described as complete DMEM medium.

Isolation of primary mesangial cells

Kidney cell suspensions were prepared from the cortex (medulla was removed) by mashing it in 250 µl of cold complete RPMI medium. The suspension was applied onto 150, 103, 63, 50 and 45 µm sieves, rinsed with cold PBS, centrifuged (4000 rpm for 7 min), re-suspended in complete RPMI medium and applied onto 30 µm pre-separation filters. Glomeruli remained on the filter. The filter was swapped upside down and rinsed with PBS containing 1 mg/ml collagenase IV. Glomeruli were incubated in this solution for 15-20 min at 37 °C. The cells were then centrifuged and re-suspended and plated in RPMI medium supplemented with 20 % FCS, 1 % PS and 1 % ITS (insulin, transferrine, selenium). Medium was changed every 4-6 days; the first passage was made after 16-20 days.

Stimulation experiments

Mesangial cells were treated with medium control or different concentrations of non CpG-DNA, 3P-RNA (dose mentioned in results). TLR9 ligand CpG-ODN 1668 and pI:C RNA were used as a control in some experiments. All stimulation experiments were done without starving conditions (unless mentioned otherwise). After stimulation cell supernatants were collected for cytokine measurements and cells were harvested either for RNA isolation as described below or for flow-cytometric analysis.

3.2.2 RNA isolation, cDNA synthesis and real-time RT-PCR

RNA isolation from cultured cells

Cells were harvested for RNA isolation after stimulation with different ligands using RNeasy Mini Kit, according to the manufacture protocol. Cells were washed with sterile PBS to remove residual medium. 350 µl RLT buffer (lysis buffer) containing 10 µg/ml beta-mercaptoethanol was added to the cells and scrap the cell with scrapers later lysed the cells while pipetting vigorously. Cell lysate was transferred to micro centrifuge tubes and frozen at -80°C until RNA isolation. At the time of RNA isolation the cell lysates were thawed, later 350 µl of 70 % ethanol made in 1% diethyl pyrocarbonate treated water (DEPC water) was added to it and mixed well. This mixture was transferred to RNeasy mini columns held in 2 ml collection tubes and centrifuged at 13000 rpm for 30 seconds. The flow-through was discarded and then 350 µl of RW1 buffer added to the column again centrifuged at 13000 rpm for 30 seconds. Discard the flow through and treated the column with DNase1 solution to prevent DNA contamination in RNA samples. Later on 350 µl RW1 buffer was added to the column and centrifuged at 13000 rpm for 30 seconds. Discarded the collection tubes and transferred the column in to fresh 2 ml collection tubes. 500 µl of RPE buffer was added to the column, centrifuged at 1300 rpm for 30 seconds and the flow-through was discarded. This step was repeated again. The column was placed in a 1 ml fresh collection tube, added 35 µl of RNase free water to column and centrifuged 1200 rpm for 30 sec to collect the RNA. RNA quality was determined by running RNA on agarose-formaldehyde gel.

Isolation of RNA from tissues

When mice were sacrificed on termination of the study, tissues from each mouse were preserved in RNA-Later and stored at -20°C until processed for RNA isolation. RNA isolation was carried out using RNeasy Mini Kit. In short tissues (30 mg) preserved in RNA-Later were homogenized using a blade homogenizer for 30 seconds at 14500 rpm in lysis buffer (600 µl) containing β -mercaptoethanol (10 ul/ml). The homogenate was centrifuged at 15000 rpm for 3 min. and 350 µl of supernatant was transferred to fresh DEPC (Diethylpyrocarbonate) treated tube. 350 µl of 70 % ethanol was added and the

whole mixture was loaded on a RNA column and processed for RNA isolation as mentioned. Isolated RNA was stored at -80°C until further used.

RNA quality was determined by running RNA on agarose-formaldehyde gel. The RNA was quantified by using a UV-Spectrophotometer at 260 nm. 260/280 ratio were also measured and values approximately close to 1.6 to 1.9 was considered.

Complementary DNA synthesis and real-time PCR analysis

The RNA samples were diluted in DEPC water (1 $\mu\text{g}/20\ \mu\text{l}$) and a master mix was prepared. The master mix contained, 4.5 μl of 5 x buffer, 0.5 μl of 25 mM dNTP mixture, 1 μl of 0.1 M DTT, 0.5 μl of 40 U/ μl RNasin, 0.25 μl of 15 $\mu\text{g}/\text{ml}$ acrylamide, 0.25 μl of hexanucleotides and 0.5 μl of superscript or ddH₂O in case of the negative controls. 7 μl of this master mix was added to each RNA samples and incubated at 42°C on a thermal shaker incubator for 1 hour 30 minutes. Complementary DNA (cDNA) samples were collected and stored at -20°C . For real-time RT-PCR, the cDNA samples were diluted for 10 times in ddH₂O.

TaqMan® quantitative real time – PCR

The real-time RT-PCR was performed on a TaqMan® ABI Prism 7000. The quantitative PCR for mRNA is based on the employment of sequence-specific primers and likewise sequence-specific probes. The latter are tagged at both ends with a fluorescent molecule. The quencher absorbs TAMRA (at the 3'-End) the fluorescence of the other reporter tagged material such as FAM or VIC at the 5'-End. The TaqMan® universal PCR master mix contained Taq polymerase possessing a 5' -3' polymerase activity and a 5'-3' ' exonuclease activity. During the elongation phase of the PCR, specifically bound probe was hydrolyzed by the exonuclease and the 5'-tag was set free. With every newly synthesized DNA strand fluorescent tag material was set free and the resulting fluorescence was measured at 488 nm. The resulting fluorescence signal is directly proportional to the quantity of DNA synthesized. The CT value (= "Cycle Threshold") was computed for each sample. This is the cycle number, of which the reporter fluorescence signal breaks through a user-defined threshold. The TaqMan® universal PCR master mix contained the forward and reverse primers and the probe was placed on ice. The TaqMan® universal PCR master mix

contained PCR buffers, dNTPs and the AmpliTaqGold® as previously mentioned (Taq polymerase without 3' to 5' exonuclease activity). 18 µl of the mastermix was pipetted into each well of a 96-well plate and 2 µl of template (DNA dilution) was added to each of these wells. The plate was sealed and centrifuged at 1000 rpm and analyzed using TaqMan® ABI PRISM 7700. For the TaqMan® RT-PCR the following temperature settings were used: The first incubation was carried out for 2 minutes at 50 °C followed by 95 °C for 10 minutes to activate the polymerase. Templates were amplified during 40 cycles each comprising 15 seconds incubation at 95 °C followed by 1 minute incubation at 60 °C. The RT-PCR for the housekeeping gene 18S rRNA was carried out under similar conditions. The CT values were recorded using the ABI PRISM Sequence Detection software (version 1.0) and the results were evaluated in relation the respective housekeepers. In all cases, controls consisting of ddH2O were negative for target and housekeeper genes. For all quantitative analyses the cDNA content of each sample was compared with another sample following the $\Delta\Delta C_t$ equation $A_0/B_0 = (1+E)^{(C_{t,B}-C_{t,A})}$ where A_0 is the initial copy number of sample A; B_0 is the initial copy number of sample B; E, efficiency of amplification; $C_{t,A}$, threshold cycle of sample A; and $C_{t,B}$ threshold cycle of sample B. The amplification efficiency was defined as 1. All analyses were performed during the same runs including control dilution series. Similar amplification efficiencies for targets and housekeeping genes were demonstrated by analyzing serial dilutions showing an absolute value of the slope of log input cDNA amount versus ΔC_t (C_t housekeeping gene - C_t target) of < 0.1 .

The Taqman probes used in the study were:

IL-6: ID Mm00446190_m1 FAM 5'-AAATGAGAAAAGAGTTGTGCAATGG-3'
 MX1: ID Mm00487796_m1 FAM 5'-TGTA CTGCTAAGTCCAAAATTAAG-3'
 CCL2: ID Mm00441242_m1 FAM 5'-GCTCAGCCAGATGCAGTTAACGCCC-3'
 CCL5: ID Mm01302428_m1 FAM 5'-CCAATCTTGCAGTCGTGTTTGTAC-3'
 TBX21: ID Mm00450960_m1 FAM 5'-GCAAGGACGGCGAATGTTCCCATTC-3'
 GATA3: ID Mm00484683_m1 FAM 5'-CCCACCACGGGAGCCAGGTATGCCG-3'
 FoxP3: ID Mm00475156_m1 FAM 5'-ACCCAGCCACTCCAGCTCCCGGCAA-3'
 Rorc: ID Mm00441139_m1 FAM 5'-CCCACACCTCACAAATTGAAGTGAT-3'
 TLR3: ID Mm01207403_m1 FAM 5'-CTTTCAAAAACCAGAAGAATCTAAT-3'
 TLR7: ID Mm00446590_m1 FAM 5'-AAAATGGTGTTCGATGTGGACAC-3'

Ddx58: ID Mm00554529_m1 FAM 5'-CCAAACCAGAGGCCGAGGAAGAGCA-3'
 IFIH1: ID Mm00459183_m1 FAM 5'-GACACCAGAGAAAATCCATTTAAAG-3'
 IFN γ : ID Mm00801778_m1 FAM 5'-CTATTTTAACTCAAGTGGCATAGAT-3'
 IPS-1: ID Mm00523168_m1 FAM 5'-AGTGACCAGGATCGACTGCGGGCTT-3'
 TNF: ID Mm00443258_m1 FAM 5'-GTCCCCAAAGGGATGAGAAGTTCCC -3'
 IL-23: ID Mm00518984_m1 FAM 5'-CAAGGACAACAGCCAGTTCTGCTTG -3'
 IP10: ID Mm00445235_m1 FAM 5'-GACTCAAGGATCCCTCTCGCAAGG-3'
 DAI: forward primer 5'-CAGGGAAGCACCCCTCTTAT-3', reverse primer 5'-GAATGAAG
 CTCCTGGGTCAG-3', core sequence FAM 5'-CCCCAGAAGTGTCACCACCCT-3'
 COX2: forward primer 5'-GGACTGGATTCTATGGTGAAAAGT-3', reverse primer 5'-GGC
 TTCAGCAGTAATTTGATTCTTG-3', core sequence FAM 5'-ACTACACCTGAATTTTC-3'
 TGF β : forward primer 5'-CACAGTACAGCAAGGTCCTTGC-3', reverse primer 5'-AGTAGA
 CGATGGGCAGTGGCT-3' (r), core sequence FAM 5'-C GCTTCGGCGTCACCGTGCT-3'
 IL-2: forward primer 5'-GACTGGTTCTTCTGGTGGAAAGCT-3' (f), 5'-TGGGATGCTTGG
 CCATATG-3' (r), core sequence FAM 5'-TGGGAGTCCAGCCACCAACATTACTTCT -3'

SYBR green quantitative real time – PCR

In addition to the use of pre-developed TaqMan assay reagents (PDAR) or primers and probe, we also used SYBR green method to analyse the gene expression of interest. SYBR green-based detection for real-time PCR only works if only one gene-specific amplicon is generated during the reaction. Unlike TaqMan-based assays, SYBR green detection also uniquely allows to check the specificity of the PCR using melting. At low temperature, the PCR DNA product is double stranded, and it binds fluorescent SYBR green. With increasing temperature, the DNA product melts or dissociates becoming single stranded, releasing SYBR Green and decreasing the fluorescent signal. Most real-time instruments usually plot melting curves as a first derivative.

Preparation of SYBR green master mixture:

2x SYBR green master mix (500 μ l Volume)	
10x Taq Buffer without detergent	100 μ l
dNTPs (25 mM)	5 μ l
Rox	20 μ l
PCR Optimizer	200 μ l

BSA	10 μ l
Sybergreen (stock 1:100 in 20% DMSO)	2 μ l
MgCl ₂ (25 mM)	120 μ l
H ₂ O	40.5 μ l added to make final volume 50 μ l

Preparation of reaction mix for each 20 μ l reaction

2x Sybergreen master mix	10 μ l
Forward primer (10 pmol)	0.6 μ l
Reverse primer (10 pmol)	0.6 μ l
Taq polymerase	0.16 μ l
H ₂ O	6.64 μ l
cDNA (1:10 diluted)	2 μ l

The SYBR green forward (f) and reverse (r) oligonucleotide sequences used for the study were:

18S rRNA:	5'-GCAATTATTCCCCATGAACG-3' (f) 5'-AGGGCCTCACTAAACCATCC-3' (r)
IFIT1:	5'-CAAGGCAGGTTTCTGAGGAG-3' (f) 5'-GACTGGTCACCATCAGCAT-3' (r)
OASL2:	5'-TCTGTTGCACGACTGTAGGC-3' (f) 5'-GTGTCCAATCCCTGTTCCC-3' (r)
ZC3HAV1:	5'-TTGCAAGCTTAATCTGCTCG-3' (f) 5'-ACCTGGAAGTTCTGTTCCGA-3' (r)
IFIH1:	5'-GCCTGGAACGTAGACGACAT-3' (f) 5'-TCATCGAAGCAGCTGACACT-3' (r)
MX1:	5'-TCTGAGGAGAGCCAGACGAT-3' (f) 5'-CCAGGTCCTGCTCCACAC-3' (r)
IFN β 1:	5'-TCCCTATGGAGATGACGGAG-3' (f) 5'-ACCCATGCTGGAGAAATTG-3' (r)
CCL5:	5'-GTGCCACGTCAAGGAGTAT-3' (f) 5'-CACTTCTTCTCTGGGTTGG-3' (r)

CCL17: 5'-TGCTTCTGGGGACTTTTCTG-3' (f)
 5'-ATAGGAATGGCCCC TTTGAA-3' (r)

HIF-1 α : 5'-CGGCGAGAACGAGAAGAA-3' (f)
 5'-AAACTTCAGACTCTTTGCTTC G-3' (r)

IL-1 β 5'-TTCCTTGTGCAAGTGTCTGAAG-3' (f)
 5'-CACTGTCAAAAAGGTGGCATT-3' (r)

3.2.3 Microarray studies

Primary mesangial cells (pMC) were stimulated with 0.5 μ g of 3P-RNA/CL and 30 μ g of non-CpG-DNA/CL. Medium/CL-treated cells were used as control. After 6 hours total RNA was prepared using RNAeasy Mini Kit. Total RNA (6 μ g) from three independent preparations in each group were used for biotin-labeled cRNA probe synthesis and hybridization of MOE 430Av2 arrays according to the Affymetrix Expression Analysis Technical Manual (www.affymetrix.com). Triplicate arrays were scanned and analyzed using the Affymetrix GeneChip Operating software (GCOS1.0). Each array was checked for general assay quality (3'-5' ratios for glyceraldehyde-3-phosphate dehydrogenase (Gapdh) and β -actin <1.1, average background <75 fluorescence units, and scaling factors within a two-fold range. The complete data set was deposited into the GEO database (<http://www.ncbi.nlm.nih.gov/geo>; submission #GSE11898). All nine Affymetrix Microarray CEL-Files were normalized together using RMA Express version 1.0 beta 2 (<http://rmaexpress.bmbolstad.com>). As probe sets definition the default Mouse430_2.cdf (included in the library files from the Affymetrix http://www.affymetrix.com/support/technical/byproduct.affx?product=moe_430-20) was used which defines 45,101 probe sets. Probe data were background-adjusted, quantile-normalized, and summarized to probe set signals using median polish. Probe set signals were logarithmized to base 2. To exclude probe sets in the lower end of the signal range which have large signal variation, a background filter cutoff value was defined as the maximal signal value obtained from nonhuman Affymetrix-control probe sets multiplied by a factor of 1.2 [146]. Probe sets with a signal below cutoff in every array of the corresponding comparison as well as Affymetrix control probe sets were excluded from the analysis. The cutoff value in controls vs. 3P-RNA/CL was 3.24, and 22,855 probe sets were retained; in controls vs. non-CpG-DNA/CL the cutoff value was 3.10, and 24,097 probe

sets were retained. Differentially expressed probe sets between controls and 3P-RNA/CL or non-CpG-DNA/CL were computed using the Microsoft Excel plugin of SAM, version 1.21 [147]. Parameters were unpaired tests for significance analysis and 100 permutations for false discovery rate estimation. Accepting a false discovery rate of 1%, 4,575 (controls vs. 3P-RNA/CL) and 7,331 probe sets (controls vs. non-CpG-DNA/CL) were considered differentially expressed. Of these, the number of probe sets induced or reduced more than 1.5-fold were 855 in controls vs. 3P-RNA/CL, and 2,576 in controls vs. non-CpG-DNA/CL.

3.2.4 RNA silencing studies

Rig-1 (DDX58) and Dai (Zbp1) genes were knockdown using DDX58 siRNA ON-TARGETplus SMART pool oligonucleotides and Dai siRNA. Negative control siRNA (Ambion/Applied biosystems, Darmstadt, Germany) was used as control. The siRNA sequences were as follows: DDX58 (Rig-1), 5'-CAAGAAGAGUACCACUAAU-3', 5'-GUUAGAGGAACACAGAUUAU-3', 5'-GUUCGAGAU UCCAGUCAUAU-3', 5'-GAAGAGCACGAGAUAGCAAU-3'; Dai, 5'-ACAGUCCAGACAGUCCACAU CAAU-3', 5'-GGCAACAAGAUGACCAUCCACCUA-3', 5'-GGAAGACACAG GUACAAGCUCUGAA-3'. 1×10^5 MMC were plated in 12 well plates in antibiotic free 2% fetal calf serum-DMEM medium. 40nM siRNA was transfected twice with cationic lipids (CL) as mentioned above. After 24 hours of second transfection cells were stimulated with 1 μ g of 3P-RNA and 5 μ g of non-CpG-DNA for 6 hours. Later on RNA was isolated from the cells. To check knock down efficiency realtime-PCR and Western blotting were performed for the Rig-1 and Dai. CXCL10 and IL-6 were measure by realtime-PCR and ELISA. To check mRNA level and protein level, respectively.

3.2.5 Western blotting

The following Western blotting protocol was used

A. Preparation of cell lysates

1. Collected cells
2. Lysed the pellet with RIPA lysis buffer on ice for 30 min with rotation
3. Spin at 14,000 rpm (16,000 g) in an Eppendorf microfuge for 10 min at 4 °C

4. Transferred the supernatant to a new tube and discard the pellet.
 5. Determined the protein concentration (Bradford assay from Bio-Rad)
 6. Mixed the protein extract with 6x sample buffer.
 7. Boiled for 5 min at 95 °C
 8. Cool at room temperature for 5 min.
 9. Flash spinned the sample
- B. 10% Polyacrylamide gel was prepared
- C. Running the gel
1. After flash spinning the samples, loaded into the wells.
 2. Ran with constant current (80V for stacking and 120V for resolving).
- D. Preparation of membrane
1. Cut a piece of PVDF membrane.
 2. Wet for about 5 min in methanol on a rocker at room temp.
 3. Removed the methanol and added 1x Blotting buffer until ready to use.
- E. Membrane transfer
1. Kept the membrane on blotting sheet
 2. Take out the SDS-Gel from transfer buffer and keep the gel onto the membrane and transfer the protein at 25 Volts for 45 minutes.
 3. When finished, immerse membrane in blocking buffer and block 1 hours or overnight according to antibody optimal protocol.
- F. Antibodies and detection
1. Incubate with primary antibody diluted in blocking buffer for 60 min at room temp/overnight according to antibody.
 2. Wash three times with 0.05% Tween 20 in TBS.
 3. Incubate with secondary antibody diluted in blocking buffer for 45 min at RT
 4. Wash three times with 0.05% Tween 20 in TBS.
 5. Detect with ECL kit and develop the film.

3.2.6 Animals and experimental protocol

Ten week old female MRLlpr/lpr mice were obtained from Harlan Winkelmann (Borchen, Germany) and kept in filter top cages under a 12 hour light and dark cycle. Water and standard chow (Sniff, Soest, Germany) were available ad libitum. All experimental procedures have been approved by the local government authorities. Mice were distributed into four groups, each group consisting of 10 to 14 mice. From weeks 16 to 18 of age, groups of 12 MRLlpr/lpr mice received intraperitoneal injections every other day with either 5% glucose or 20 µg phosphodiester 3P-RNA (5'PPP-GAAAAGGGGACACACACACACACACACAC-3') dissolved in transfection agent in vivo-JetPEI™ according to the manufactures recommendations. 3P-RNA, devoid of TLR7 activation, was prepared using *in vitro* transcription assay kit. A third group of MRLlpr/lpr mice was injected with 50 µg phosphodiester non-CpG-dsDNA, (sense 5'TACAGATCTACTAGTGATCTATGACTGATCTGTACATGATCTACA3'). Non-CpG-DNA was generated by annealing complementary single strands of DNA [101] and dissolved in JetPEI. JetPEI was used to facilitate the uptake of both ligands into the cellular cytosol in vivo. As a positive control for the immunostimulatory effects of DNA, a group of mice were injected with 40µg of the immunostimulatory A-class phosphothioate CpG-ODN 1668, 5`-TCG ATG ACG TTC CTG ATG CT-3` dissolved in saline as described [132]. Endotoxin levels of all synthetic nucleic acids were negligible as tested by the Limulus Assay. Phosphorothioate or phosphodiester backbones of synthetic CpG oligonucleotides can modulate their binding affinity to DNA autoantibodies [148]. Neither of the aforementioned ODN bound to serum IgG from C57BL/6 mice but all of them bound to serum IgG of MRLlpr/lpr mice. Binding affinity was strongest for phosphorothioate CpG-DNA particularly at lower concentrations. Binding affinity of phosphodiester non-CpG-DNA was less potent and was not much affected by complexing non-CpG-DNA to JetPEI. At a concentration of 10 µg/ml the binding affinity of all nucleic acid ligands tested was almost identical. All mice were sacrificed by cervical dislocation at the end of week 18 of age. To assess the renal distribution of injected 3P-RNA and non-CpG DNA in vivo 5'-rhodamine-labeled forms of 3P-RNA/Jet-PEI and non-CpG DNA/Jet-PEI complexes were intravenously injected into MRLlpr/lpr mice at 18 weeks of age. Frozen renal sections were collected 2 hours later, stained with FITC-labeled phalloidin (1:50) and 4',6-diamidino-2-

phenylindol (DAPI) and subjected to immunofluorescence imaging. In some experiments single dose studies were performed in C57BL/6 mice that were obtained from Charles River, Sulzfeld, Germany, or in MyD88-deficient mice that had been backcrossed for 6 generations to the same background [149].

3.2.7 Morphological and histological analysis

The weight ratio of spleen and the bulk of mesenterial lymphnodes to total body weight were calculated as markers of the lupus-associated lymphoproliferative syndrome. From all the mice, the tissues isolated from kidneys and spleens were placed in plastic histocassettes and immediately fixed in 10% buffered formalin (formaldehyde in PBS) for overnight. Next day the tissue was processed with an automatic tissue-processor, which processes tissues sequentially in 70% ethanol for 5 hours, 96% ethanol for 2 hrs, 100 % ethanol 3.5 hrs, xylene 2.5 hrs and paraffin for 4 hrs. Histocassettes were taken out from the automatic tissue-processor and paraffin blocks were prepared with hot liquid paraffin using a Microm- EC 350 machine. These blocks were used for making fine sections for different staining (PAS or immuno staining). 5 µm thick paraffin-embedded sections were cut. De-paraffinization followed by dehydration was carried out by incubating the sections in xylene, 100% absolute ethanol, 95%, 80% and 50% ethanol followed by rinsing with PBS (2 changes, 3 minutes each). Silver and periodic acid-Schiff stains were done following routine protocols. The severity of the renal lesions was graded using the indices for activity and chronicity as described for human lupus nephritis [150]. Activity index was considered as the sum of individual scores of the following items considered to represent measures of adaptive lupus nephritis: glomerular proliferation, leucocyte exudation, karyorrhexis/fibrinoid necrosis (X2), cellular crescents (X2), hyaline deposits, and interstitial inflammation [150]. The maximum score was 24 points for activity index. Chronicity index was considered to be the sum of individual scores of the following items considered to represent measures of chronic irreversible lupus nephritis: glomerular sclerosis, fibrous crescents, tubular atrophy and interstitial fibrosis. The maximum score was 12 points for the chronicity index.

For immunostaining all sections were incubated with different primary antibodies either for 1 hour at room temperature or overnight at 4 °C in a wet chamber followed by a wash with PBS (2x 5 min). After washing, sections were incubated with biotinylated secondary antibodies (1:300, dilution in PBS) and the ABC reagent (Vector, Burlingame, CA USA). Slides were washed in phosphate buffered saline between the incubation steps. 3,3'-Diaminobenzidine (DAB) with metal enhancement was used as detection system, resulting in a black coloured product. Methylgreen was used as counterstain and slides were washed with alcohol (96%) to remove excess stain and xylene. Sections were dried and mounted with Vecta Mount.

The following rat and rabbit antibodies were used as primary antibodies: rat anti-Mac2 (glomerular macrophages, 1:50), rat anti-F4/80 (macrophages, 1:50), anti-Ki-67 (cell proliferation, 1:25), anti-CD3 (1:100), anti-mouse Mac-2 (monocytes/macrophages, 1:50), anti mouse B220 (early Pro-B to mature B cells, 1:400), anti-mouse IgG1 (1:100), anti mouse IgG2a (1:100), anti-mouse C3 (1:20, GAM/C3c/FITC). For each immunostaining negative controls staining was performed by incubation with a respective isotype antibody instead of the primary antibody. For quantitative analysis for evaluation of glomerulonephritis glomerular cells were counted using a microscope in 15 cortical glomeruli per section. The severity of the renal lesions was graded using the indices for activity and chronicity of lupus nephritis (100). Activity index included semi-quantitative score of 4 active inflammatory lesions: 1. glomerular leukocyte infiltration, 2. interstitial inflammation, 3. glomerular karyorrhexis and 4. cellular crescents; while chronicity index included semi-quantitative score of 3 inflammatory lesions: 1. glomerular sclerosis, 2. interstitial fibrosis and 3. tubular atrophy. Semi quantitative scoring of glomerular IgG deposits from 0 to 3 was performed on 15 cortical glomerular sections using a semiquantitative index as follows: 0 = no signal, 1 = low signal, 2 = moderate signal, and 3 = strong signal intensity. Peribronchial and pulmonary inflammation was arbitrarily graded from 0 (no inflammation) to 3 (severe inflammation).

3.2.8 Evaluation of serum autoantibodies

Blood and urine samples were collected from each animal at the end of the study period from each group of mice. Blood samples were collected under anesthesia by retroorbital puncture using capillaries and collected in 1.5 ml micro centrifuge tubes. Serum was collected after a settle time of 15 min at room temperature followed by centrifugation of blood at 10000 rpm for 5 min. Proteinuria and creatinine were determined using an automatic autoanalyzer (Integra 800, Roche Diagnostics, Germany).

Analysis of serum anti-dsDNA autoantibodies by ELISA

Serum dsDNA autoantibodies were determined by using commercial ELISA kits using the following antibodies: anti-mouse IgG1, IgG2a and IgG2b following the manufacturer's protocols. First coat the NUNC maxisorp 96 well flat bottom ELISA plate with 100 µl of poly-L-Lysine (Trevigen, Gaithersburg, MD, USA) for 1 hour at room temperature. Later on wash the plate with PBS and then incubated the wells with 100 µl of dsDNA (1 µg/ml) which was diluted in SSC buffer (1X) for over night at 4 °C. For standards, the wells were captured with the capture antibody in coating buffer. Washed the plate and blocking solution was added for one hour, later on standard and samples were added in respective wells and incubated for 2 hours. After washing the plate the wells were incubated for 1 hour with secondary antibody. The plate was developed by adding TMB substrate to the wells and incubated for 15 min. The reaction was stopped by adding 1 M H₂SO₄ and absorbance was measured at 450 nm.

***Crithidia luciliae* assay**

To detect anti-dsDNA more specifically *Crithidia luciliae* assay was carried out. Diluted serum samples (1:100) were applied to fixed *C. luciliae* slides (Bio Rad Laboratories, Munich, Germany) and incubated for 30 min at room temperature. After washing the slides with PBS, FITC-labeled goat anti-mouse IgG was used as a detection reagent. Slides were mounted with DAPI. *C. luciliae* DNA colocalized with DAPI and the kinetoplast staining intensity was quantified from digital images with Adobe Photoshop software.

Anti-nuclear antibodies

Anti-nuclear antibodies (ANA) were determined by incubating serum samples (1:200 in PBS) with Hep-2 slides. Fluorescein-labeled goat anti mouse IgG was used as secondary antibody (1:50 in PBS). Serum of 6-10 week old C57BL/6 mice was used as negative control. The fluorescent patterns of ANA were classified as homogenous nuclear, speckled nuclear, cytoplasmic and mitotic patterns [137].

Anti-Sm and anti Sm-RNP antibodies

NUNC maxisorp ELISA plates were coated with 1:250 diluted Smith (Sm) antigen (Immunovision, Springdale, AR, USA). An anti-Sm IgG (Y12) antibody was used as standard. A horseradish peroxidase-conjugated goat anti-mouse IgG (2 mg/ml) was used as secondary antibody at a dilution of 1 µl in 50 ml in PBS (pH 7). After that TMB substrate was added to develop colour and kept for 20 min in dark. Later on reaction was stopped by using 1M H₂SO₄. Absorbance was measured at 450 nm using spectrophotometer (TECAN). The same procedure was followed for anti-SmRNP ELISA. Here the ELISA plates were captured with Sm-RNP complex (1000 units/ml) (Immunovision) at a dilution of 1:250 instead of Sm antigen.

Rheumatoid factor

NUNC maxisorp ELISA plates were coated with rabbit IgG at a concentration of 10µg/ml (Jackson Immunoresearch, West Grove, PA, USA) overnight at 4 °C. Serum samples were diluted 1:100 in PBS (pH 7), 10 week old C57BL/6 mouse serum was used as negative control. HRP conjugated goat anti-mouse IgG (2 mg/ml, Rockland Immunochemicals Research, Gilbertsville, PA, USA) was used as secondary antibody at a dilution of 1 µl in 50 ml of PBS (pH7). TMB Substrate was used to develop the colour and reaction was stopped by using 2N H₂SO₄. The absorbance was measured at 450 nm by using spectrophotometer.

Cytokines and serum IgG antibodies

Cytokine levels in sera or cell culture supernatants were determined using commercial ELISA kits: IL-6, IL-12p40, CCL2 or CXCL2, IFN-γ (OptEiA, BD, Biosciences,

Heidelberg, Germany), IFN- α , IFN- β (PBL Biomedical Labs, NJ), TNF α (BioLegend, San Diego, CA) following the protocol provided by the respective manufacturers. The 96-well plate was first coated with 100 μ l/ well capture antibody (anti-mouse cytokine) at recommended dilution and placed overnight at 4 °C. The wells were then aspirated, washed with wash buffer and the plate was blocked with assay diluent and incubated at room temperature for 1 hour. After washing the plate 100 μ l of standard or samples were added to the wells and incubated for 2 hours at room temperature. After washing the plate it was incubated for one hour with the secondary antibody (avidin-horse raddish peroxidase conjugated). This was followed by another wash step. The TMB substrate solution was then added to each well at a volume of 100 μ l and incubated for 30 minutes. The stop solution (2N H₂SO₄) was then added to each well, and absorbance was measured at prescribed wave length (nm), using an automatic plate reader.

For quantification of serum IgG antibodies NUNC maxisorp ELISA plates were coated with a capture antibody (anti mouse IgG1 or IgG2a or IgG2b or IgG) in coating buffer. Washed the plate and blocking solution was added for one hour, later on standard and samples were added in respective wells and incubated for 2 hours. After washing the plate the wells were incubated for 1 hour with secondary antibody. The plate was developed by adding TMB substrate to the wells and incubated for 15 min. The reaction was stopped by adding 1 M H₂SO₄ and absorbance was measured at 450 nm. For antibody binding assay ELISA plates were coated overnight at 4° C with CpG-DNA, non-CpG-DNA complexed with JetPEI and mouse genomic DNA diluted to various concentrations in SSC solution 1:100 diluted sera from 20 week old MRLlpr/lpr or C57BL/6 mice were added for one hour. After washing HRP conjugated anti-mouse IgG was used as secondary antibody. Reading was taken at OD 450nm.

3.2.9 Flow cytometry

Spleens were isolated from the mice of each group after sacrificing mice. Each spleen was collected in a sterile petri plate containing the 2-3 ml of ice-cold media (RPMI+ 10 %FCS + 1 % PS) on ice. Cell suspension was prepared by mashing the tissue in to fine fine pieces. Cell suspension was passed through 70 μ m plastic filter (BD Biosciences) and centrifuged

at 1600 rpm at 4°C for 5 min. The supernatant was discarded and the pellet was resuspended in to ammonium chloride to lyse red blood cells and incubated for 3 min at room temperature. Cells were centrifuged again at 1600 rpm for 5 min. Cells were washed twice with PBS and filtered by using 70 µm plastic filters. The cells were resuspended in PBS and cell number was counted using Neubauer's chamber under the microscope. Cells were incubated with labelled antibody for 30 min in dark. After washing the cells FACS analysis was carried out. The following antibodies were used in this study. Anti-mouse CD3, CD4, CD8, CD25, B220 and CD138 antibodies were used to detect CD3⁺CD4⁻CD8⁻ double negative T cells, CD4⁺CD25⁺ regulatory T cells and B220⁺CD138⁺ plasma cell populations in spleens. CD11c has been stained to identify plasmacytoid and myeloid dendritic cells and their activation was assed by costaining for CD40 and MHCII. Respective isotype antibodies were used to demonstrate specific staining of cell subpopulations.

3.2.10 Other methods

Proliferation assay

Proliferation of cells was assessed using CellTiter 96 Proliferation Assay (Promega, Mannheim, Germany). The CellTiter 96 Aqueous One Solution contains a novel tetrazolium salt compound (MTS) and phenazine ethosulfate that serves as an electron coupling reagent. The solution remains stable normally, while the MTS is bioreduced by the NADPH or NADH produced by dehydrogenase enzymes in metabolically active cells (such as proliferating cells). PMC were grown in 96 well plates for 24 hours before stimulation with various doses of 3P-RNA/CL and non-CpG-DNA/CL. After 72 hours 20 µl CellTiter 96 Aqueous One Solution was added and cells were incubated at 37 °C in 5% CO₂ for 2 hours and later the optical density (OD) was measured at 492 nm for comparing the cell proliferation.

Immunofluorescence microscopy

Mesangial cells were grown on glass coverslips and then cells were stimulated with 5'-rhodamine-labeled 3P-RNA and non-CpG-DNA complexed with or without CL. After 2 hours cells were fixed with 2% paraformaldehyde, 10 mM Pipes, 15% saturated picric acid

at pH 6.0. Wash the cells with PBS/glycin and incubated overnight with mouse anti-Rab5 (BD, Biosciences, Heidelberg, Germany) to mark early endosomes. FITC-labeled goat anti mouse IgG was used for detection. MMC cells were scanned using a LSM510 laser scanning microscope.

Annexin V-FITC and propidium iodide (PI) assay

To check apoptosis annexin V-FITC and propidium iodide (PI) assay was performed. Cells were stimulated with various concentrations of 3P-RNA/CL or non-CpG-DNA as shown in Figure 38 for 24 hours. After stimulation, cells were washed with PBS and resuspended them into annexin V binding buffer. Annexin V and PI were added to the cells suspension and incubated for 15 min at room temperature in dark. Cells were analyzed by FACS with acquisition of 30000 events/sample.

3.2.11 Statistical analysis

Statistics were done using GraphPad Prism. Data was expressed as mean \pm SEM (standard error of the mean) or mean \pm standard deviation (SD). Data were analysed using unpaired two-tailed *t*-test for comparison between two groups. One-way ANOVA followed by post-hoc Bonferroni's test was used for multiple comparisons. For nonparametric analysis of two groups two-tailed Fisher's exact test and Mann-Whitney U test were performed.

4. Results

4.1. Results part- I

Viral infection can aggravate disease activity of autoimmune diseases SLE but the molecular mechanisms remain elusive. Antiviral immune responses might drive autoimmune tissue injury via type I interferons, Th1 cytokines or CD8⁺ T cells as these mediators regulate both conditions. Antiviral immunity is triggered by conserved viral nucleic acid formats via pattern recognition receptors. The role of nucleic acid recognition via TLRs in lupus is well studied. We hypothesized that TLR-independent viral nucleic acid recognition also aggravates lupus nephritis in experimental MRLlpr/lpr mouse model. In this study we used 3P-RNA and non-CpG-DNA as RNA and DNA receptor agonists. CpG-DNA was used as a control

4.1.1. TLR-independent IL-6 induction by 3P-RNA and non-CpG-DNA *in vivo*

3P-RNA and non-CpG-DNA have been reported to trigger cytokine release via TLR-independent pathways in cultured dendritic cells [87, 101]. To extend these results *in vivo* serum IL-6 levels were measured before and 6 hours after a single injection of 3P-RNA or non-CpG-DNA into MyD88-deficient and wild-type mice. These results show that MyD88 was not required to induce IL-6 with either of these two ligands *in vivo* (Figure 11).

4.1.2. 3P-RNA and non-CpG-DNA dose dependent studies in MRLlpr/lpr mice

To select the compatible dose we did dose studies with 3P-RNA and non-CpG-DNA. These studies revealed that a single dose of 20 µg 3P-RNA or 50 µg non-CpG-DNA, but not higher doses, potently increased IL-6 or CCL2 serum levels in 16 week old MRLlpr/lpr mice (Figure 12). As this response was not dose-dependent we assumed the doses tested to be at the plateau-level of the dose response.

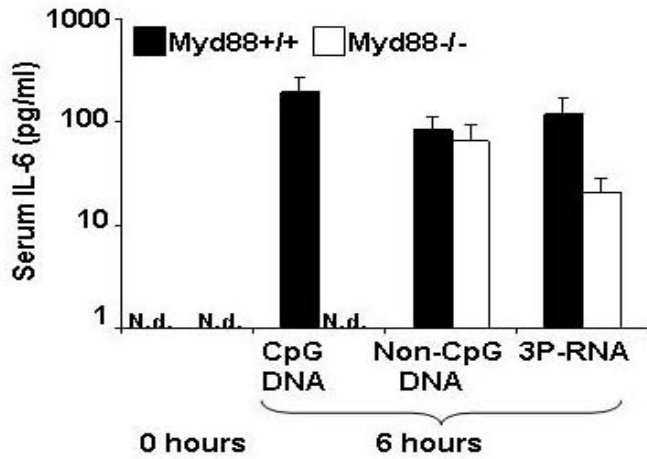


Figure 11. Serum IL-6 response in MyD88 knock out mice. C57BL/6 mice with (black bars) or without MyD88 (white bars) were injected with a single dose of 3P-RNA, non-CpG-DNA, or CpG-DNA. After 6 hours serum samples were obtained and IL-6 levels were determined by ELISA. Values are means \pm SEM from 3 mice in each group, each performed in duplicate. Note that non-CpG-DNA and 3-PRNA injected MyD88-deficient mice significantly increase serum IL-6 levels 6 hours after injection as compared to time point zero but no response to CpG-DNA ND= not detected.

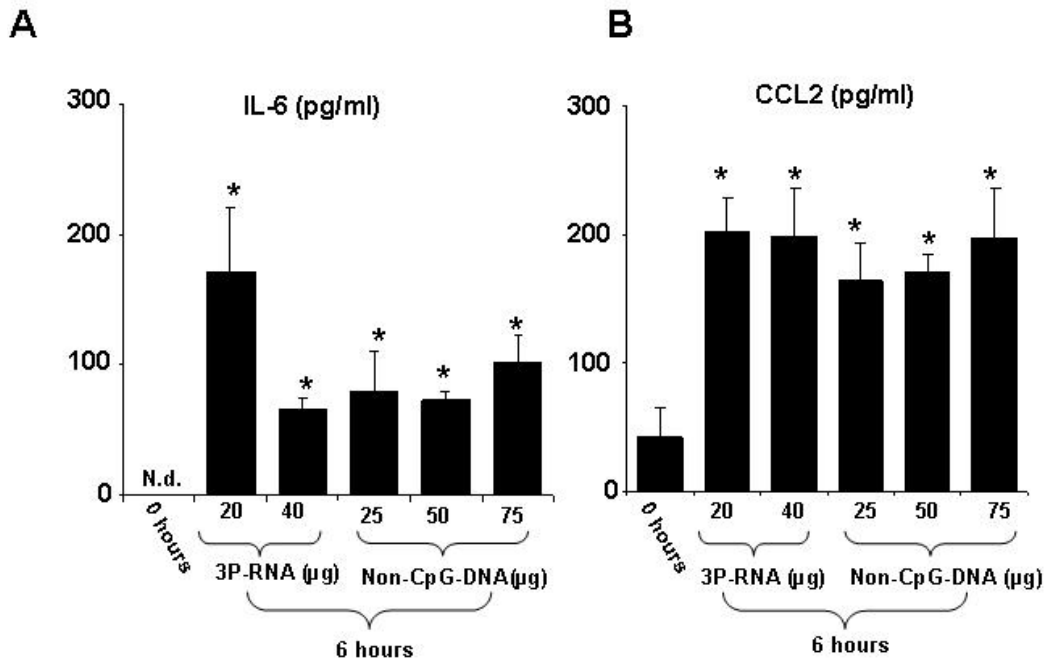


Figure 12. Dose studies in MRLlpr/lpr mice. Different concentrations of 3P-RNA and non-CpG-DNA were injected intraperitoneally into 12 week old MRLlpr/lpr mice as indicated. Serum IL-6 (A) and CCL2 (B) were measured at 6 hours after injection by ELISA. Data represent means \pm SEM from 4 mice in each group. Comparison between different doses were analyzed by ANOVA and post-hoc Bonferroni correction, * $p < 0.05$. N.d. = not detectable.

4.1.3. Non-CpG-DNA induces serum cytokines in MRLlpr/lpr mice

In order to test the effects of transient exposure to 3P-RNA and non-CpG-DNA, 16 week old nephritic MRLlpr/lpr mice with preexisting immune complex disease were repeatedly injected with 3P-RNA and non-CpG-DNA. Based on above dose studies 16 week old MRLlpr/lpr mice were injected with either 5% glucose, 20 µg of 3P-RNA, 50 µg of non-CpG-DNA or 40 µg CpG-DNA for 2 weeks. Serum cytokine levels were determined 3 hours after the last injection. Only non-CpG-DNA significantly increased serum TNF and IL-12 levels at 18 weeks, although not as high as compared with CpG-DNA (Figure 13). By contrast, 3P-RNA and non-CpG-DNA had no effect on levels of IFN- α and IFN- γ , but IFN- γ was significantly induced by CpG-DNA (Figure 13). Together, 3P-RNA and non-CpG-DNA are less potent than CpG-DNA to increase serum levels of TNF, IFN- α , IFN- γ , IL-12, IL-6 and TNF in nephritic MRLlpr/lpr mice.

4.1.4. Non-CpG-DNA induces lymphoproliferation and splenomegaly in MRLlpr/lpr mice

Repeated exposure to CpG-DNA can trigger significant lymphoproliferation [151], hence, we assessed the weight of spleens and mesenteric lymphnodes at the time of sacrifice in all mice. Non-CpG-DNA but not 3P-RNA increased the weight of spleen and mesenteric lymphnodes in MRLlpr/lpr mice to the same extent as CpG-DNA (Figure 14A and 14B). Thus, non-CpG-DNA but not 3P-RNA induces lymphoproliferation in nephritic MRLlpr/lpr mice.

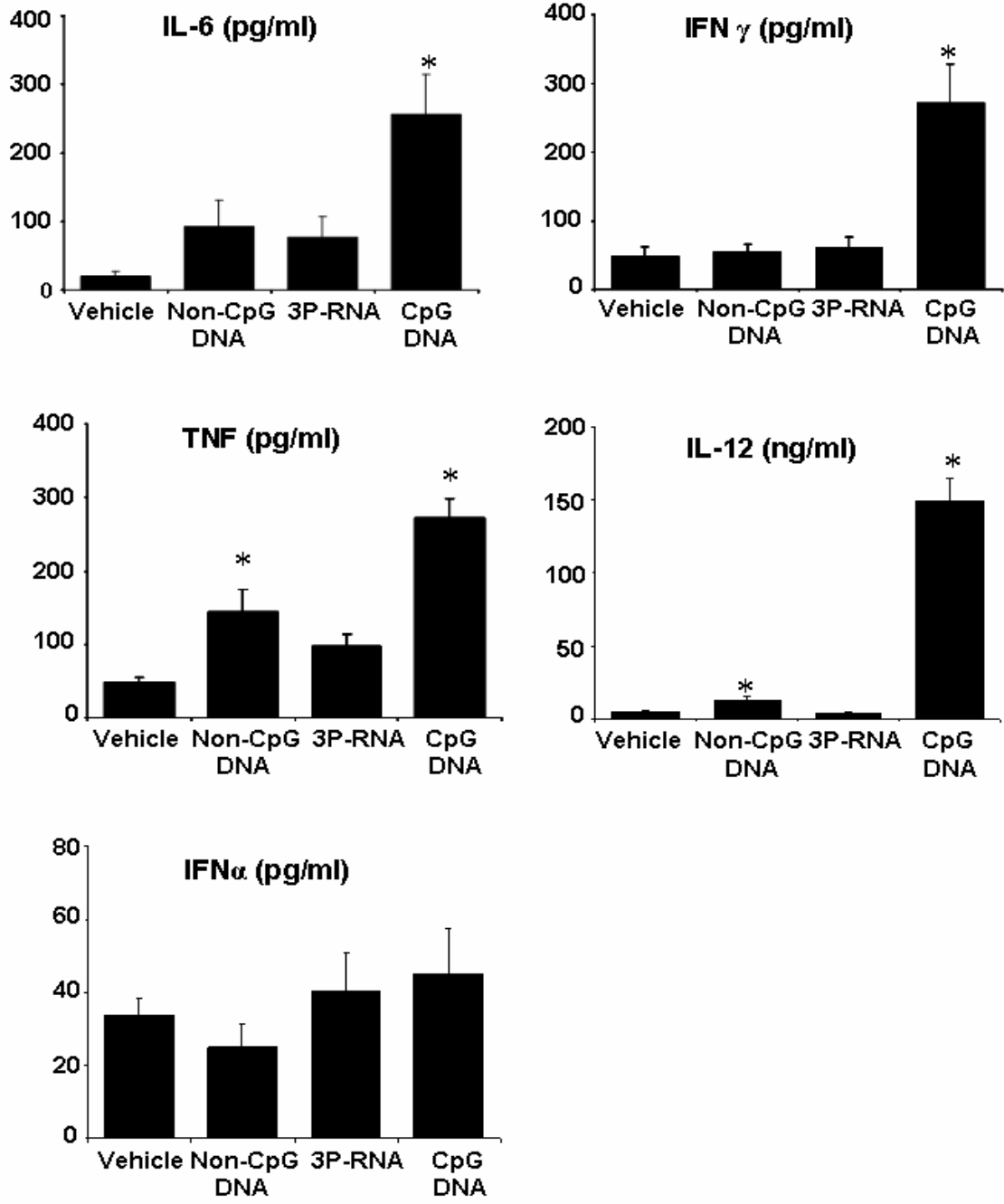


Figure 13. Serum cytokine levels in MRLlpr/lpr mice. Serum cytokine levels of 18 week old MRLlpr/lpr mice for TNF, IFN- γ , IL-6, IL-12, and IFN- α were measured by ELISA. Data represent means \pm SEM from 10-12 mice in each group. Comparison between different agonists and vehicle were analyzed by ANOVA and post-hoc Bonferroni correction, * $p < 0.05$ vs vehicle

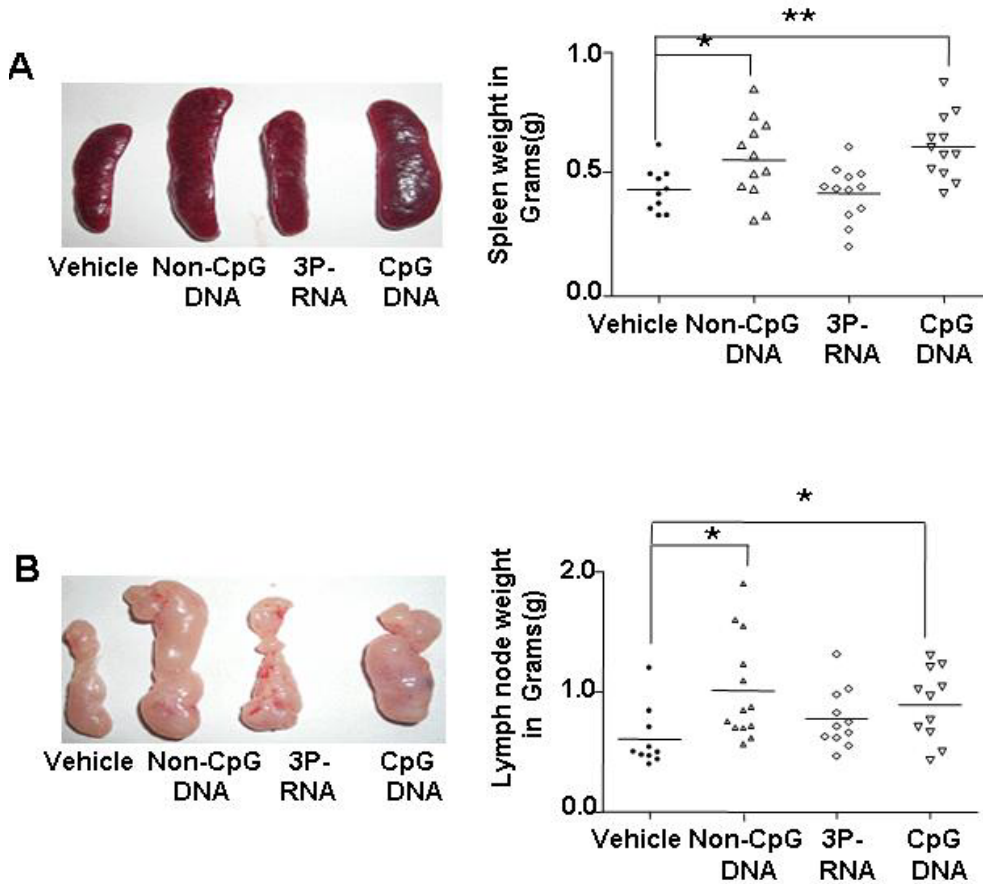


Figure 14. Spleen and lymphnodes in MRLlpr/lpr mice. Weights of spleens (A) and of mesenteric lymphnodes (B) were determined in all mice at the end of the study. Comparison between different agonists and vehicle were analyzed by ANOVA and post-hoc Bonferroni correction, * $p < 0.05$ vs. vehicle, ** $p < 0.01$ vs. vehicle.

4.1.5. Non-CpG-DNA increased negative T cells and plasma cells in MRLlpr/lpr mice

Non-CpG-DNA increased the percentage of splenic CD4/CD8 double negative T cells and B220/CD138 double positive plasma cells in MRLlpr/lpr mice (Figure 15A and 15B). But 3P-RNA did not affect these two cell population. Interestingly CpG-DNA decreased B220/CD138 double positive plasma cell population.

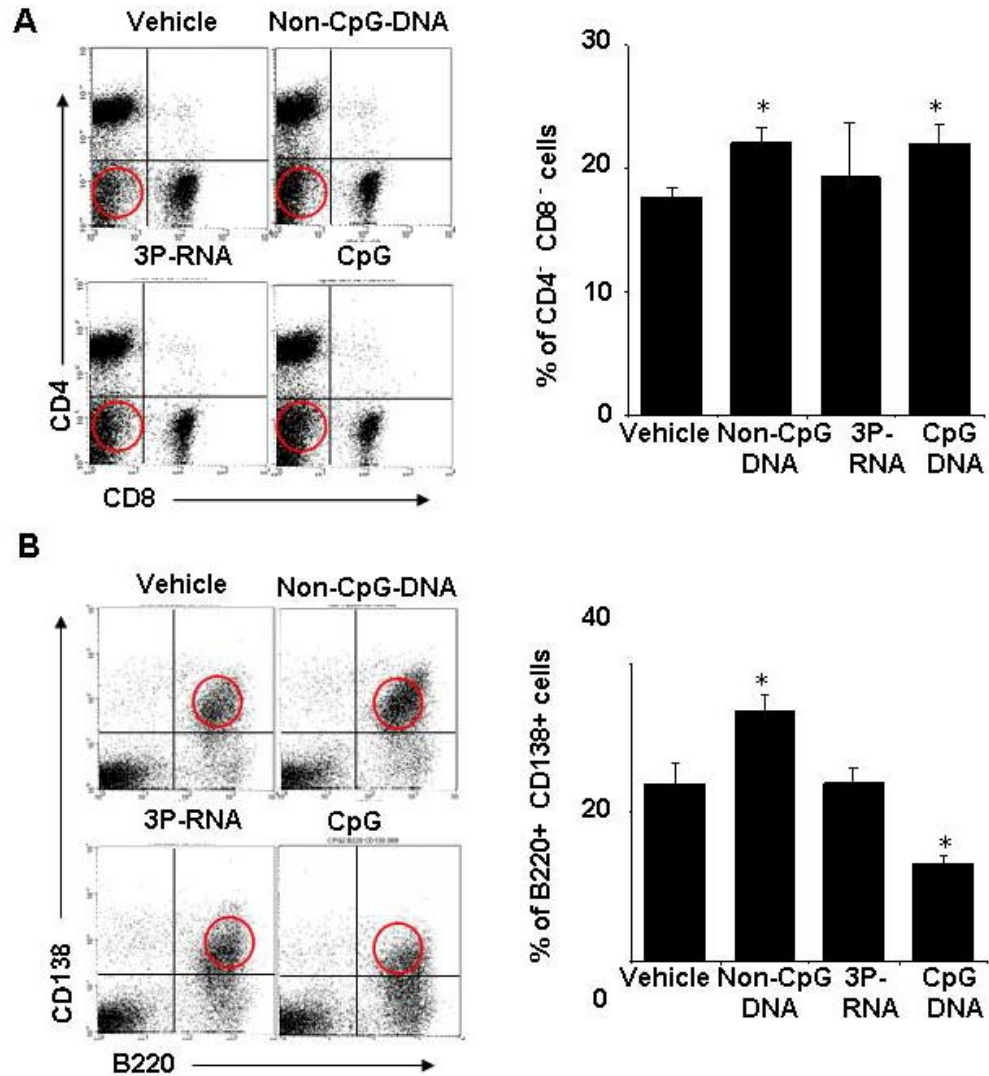


Figure 15. Spleen cell subsets in MRLlpr/lpr mice. Spleen cell subsets were determined by flow cytometry as follows: (A): CD3⁺/CD4⁻/CD8⁻ T cells by staining CD4⁺ and CD8⁺ for CD3⁺ gated T cells; the mean percentage of CD3⁺/CD4⁻/CD8⁻ T cells from the round marked lower left quadrant were shown in right side graph; (B): B220⁺CD138⁺ plasma cells, mean percentage of B220⁺CD138⁺ cells from the round marked upper right quadrant were shown in right side graph * p < 0.05 vs. vehicle. Comparison between different agonists and vehicle were analyzed by ANOVA and post-hoc Bonferroni correction, * p < 0.05 vs. vehicle.

4.1.6. Dendritic cell activation

We assessed the activation of spleen CD11c⁺ dendritic cells by flow cytometry for MHC class II and CD40 surface expression. 3P-RNA and non-CpG-DNA did not increase surface expression of MHC II and CD40 as it was observed with CpG-DNA (Figure 16).

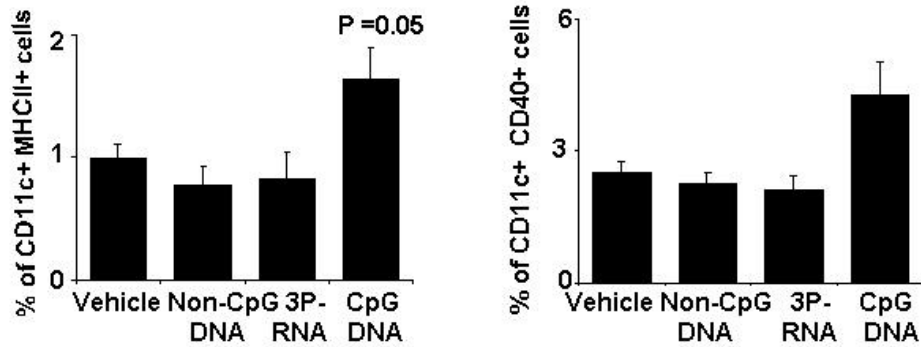


Figure 16. Dendritic cells activation in MRLlpr/lpr mice

Percentage of total splenic CD11c+ dendritic cells expressing MHCII and CD40. Comparison between different agonists and vehicle were analyzed by ANOVA and post-hoc Bonferroni correction

4.1.7. Expression of inflammatory mediators and transcription factors in spleen

We assessed spleen mRNA expression to check whether the agonist modulate the mRNA expression of inflammatory mediators and transcription factors. 3P-RNA but not non-CpG-DNA induced Mx1, a marker of type I interferon signaling, in spleens of MRLlpr/lpr mice, while IFN- γ and TNF mRNA were not induced (Figure 17). Neither 3P-RNA nor non-CpG-DNA induced IL-6 and CCL2 mRNA as seen with CpG-DNA (Figure 17). The mRNA levels of TBX21 and GATA2, respective markers of Th1 or Th2 responses, were rather decreased upon 3P-RNA exposure (Figure 17). 3P-RNA and non-CpG-DNA reduced IPS-1 mRNA levels (Figure 17). 3P-RNA suppressed Foxp3 mRNA, crucial regulator in the development and function of regulatory T cells [152]. This was consistent with reduced numbers of CD4/CD25+ T cells in 3P-RNA-treated MRLlpr/lpr mice (Table 4). IL-15 mRNA levels were not altered any of the three ligands (Figure 17). Thus, 3P-RNA induces type I IFN-dependent MX1 signaling and impairs Foxp3-driven regulatory T cells in spleens of MRLlpr/lpr mice.

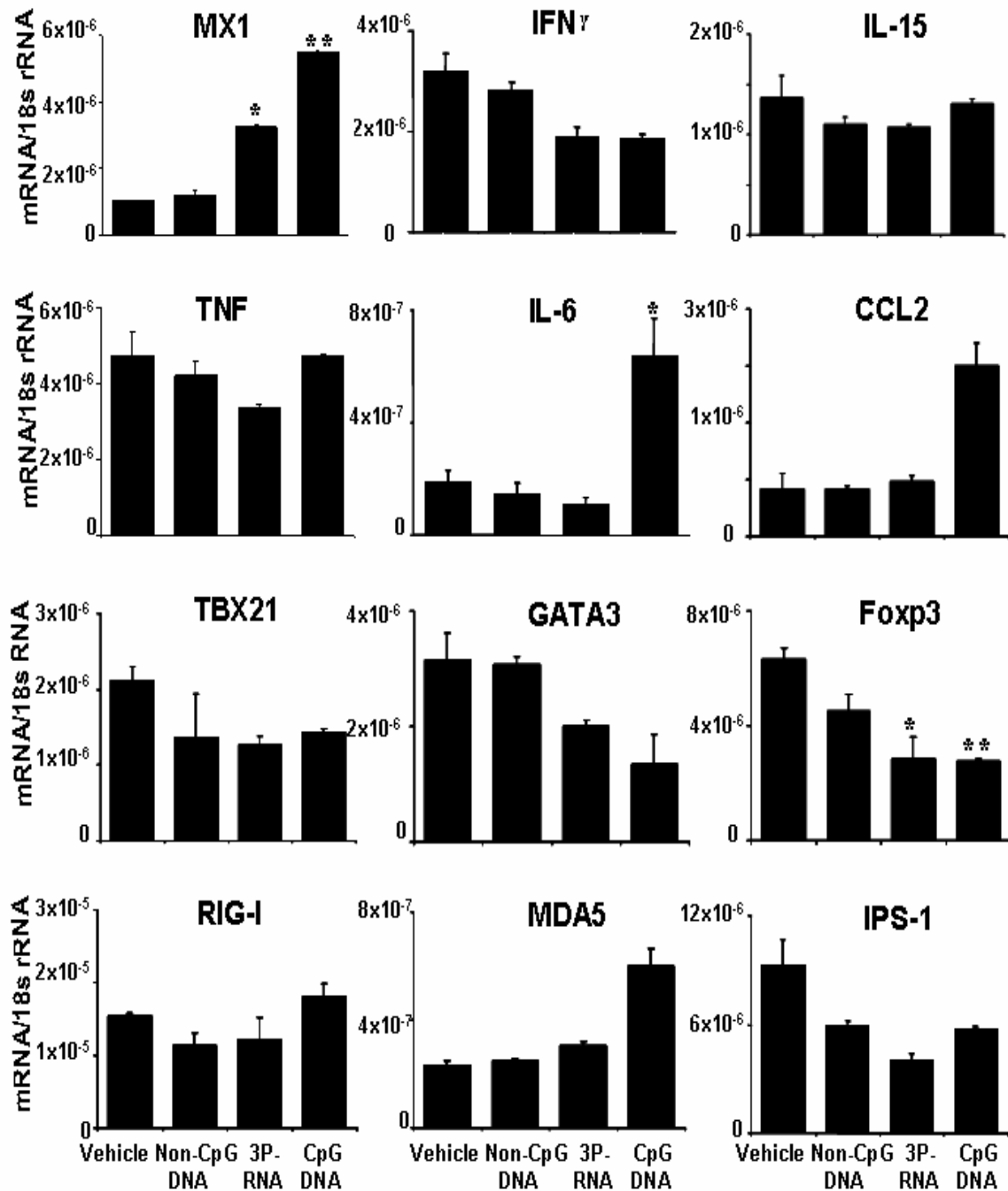


Figure 17. Spleen mRNA expression of proinflammatory mediators and transcription factors. Total spleen mRNA from 10 mice in each group was used for real-time RT-PCR. The primers for target mRNAs used are listed in methods. Data are expressed as means \pm SEM of the ratio from the target mRNA per respective 18s rRNA expression. Comparison between different agonists and vehicle were analyzed by ANOVA and post-hoc Bonferroni correction, * $p < 0.05$ vs. vehicle, ** $p < 0.01$ vs. vehicle $n = 10$ per group.

Table 4. Serum autoantibodies and spleen lymphocytes in MRLlpr/lpr mice.

	Vehicle	Non -CpG-DNA	3P-RNA	CpG-DNA
Serum IgG(mg/ml)	8 ± 1	16 ± 2**	9 ± 1	8 ± 1
IgG1(mg/ml)	15.0 ± 2.6	22.0 ± 1.6*	13.0 ± 2.2	14.0 ± 1.5
IgG2a(mg/ml)	4.0 ± 0.4	8.9 ± 1.7*	6.0 ± 1.1	6.0 ± 1.3
IgG2b(mg/ml)	2.0 ± 0.2	5.0 ± 0.8*	2.0 ± 0.3	1.0 ± 0.3
Anti-dsDNA IgG (µg/ml)	144 ± 22	203 ± 37	200 ± 30	206 ± 35
IgG1(µg/ml)	16 ± 6	108 ± 56	104 ± 37 *	85 ± 36
IgG2a (µg/ml)	462 ± 108	671 ± 142	555 ± 105	582 ± 159
IgG2b (µg/ml)	10 ± 3	43 ± 13*	46 ± 21	60 ± 21*
Anti-Sm IgG (µg/ml)	6 ± 4	8 ± 3	5 ± 2	4 ± 2
Rheumatoid factor (OD 450 nm)	0.4 ± 0.1	0.7 ± 0.1 *	0.4 ± 0.1	0.4 ± 0.1
CD4+ % of cells in spleen	53.7 ± 0.7	48.2 ± 1.7	53.3 ± 8.4	48.9 ± 1.6
CD8+ % of cells	16.3 ± 1.1	14.8 ± 1.1	12.9 ± 0.9	17.0 ± 1.3
CD4+CD25+ % of cells	2.1 ± 0.2	2.1 ± 0.2	1.4 ± 0.2	1.6 ± 0.1

Comparison between different agonists and vehicle were analyzed by ANOVA and post-hoc Bonferroni correction * p < 0.05 vs. vehicle.

4.1.8. Hypergammaglobulinaemia and DNA autoantibodies in MRLlpr/lpr mice

TLR signaling contributes to B cell activation and the production of selected autoantibodies in lupus [153]. Hence, we meticulously analyzed the effects of 3P-RNA and non-CpG-DNA on serum IgG levels and a number of common lupus autoantibodies. Consistent with its effect on spleen plasma cells only non-CpG-DNA significantly increased serum levels of total IgG including all isotypes and that of rheumatoid factor (Table 4). *Critidia luciliae* kinetoplast dsDNA binding was used to detect and quantify anti-dsDNA-IgG. A digital quantitative analysis of *Critidia luciliae* kinetoplast positivity revealed that both 3P-RNA-

and non-CpG-DNA-injected MRLlpr/lpr mice had little but statistically significant higher levels of anti-dsDNA-IgG as compared to vehicle controls (Figure 18A).

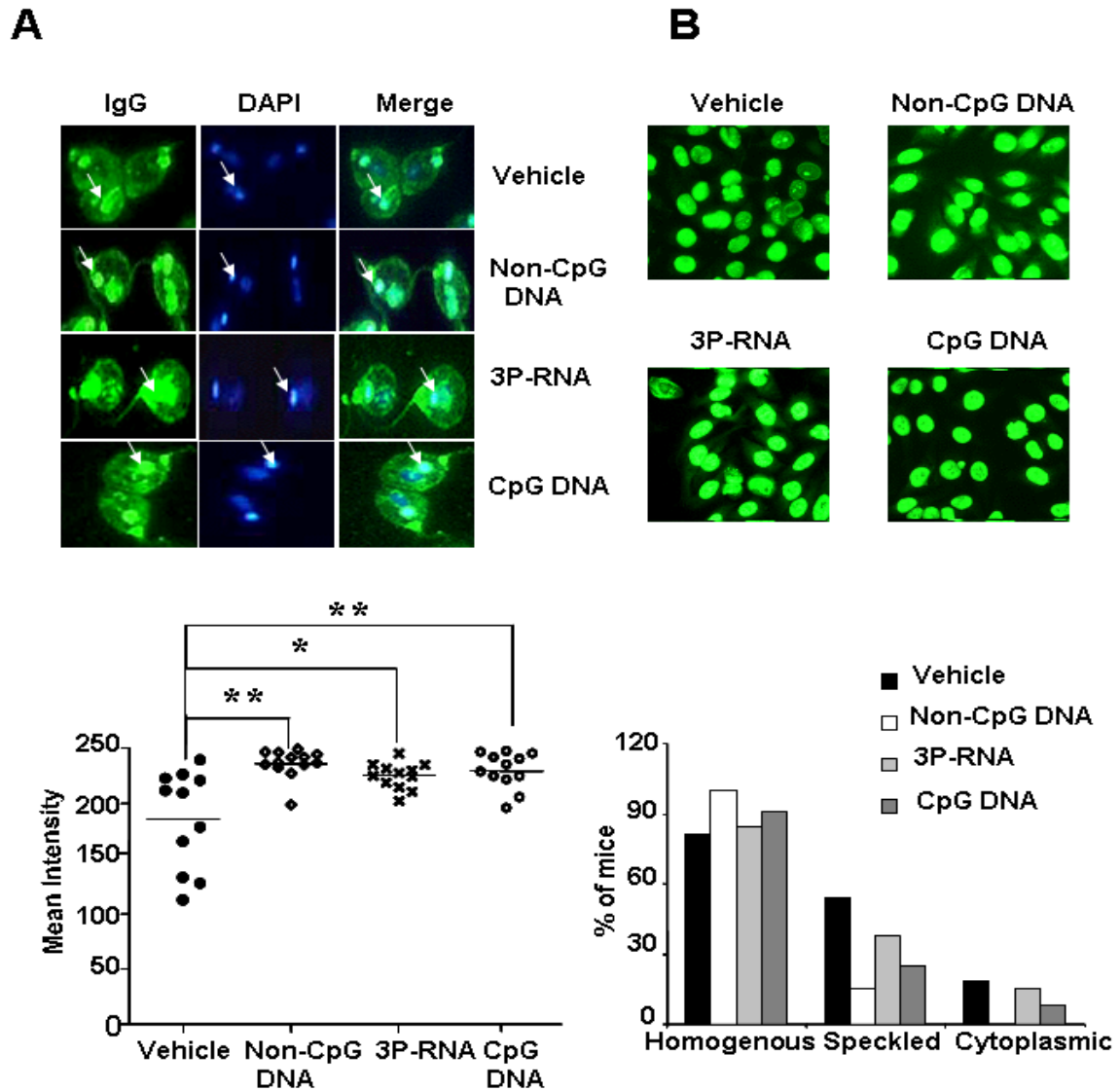


Figure 18. Lupus autoantibodies in MRLlpr/lpr mice. (A) Anti-dsDNA antibodies were assayed by binding to *Crithidia luciliae* kinetoplast dsDNA and were detected by immunofluorescence. IgG staining to *C. luciliae* dsDNA is shown in green (left), and DAPI staining of DNA is shown in blue (middle). White arrows indicate the kinetoplast. Specific anti-dsDNA antibodies are identified by colocalization of IgG and DAPI staining in the kinetoplast and appear in mixed colour (right). Specific anti-dsDNA staining of *C. luciliae* kinetoplasts mean intensity was shown in lower panel. Two-tailed Fisher's exact test was used for non-parametric analysis. * $p < 0.05$ vs vehicle. ** $p < 0.01$ vs. vehicle (B) Serum antinuclear antibodies were detected by Hep2 slide staining as described in methods. Staining patterns were classified as homogenous, speckled or cytoplasmic. Data shown on the right lower panel represent the staining pattern present in percent of mice of each group as indicated.

This was associated with increased homogenous ANA staining pattern on Hep2 cells (Figure 18B). Increased anti-dsDNA IgG antibodies were observed with both ligands also by ELISA (Table 4). 3P-RNA and non-CpG-DNA had no effect on serum levels of anti-Sm IgG (Table 4). Together, transient exposure to 3P-RNA and non-CpG-DNA both specifically enhanced the production of dsDNA autoantibodies but not anti-Sm IgG. Only non-CpG-DNA increases IgG and rheumatoid factor in sera of MRLlpr/lpr mice.

4.1.9. Renal inflammatory mediator mRNA expression in MRLlpr/lpr mice

We hypothesized that 3P-RNA and non-CpG-DNA would trigger the expression of proinflammatory mediators in kidneys of MRLlpr/lpr mice. 3P-RNA but not non-CpG-DNA induced IFN- α (Mx1) signaling in the kidney consistent with its effect in spleens of MRLlpr/lpr mice (Figure 19A). 3P-RNA but not non-CpG-DNA also induced TNF, IL-6, and CCL2 mRNA levels (Figure 19B). CpG-DNA induced a robust induction of TBX21 consistent with the Th1-like glomerular crescent formation seen in many sections. This was neither seen with 3P-RNA nor with non-CpG-DNA (Figure 19C). Also the CpG-DNA-induced a robust induction of RIG-I and MDA5 was not seen with 3P-RNA or non-CpG-DNA in kidney (Figure 19D). Together, exposure to 3P-RNA and non-CpG-DNA is associated with markedly lower changes in the renal expression of inflammatory mediators as observed with exposure to CpG-DNA.

4.1.10. Glomerular IgG and complement deposits in MRL lpr/lpr mice.

Higher levels of circulating dsDNA autoantibodies are usually associated with more severe immune complex-mediated renal injury. In fact, 3P-RNA and non-CpG-DNA both increased glomerular IgG and complement factor C3c staining as compared to control mice (Figures 20A and 20B, Table 5). Hence, increased glomerular IgG and C3c deposits were rather associated with the consistent effect of 3P-RNA and non-CpG-DNA on dsDNA autoantibody production than with hyperglobulinaemia which was selectively induced by non-CpG-DNA.

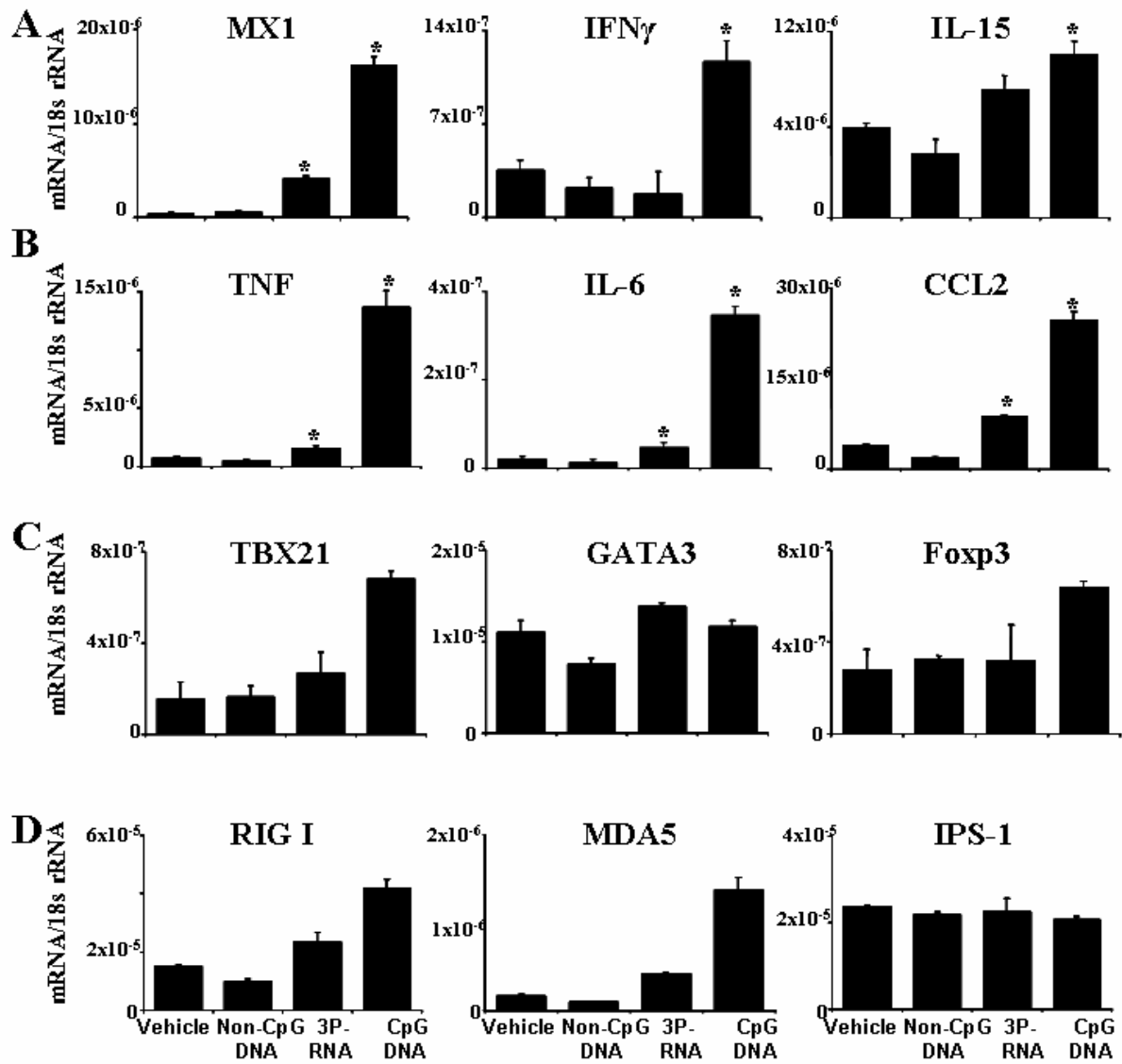


Figure 19. Renal mRNA expression of proinflammatory mediators and recognition molecules. Total kidney mRNA from 10 mice in each group was used for real-time RT-PCR. The primers for target mRNAs used are listed in methods. Data are expressed as means \pm SEM of the ratio from the target mRNA per respective 18s rRNA expression. * $p < 0.05$ vs Vehicle.

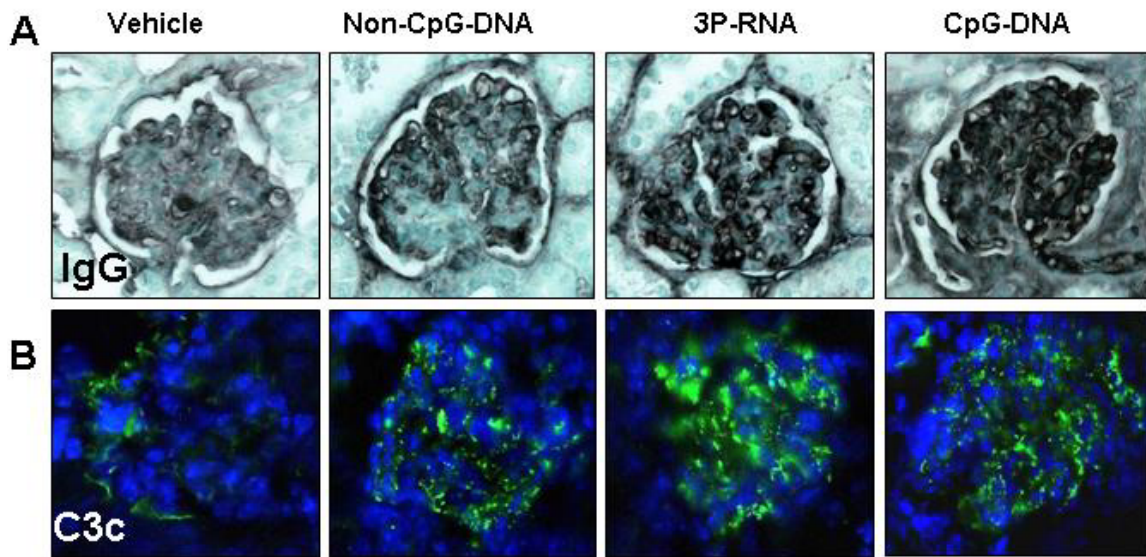


Figure 20. Glomerular immune complex deposits in kidneys of MRLlpr/lpr mice. (A): Immunostaining for total IgG was performed on paraffin-embedded renal sections from 18 week old MRLlpr/lpr mice of all groups. Original magnification x400. (B): Frozen sections of the same kidneys were used for immunostaining for complement factor C3 with a FITC labeled antibody (green). Cell nuclei are stained with DAPI (blue). Original magnification x400.

4.1.11. Kidney histopathology

From the above results one could predict that 3P-RNA and non-CpG-DNA also aggravate glomerular pathology, i.e. lupus nephritis, in MRLlpr/lpr mice. Control MRLlpr/lpr mice had diffuse proliferative glomerulonephritis with moderate mesangial hypercellularity, increase of mesangial matrix, and few periglomerular inflammatory cell infiltrates at week 18 (Figure 21). 3P-RNA and non-CpG-DNA injections both increased disease activity of lupus nephritis as evaluated by the histomorphological activity and chronicity scores for lupus nephritis (Figure 21 and Table 5). These effects were less severe and specifically were not associated with glomerular crescents or aggravated albuminuria as seen with CpG-DNA injections (Table 5). Aggravation of renal pathology was associated with some increase in the numbers of glomerular and interstitial macrophages and T cells (Figure 21), but again these effects were less prominent as with CpG-DNA. 3P-RNA also increased the number of Ki-67 positive proliferating cells in the renal interstitium but not in tubular

epithelial cells. Taken together, transient exposure to 3P-RNA and non-CpG-DNA aggravates immune complex disease and proliferative lupus nephritis in MRLlpr/lpr mice.

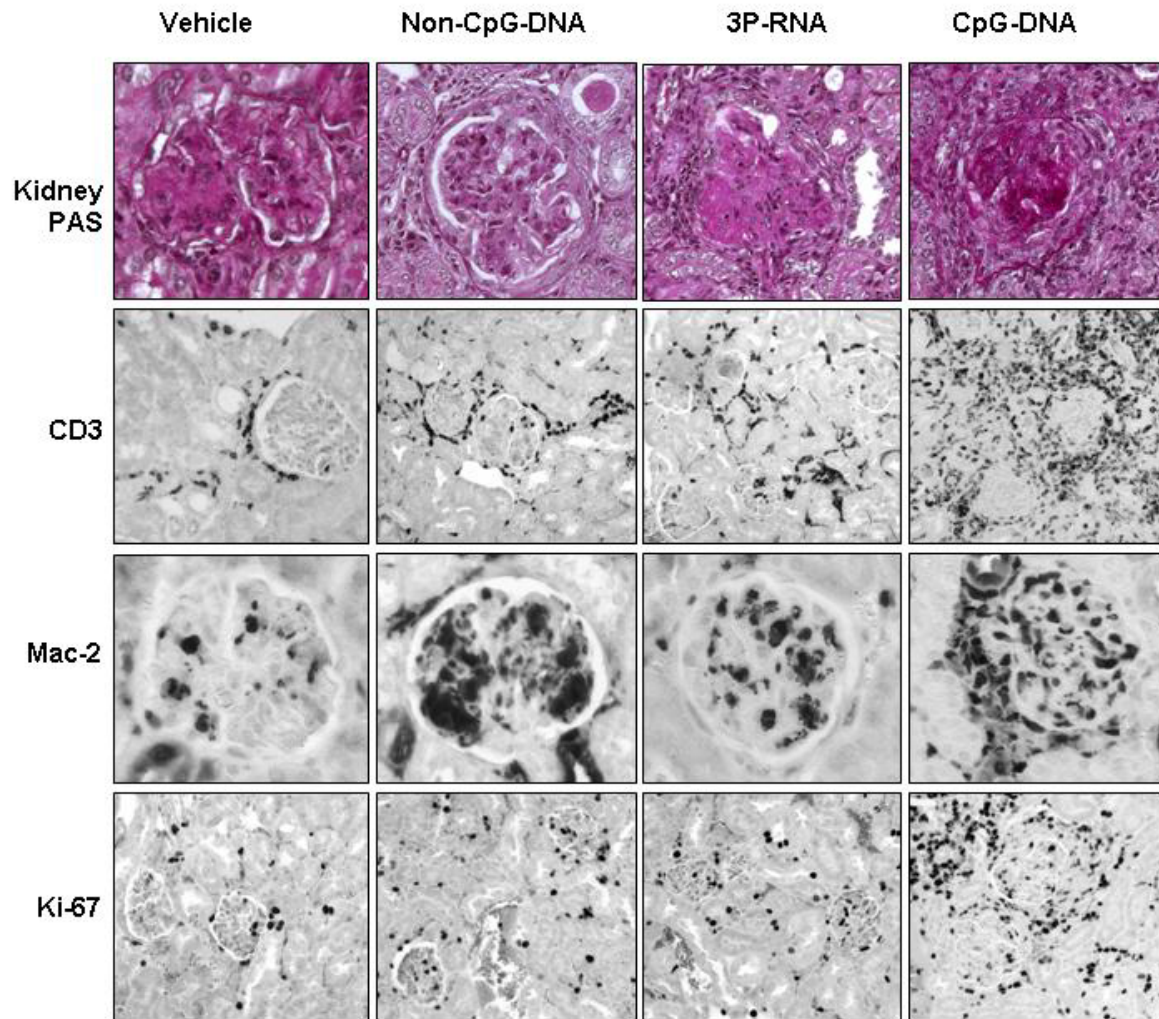


Figure 21. Histopathology of kidney MRLlpr/lpr mice. Paraffin-embedded lung sections were stained with PAS, CD3, Mac-2, and Ki-67 as indicated (original magnification x200-x400). Note that 3P-RNA, non-CpG-DNA and CpG-DNA treated MRLlpr/lpr mice show higher periglomerular and interstitial inflammatory cell infiltrates as compared to vehicle-treated MRLlpr/lpr mice.

Table 5. Parameters of lupus nephritis in 18 weeks old MRLlpr/lpr mice.

	Vehicle	Non –CpG-DNA	3P-RNA	CpG-DNA
Proteinuria (mg/mg)	33 ± 11	37 ± 14	67 ± 39	108 ± 55
Glom. deposit scores (0-3)				
IgG	1.2 ± 0.1	1.5 ± 0.1	1.9 ± 0.2	2.1 ± 0.2*
C3c	0.8 ± 0.1	1.5 ± 0.1*	1.8 ± 0.1*	1.8 ± 0.1*
Histological scores				
Activity index	6.3 ± 1.5	12.4 ± 2.0	11.0 ± 1.7	15.4 ± 1.7
Chronicity index	0.6 ± 0.5	2.5 ± 0.9	1.8 ± 0.6	3.6 ± 0.9
Cellular response [cells/glom. or hpf]				
Glom. Mac2+(cells/glom)	6.9 ± 0.9	8.5 ± 0.8	10.1 ± 0.9	15.3 ± 1.6*
CD3+ (cells/glom)	0.7 ± 0.1	1.4 ± 0.2	1.2 ± 0.2	2.2 ± 0.2*
Ki67+ (cells/glom)	2.3 ± 0.4	2.5 ± 0.2	2.1 ± 0.2	4.6 ± 0.2*
Interst. Mac2+ (cells/hpf)	8.0 ± 1.3	10.3 ± 1.0	17.4 ± 3.4	29.3 ± 4.6*
CD3+ (cells/hpf)	11.6 ± 1.8	16.0 ± 1.9	17.1 ± 3.0	34.6 ± 4.1*
Ki67+ (cells/hpf)	5.8 ± 1.4	6.9 ± 1.2	10.4 ± 1.6	35.3 ± 1.5*
Tubular Ki67+ (cells/hpf)	13.9 ± 3.1	12.5 ± 1.7	10.5 ± 1.4	40.2 ± 3.8*

* p < 0.05 versus vehicle.

4.1.12. Localization of 3P-RNA and non-CpG DNA in mice kidneys

TLR-independent recognition of viral nucleic acids is not restricted to immune cells [85, 99, 100], Hence, 3P-RNA and non-CpG-DNA might elicit local immunostimulatory effects in renal cells and infiltrating immune cells in addition to their systemic effects. To test this hypothesis we injected fluorescently labeled 3P-RNA and non-CpG-DNA into 18 weeks

old MRLlpr/lpr mice and harvested the kidney for fluorescence microscopy 2 hours later. Labeled 3P-RNA and non-CpG-DNA were both found in the kidney and colocalized with glomerular cells and tubular epithelial cells in a cytoplasmic staining pattern (Figures 22). Obviously, 3P-RNA and non-CpG-DNA localize to the cytosolic compartment of renal cells suggesting that they might elicit local effects in addition to their effects on autoimmunity.

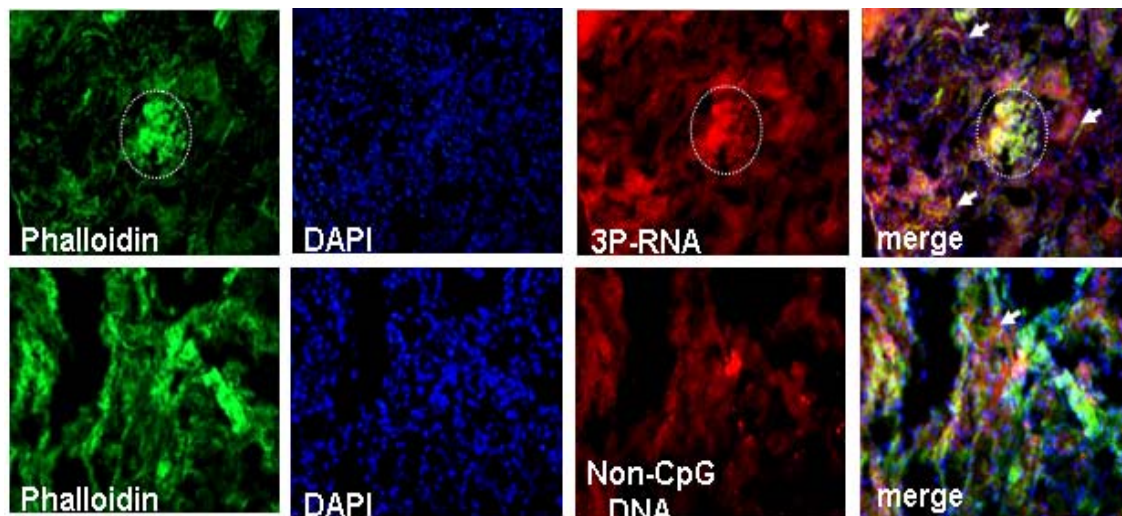


Figure 22. Distribution of 3P-RNA and non-CpG-DNA in kidneys of MRL lpr/lpr mice. Rhodamine-labeled 3P-RNA and non-CpG-DNA were intravenously injected into 16 week old MRLlpr/lpr mice. Renal tissue was harvested two hours later and frozen sections underwent fluorescence microscopy. Rhodamine-labeled nucleic acids appear in red. FITC phalloidin staining appears in green and DAPI-stained cell nuclei are blue. Glomeruli are encircled. Original magnification x200.

4.1.13. 3P-RNA and non-CpG-DNA injections induce interferon-related mediators in kidney glomeruli of C57BL/6 mice

Localization experiments showed that 3P-RNA and non-CpG-DNA interacting with glomerular cells. However, we do not know whether these ligands could induce cytokine production at the glomerular level. MRL lpr/lpr mice are already diseased mice and have systemic inflammation. So we injected C57BL/6 mice with either CL (Dotap), 30 μ g of 3P-RNA or 100 μ g of non-CpG-DNA in C67BL/6 mice on alternate days for three times. Glomeruli were isolated from kidney and mRNA expression profiles were determined by real time RT-PCR. 3P-RNA and non-CpG-DNA both induced the glomerular expression of

CXCL10/IP10, IFIT1, OASL2, ZC3HAV1, CCL2 and IL-6 (Figure 23). Thus, 3P-RNA and non-CpG-DNA injections induce multiple IFN-related mediators and cytokines in kidney glomeruli of C57BL/6 mice.

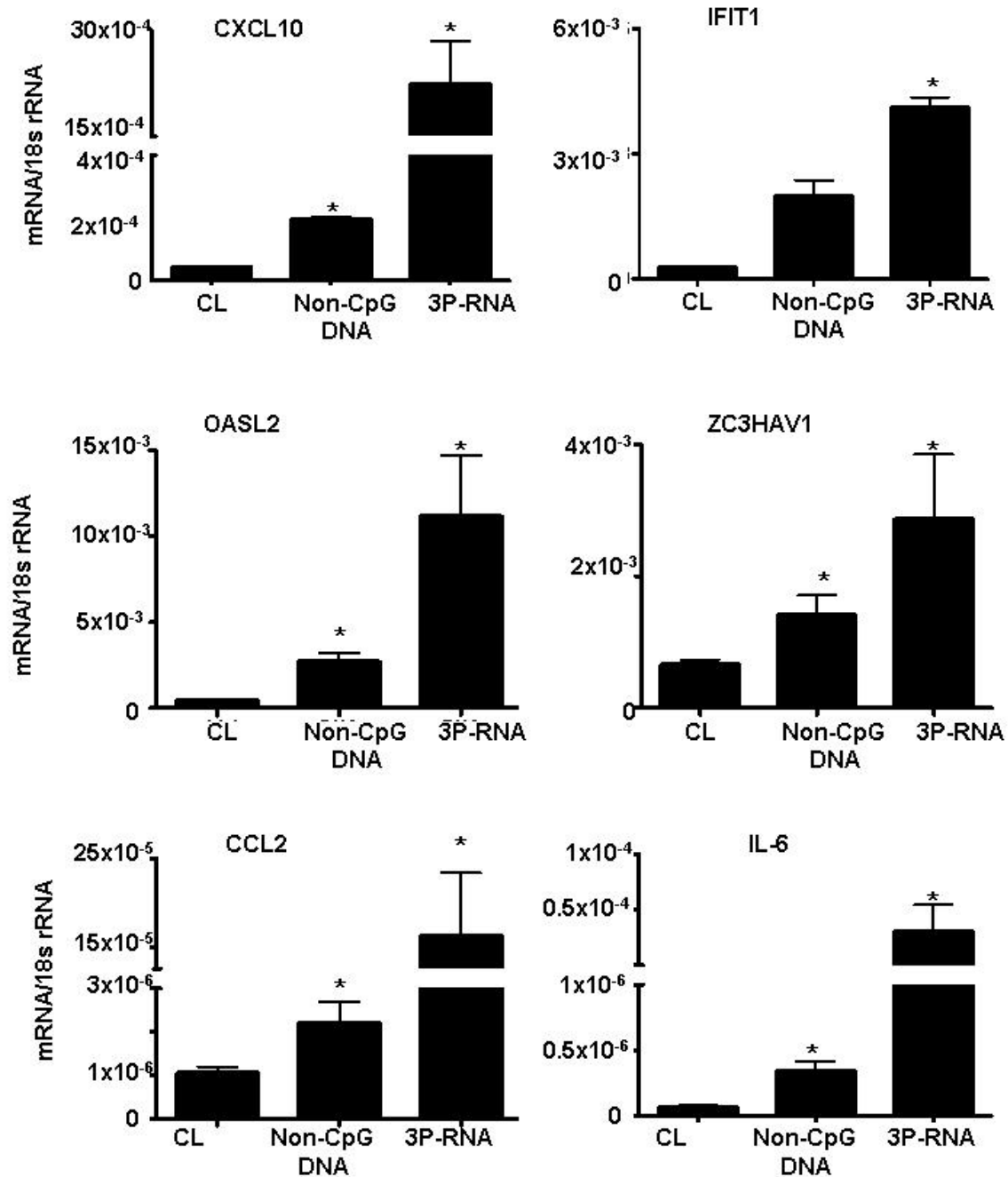


Figure 23. 3P-RNA and non-CpG-DNA induced interferon-related mediators in kidney glomeruli. C57BL/6 mice were injected 3 times on alternate days with CL, CpG-DNA dissolved in CL or 3P-RNA in CL (n=6), and glomerular RNA was isolated 12 hours after the last injection as described in methods. Data are means ± SD. * p<0.05 vs. CL.

4.1.14. Backbone chemistry of DNA affects their affinity to lupus autoantibodies

Phosphorothioate or phosphodiester backbones of synthetic CpG oligonucleotides were shown to modulate their binding affinity to DNA autoantibodies [148], hence, any differences the phenotype of non-CpG-DNA- or CpG-DNA-treated MRLlpr/lpr mice may be at least partially relate to this effect. We therefore assessed the binding affinities of serum IgG from MRLlpr/lpr or C57BL/6 mice to phosphodiester non-CpG-DNA and phosphorothioate CpG-DNA, respectively. Neither of the nucleic acids bound to serum IgG from C57BL/6 mice but all of them bound to serum IgG of MRLlpr/lpr mice. Binding affinity was strongest for phosphorothioate CpG-DNA particularly at lower concentrations (Figure 24). Binding affinity of phosphodiester non-CpG-DNA was less potent and was not much affected by complexing non-CpG-DNA to JetPEI (Figure 24). The lowest binding affinity was noted for mouse genomic DNA. However, at a concentration of 10 $\mu\text{g/ml}$ the binding affinity of all nucleic acid formats tested was almost identical. Thus, the backbone chemistry of DNA may affect their binding affinity to lupus autoantibodies at certain concentrations.

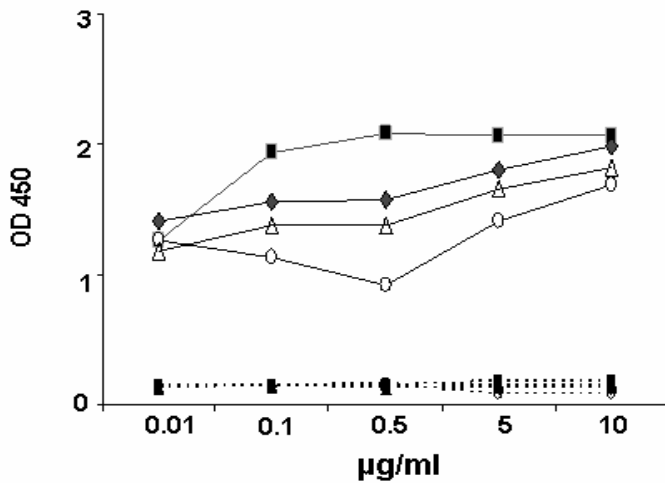


Figure 24. DNA autoantibody binding assay. Binding of MRLlpr/lpr and C57BL/6 serum to CpG, non-CpG-DNA, non-CpG-DNA complexed with JetPEI and mouse genomic DNA by ELISA. 1:100 dilutions of sera from MRLlpr/lpr or C57BL/6 mice were tested on CpG (black squares), non-CpG-DNA (black diamonds), non-CpG-DNA complexed with JetPEI (open triangles) and mouse genomic DNA (open circles) coated to polystyrene at concentrations indicated. The solid lines indicate MRLlpr/lpr mouse serum while the broken lines indicate sera from C57BL/6 mice.

4.2. Results part- II

Interaction of local glomerular cells with immune complexes, that contain viral nucleic acids might drive inflammation and further lead to glomerulonephritis. Mesangial cells are localized in side glomeruli and play an important role in glomerulonephritis. So we hypothesized that 3P-RNA and non-CpG-DNA could directly activate mesangial cells and release inflammatory cytokines. Furthermore we analysed gene expression profiles induced by 3P-RNA and non-CpG-DNA in mesangial cells.

4.2.1 Characterization of mesangial cells

Primary mesangial cells (pMC) were prepared from C57BL/6 mice and after five passages, immunostaining was performed either with phalloidin or cytokeratin 18 or alpha-smooth muscle actin (SMA) to check purity of pMC. pMC were >99% positive for smooth muscle actin and >99% were negative for cytokeratin 18 (Figure 25) .

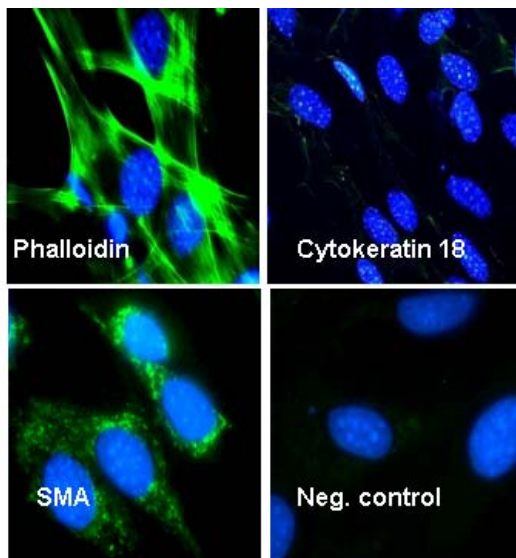


Figure 25. Immunostaining of primary mesangial cells. Immunostaining was performed for pMC either with phalloidin or cytokeratin 18 or alpha-smooth muscle actin (SMA). Original magnification x1000.

4.2.2. Mesangial cells express nucleic acid-specific pattern recognition molecules

Primary mesangial cells mRNA expression was determined by the RT-PCR for the nucleic acid-specific pattern recognition molecules TLR-3, -7, -8, -9, Rig-1, Mda5, Dai, and Mavs

(IPS). Under basal culture conditions pMC expressed Rig-1 and Mavs but not TLR-3, -7, -8, 9, Dai or Mda5 mRNA (Figure 26). Prestimulation with IFN- β induced TLR3, Dai, Rig-1, and Mda5 mRNA but suppressed Mavs mRNA expression.

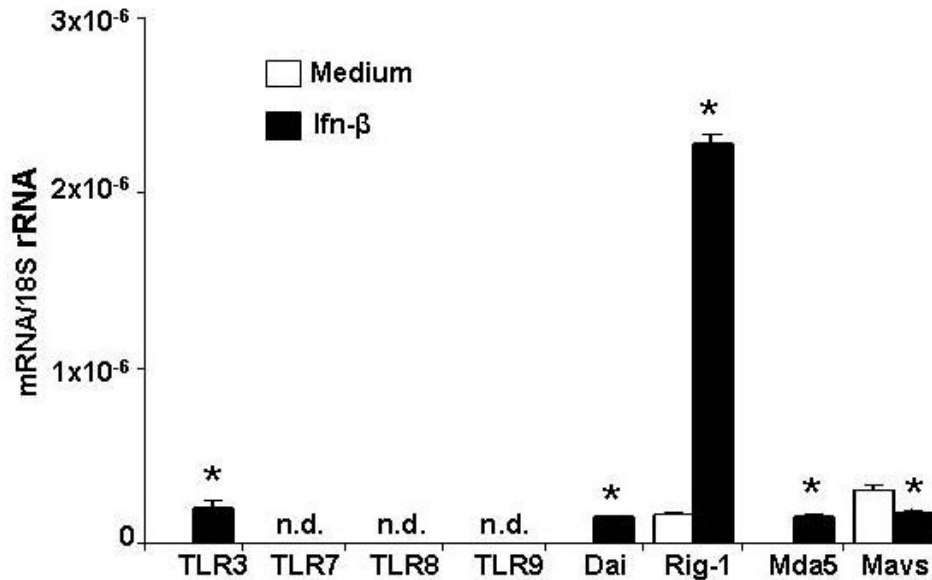


Figure 26. IFN- β induces TLR3, Dai, Rig-1, and Mda5 mRNA in primary mesangial cells. Total RNA was isolated from pMC after 6 hours exposure to medium or 2000u IFN- β . Real-time RT-PCR data for TLR3, TLR7, TLR8, TLR9, Dai, Rig-1, Mda5, and Mavs mRNA are expressed as per respective 18S rRNA expression. Data are means \pm SD from three experiments each analyzed in duplicates. N.d. = not detectable. * $p < 0.05$ vs. medium.

4.2.3. Cationic lipid enhances the uptake of non-CpG-DNA and 3P-RNA in mesangial cells.

In dendritic cells and embryonic fibroblasts 3P-RNA and non-CpG-DNA needs to be transfected with CL to reach the intracellular cytosol, for their activation and release of cytokines, chemokines or interferons [87, 101]. Consistently, rhodamine-labeled 3P-RNA or non-CpG-DNA was hardly detectable in the intracellular cytosol of pMC unless being complexed with CL as assessed by confocal microscopy (Figure 27).

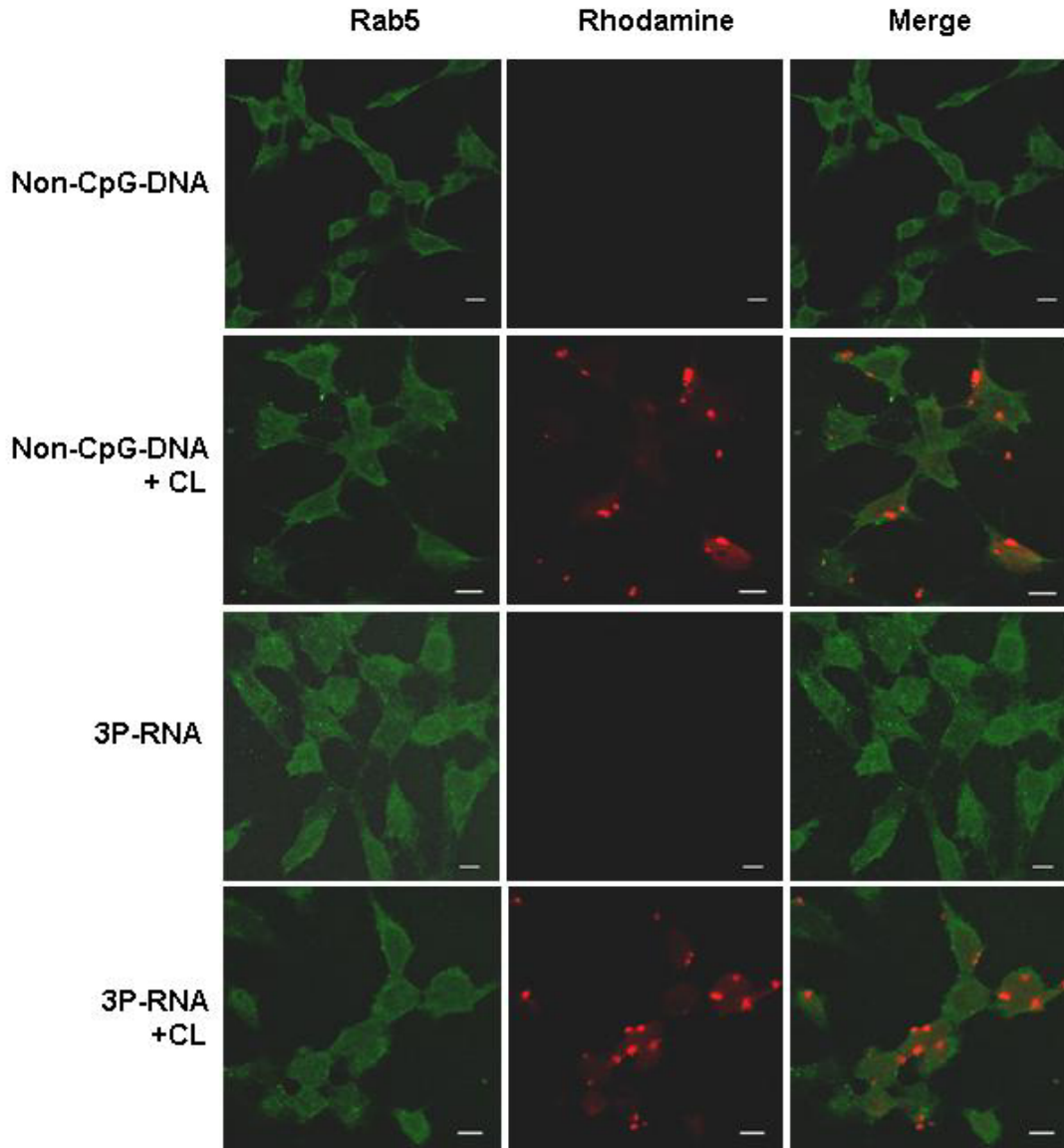


Figure 27. Cationic lipid enhances the uptake of non-CpG-DNA and 3P-RNA in mesangial cells. PMC were exposed to either 1 μ g of rhodamine-labeled 3P-RNA or 5 μ g rhodamine-labeled non-CpG-DNA in the presence or absence of cationic lipid (CL) for 2 hours. Intracellular uptake was detected by confocal microscopy and appears as red staining inside of MC. FITC-labeled anti-Rab5 was used to mark early endosomes of MC and appears as green staining. Note that the intracellular uptake strongly increased when 3P-RNA or non-CpG-DNA were complexed with CL. Images are representative for 3 independent experiments. Original magnification x400, scale bar = 10 μ m.

4.2.4. 3P-RNA and non-CpG-DNA activates pMC to produce IL-6

In the cytosol 3P-RNA and non-CpG-DNA should be able to access their respective recognition receptors and activate pMC. In fact, 3P-RNA and non-CpG-DNA both induced pMC to produce IL-6 in a dose-dependent manner, only when being complexed with CL

(Figure 28A). Pretreatment with either RNase or DNase drastically reduced the release of IL-6, which was induced by 3P-RNA and non-CpG-DNA, respectively. This indicates that the immunostimulatory effect of these complexes derives from specifically their RNA or DNA content only (Figure 28B).

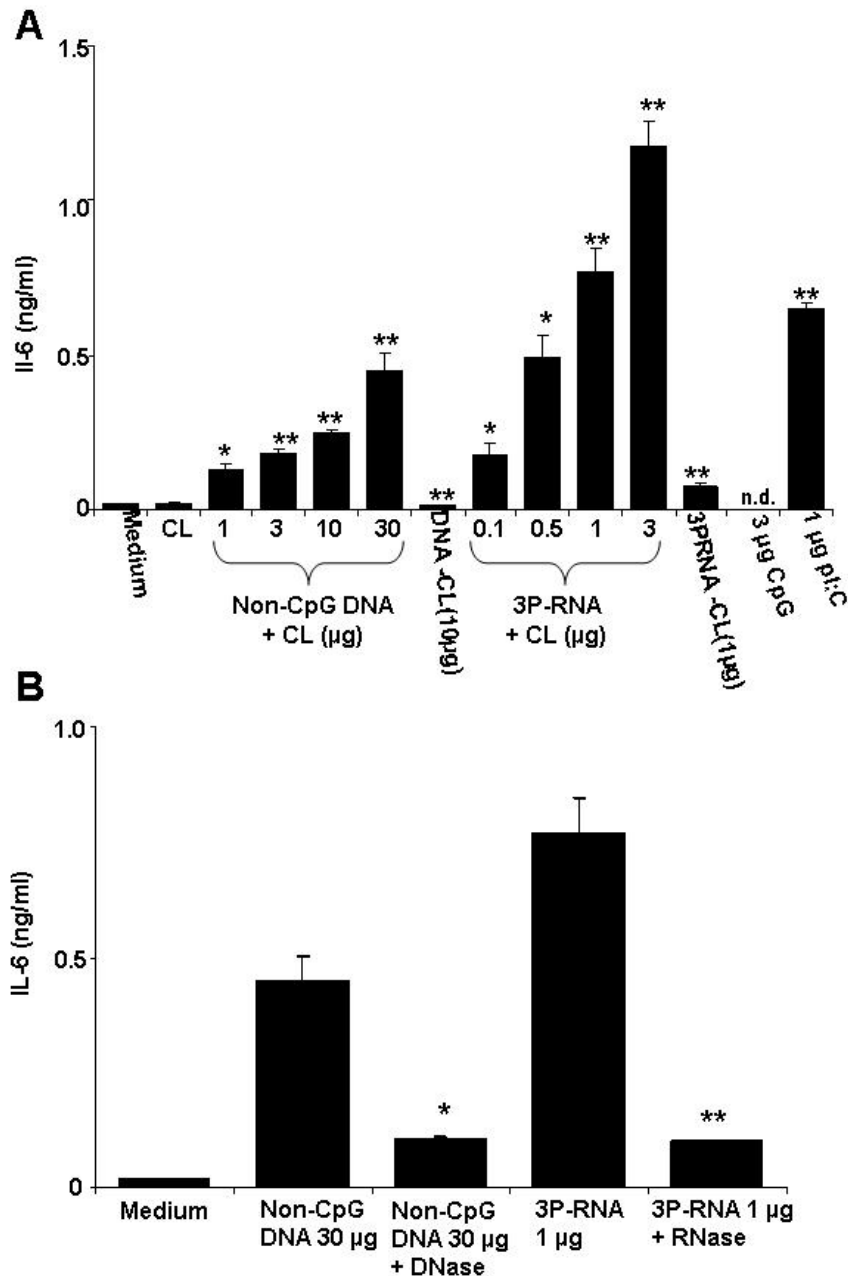


Figure 28. 3P-RNA and non-CpG-DNA induce IL-6 release in mesangial cells. (A): Primary mesangial cells were stimulated with increasing doses of 3P-RNA/CL and non-CpG-DNA/CL complexes. The highest doses were also tested in the absence of CL (-CL). PolyI: PolyC (pI:C) RNA and CpG oligodeoxynucleotide 1668 were used as positive and negative controls, respectively. (B): In similar experiments 3P-RNA/CL and non-CpG-DNA/CL were preincubated with either RNase or DNase. Supernatants were harvested after 24 hours and analyzed by IL-6 ELISA. Data represent means \pm SD. * $p < 0.05$ vs. medium, ** $p < 0.01$ vs. medium.

4.2.5. 3P-RNA and non-CpG-DNA activate pMC through TLR-independent pathway

Most TLRs except TLR3 signal through MyD88 adaptor protein, while TLR3 depends on Trif. Consistent with multiple previous studies in other cell types 3P-RNA and non-CpG-DNA activated pMC via TLR-independent pathways because pMC prepared either from MyD88-deficient, Trif-mutant or wild-type mice showed comparable CXCL10, IL-6 and CCL5 induction upon 3P-RNA and non-CpG-DNA stimulation (Figure 29).

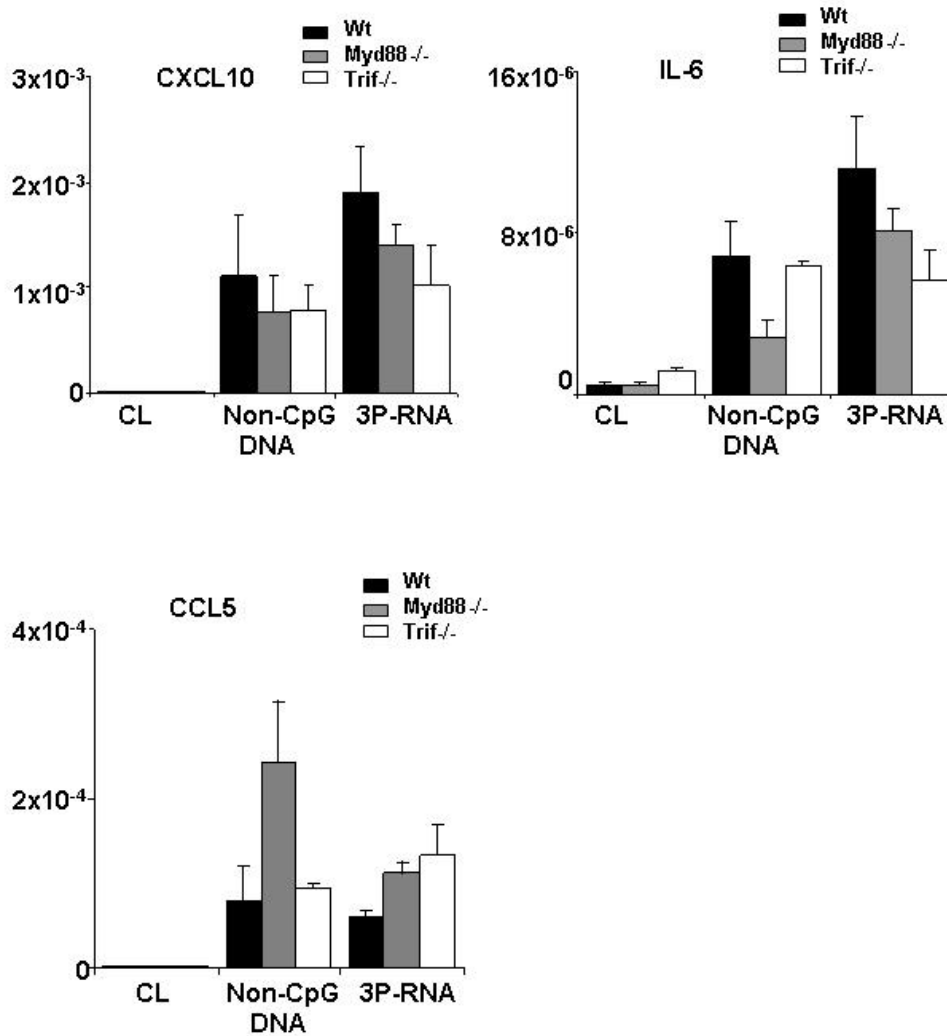


Figure 29 TLR-independent pathway signaling. MyD88^{-/-}, Trif mutant and WT pMC mRNA was isolated after 6 hours exposure to 3P-RNA/CL or non-CpG-DNA/CL. Real-time RT-PCR was performed for the indicated targets as described in methods. Data are expressed per respective 18S rRNA expression and represent means \pm SD from three experiments each analyzed in duplicates.

4.2.6. Rig-1 mediates 3P-RNA- but not non-CpG-DNA-induced activation of mesangial cells

The recognition of 3P-RNA was reported to involve Rig-1 in dendritic cells [87], hence, Rig-1-specific siRNA studies were carried out to confirm the role of Rig-1 for 3P-RNA recognition in mesangial cells. Rig-1-specific siRNA significantly suppressed Rig-1 mRNA levels and protein levels (Figure 30A) and largely prevented IL-6 or CXCL10 mRNA expression and protein secretion in MC upon exposure to 3P-RNA (Figure 30B and C). The 3P-RNA-induced cytokine release was not completely prevented by Rig-1 siRNA which may either relate to other contributing signaling pathways or to the technically incomplete knock down of Rig-1. By contrast, knock down of Rig-1 did not significantly impair the non-CpG-DNA-induced expression of CXCL10 mRNA in MC and had no effect on CXCL10 release of MC (Figure 30 D and E). Suppression of Rig-1 somewhat reduced the non-CpG DNA-induced expression of IL-6 mRNA at 6 hours but this did not translate to the protein level during 24 hours of stimulation (Figure 30 D and E). These data show that Rig-1 mediates 3P-RNA but not non-CpG-DNA-induced activation MC cells.

4.2.7 Dai contributes to 3P-RNA but not to non-CpG-DNA induced activation of mesangial cells

Dai has been suggested to mediate the recognition of double-stranded B-DNA in *in vitro* [105]. But a recent study reported that mouse embryonic fibroblasts and bone marrow-derived dendritic cells from Dai knockdown mice showed considerable response to B-DNA compared with wild type cells [106]. To test whether Dai is involving in recognition of 3P-RNA and non-CpG-DNA in MC, Dai-specific siRNA studies were carried out. Dai-specific siRNA effectively suppressed Dai mRNA levels in MC (Figure 31A). However, non-CpG-DNA-induced CXCL10 or IL-6 mRNA expression and protein release was independent of Dai (Figure 31B and C). Interestingly, suppression of Dai significantly reduced the 3P-RNA-induced expression of CXCL10 and IL-6 mRNA and protein release in MC (Figure 31D and E). Thus, Dai contributes to 3P-RNA but not to non-CpG-DNA-induced activation of MC.

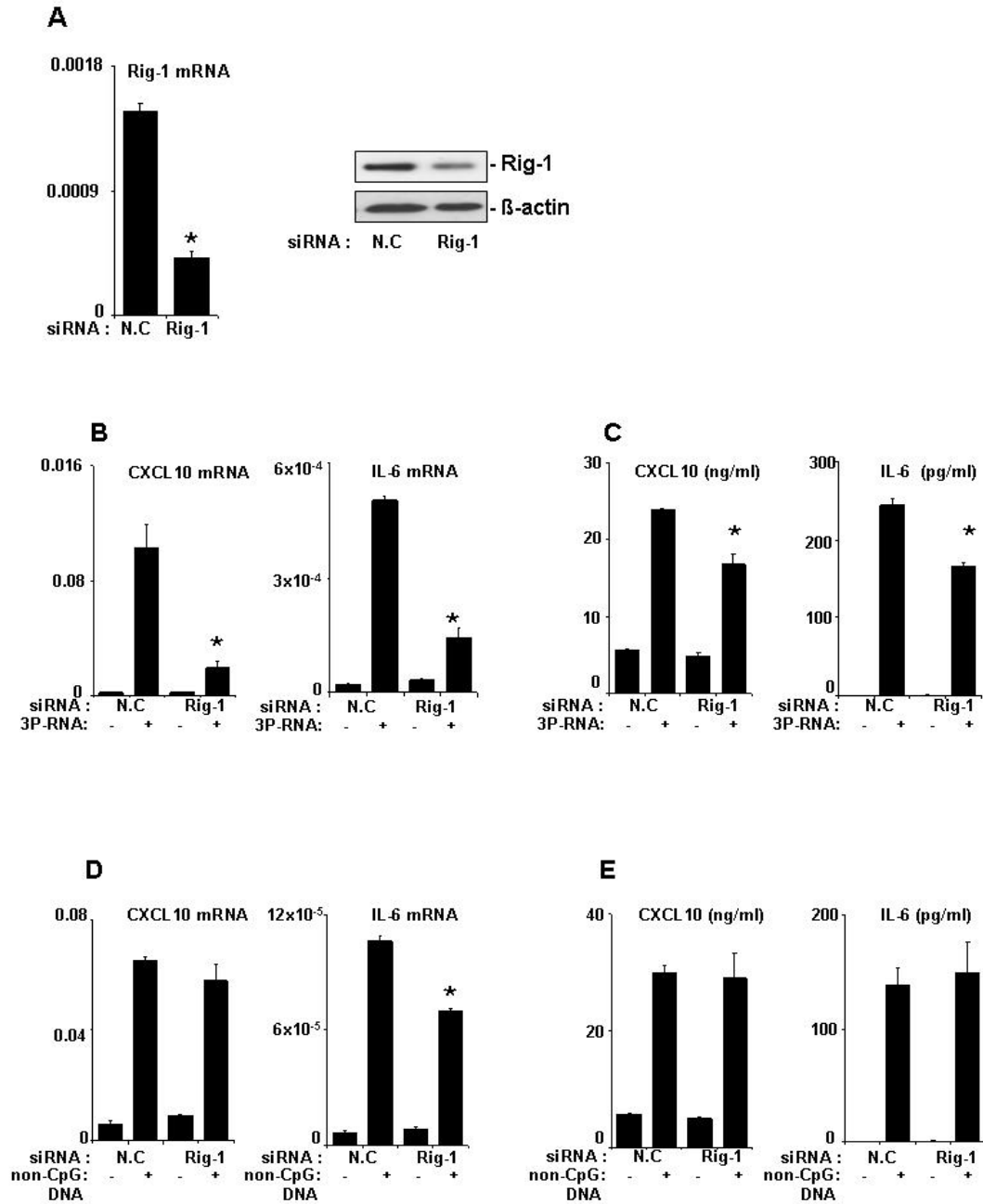


Figure 30. Rig-1 siRNA studies in mesangial cells. (A): MMC were transfected with Rig-1-specific siRNA or non-specific control siRNA and subjected to real-time RT-PCR and Western blotting to evaluate the expression of Rig-1. (B) The mRNA expression of CXCL10 and IL-6 in siRNA treated MMC was measured by real-time RT-PCR after 6 hours treatment with 3P-RNA. (C) CXCL10 and IL-6 protein levels were measured by ELISA in siRNA-treated MMC after 24 hours treatment with 3P-RNA. (D) and (E) mRNA expression and protein levels of CXCL10 and IL-6 were measured by real-time RT-PCR and ELISA, respectively, after treatment with non-CpG-DNA. All RT-PCR data was expressed as per respective 18S rRNA expression. Data are means \pm SD from three experiments each analyzed in duplicate. * $p < 0.05$ Rig-1 siRNA vs. non-specific control RNA.

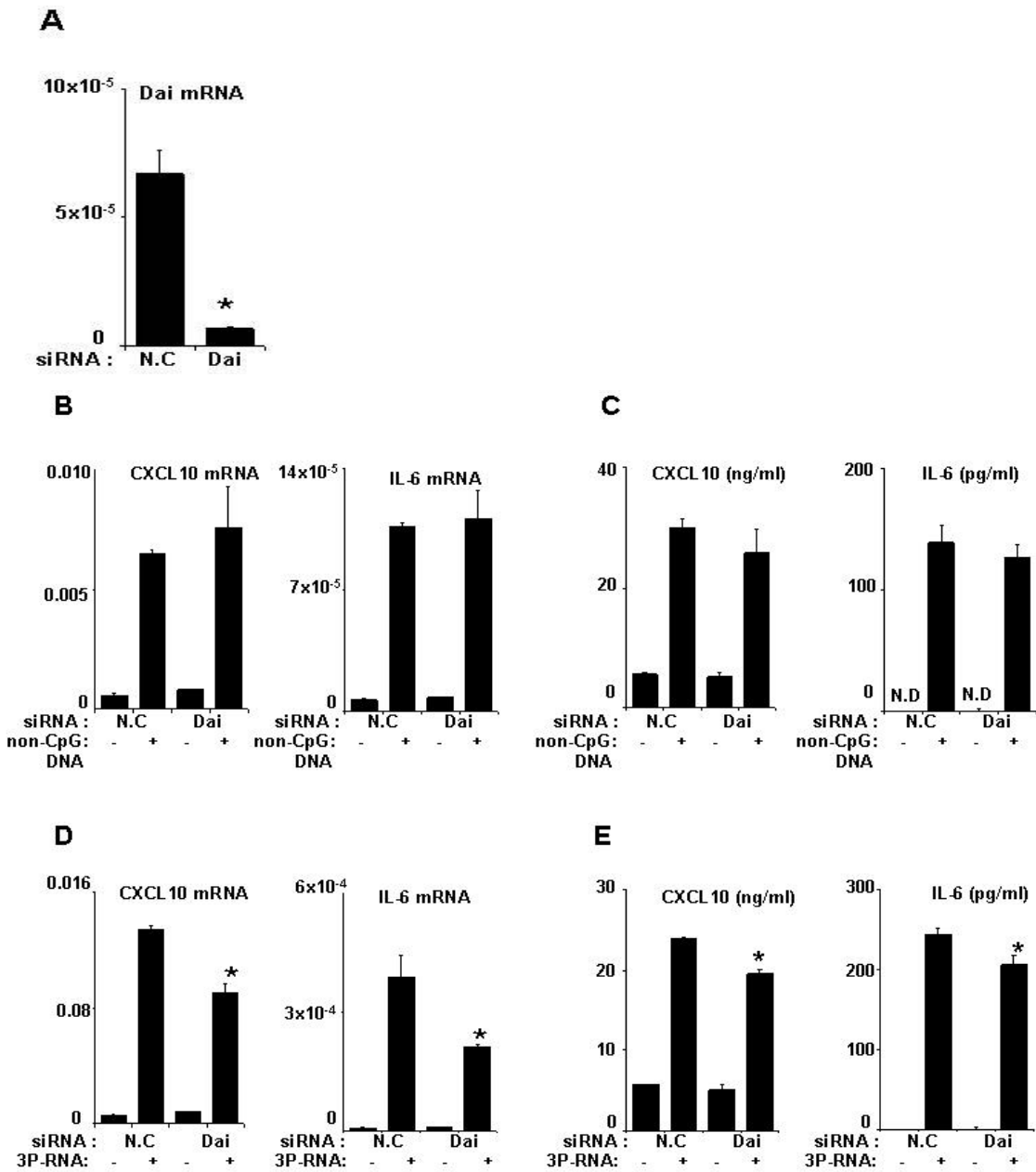


Figure 31. Dai siRNA studies in mesangial cells. (A): MMC were transfected with Dai (Zbp1) specific siRNA or non-specific control siRNA and subjected real-time RT-PCR to evaluate the expression of Dai. (B): The mRNA expression of CXCL10 and IL-6 in siRNA-treated MMC was measured by real-time RT-PCR after 6 hours treatment with non-CpG-DNA. (C) CXCL10 and IL-6 protein levels were measured by ELISA in supernatants of siRNA-treated MMC after 24 hours treatment with non-CpG-DNA. (D) and (E) mRNA expression and protein levels of CXCL10 and IL-6 were measured by real-time RT-PCR and ELISA, respectively, after treatment with 3P-RNA. All RT-PCR data are expressed as per respective 18S rRNA expression. Data are means \pm SD from three experiments each analyzed in duplicate. * $p < 0.05$ Dai siRNA vs. non-specific control RNA.

4.2.8. 3P-RNA and non-CpG-DNA both activate interferon-regulated factor-3 in mesangial cells

Innate RNA and DNA recognition receptors can specifically activate a group of transcription factors called the interferon regulatory factors (IRF) [154]. To check this concept nuclear extracts were isolated from MC after stimulating them with 3P-RNA or non-CpG-DNA for 2 hours. 3P-RNA and non-CpG-DNA both increased the phosphorylation of IRF3 suggesting that despite different recognition machineries 3P-RNA and non-CpG-DNA both share IRF3 as a transcription factor to induce gene expression in glomerular MC (Figure 32).

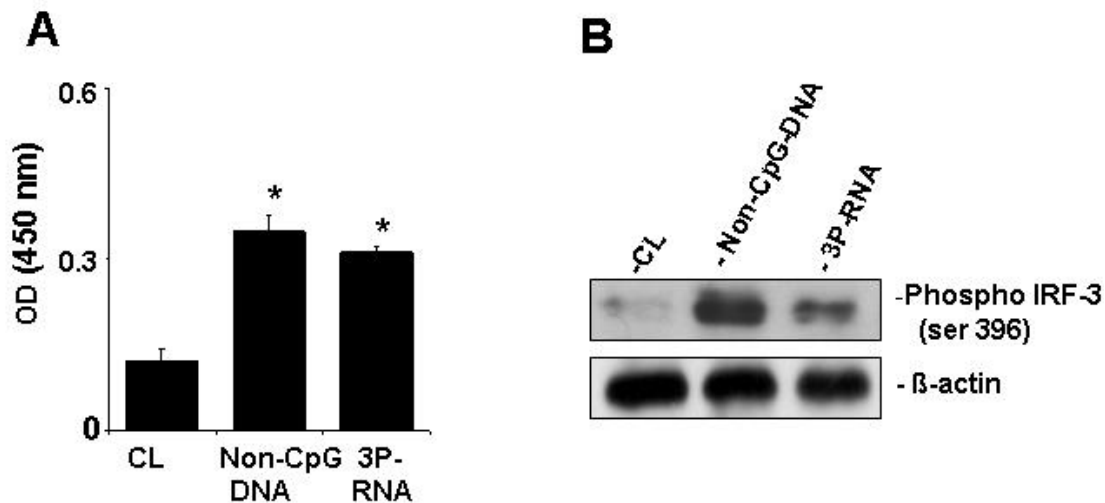


Figure 32. IRF3 activation in 3P-RNA- and non-CpG-DNA-stimulated mesangial cells. MMC were stimulated with 3P-RNA/ CL and non-CpG-DNA/CL complexes. Nuclear extracts were harvested after 2 hours and analyzed for phosphorylated Irf3 by ELISA and Western blotting. Data represent means \pm SD. * $p < 0.05$ vs. CL

4.2.9 Unique but overlapping gene-expression program triggered by 3P-RNA and non-CpG-DNA in MC

Shared IRF3 phosphorylation would propose that 3P-RNA and non-CpG-DNA induce similar rather than different gene expression patterns in MC. Microarray experiments were carried out with Affymetrix mouse genome 430 2.0 array to characterize the pMC mRNA expression profiles upon stimulation with complexes of 0.5 μ g/ml 3P-RNA/CL and 30

$\mu\text{g/ml}$ non-CpG-DNA/CL, two doses that stimulated pMC to secrete comparable levels of Il-6 within 24 hours of stimulation (Figure 28A). A large number of genes were found to be coinduced by 3P-RNA/CL and non-CpG-DNA/CL (Figure 33), the 30 most coinduced genes are listed in table 7. Some genes are specific to either 3P-RNA or non-CpG-DNA (Table 6).

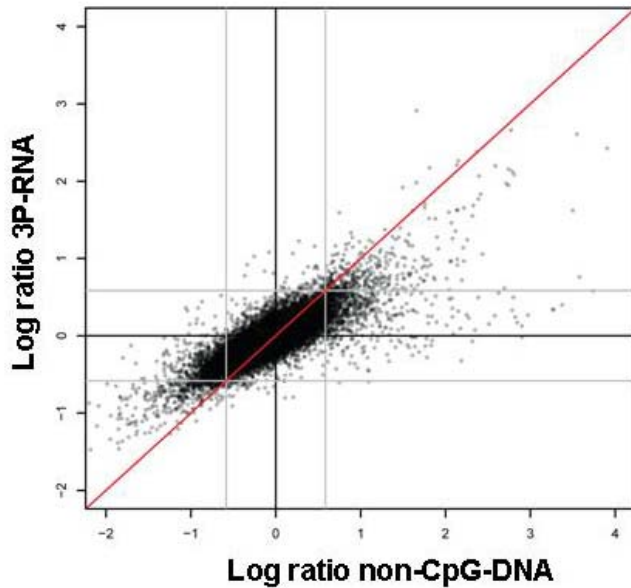


Figure 33. Microarray analysis comparing the 3P-RNA and non-CpG-DNA induced response pMC were stimulated for 6 hr with 3P-RNA or non-CpG-DNA and total RNA was prepared for microarray analysis. For all expressed genes, the change relative to untreated cells after 3P-RNA (y axis) or non-CpG-DNA (x axis) stimulation is plotted in log₂ format. Data are from one of three independent experiments.

Table 6. Genes induced by 3P-RNA and non-CpG-DNA in mesangial cells.

Gene name	Affymetrix ID	Fold change non-CpG-DNA	Fold change 3P-RNA
Ifit1	1450783_at	199	14.5
Cxcl10	1418930_at	61.7	4.4
Amphiregulin	1421134_at	52.7	11.6
Usp18	1418191_at	52.4	2.2
Isg15	1431591_s_at	34.6	3.2
Il-6	1450297_at	25.2	14.1
Ccl5	1418126_at	19.9	4.6
Epiregulin	1419431_at	14.9	5.3
Ptgs2	1417263_at	7.0	4.2
Hmox1	1448239_at	6.8	6.3
Stanniocalcin 1	1450448_at	5.2	4.1
Nr4a2	1447863_s_at	5.1	5.2
Ccl2	1420380_at	4.4	3.0
Ccl7	1421228_at	4.2	2.7
Zfp36	1452519_a_at	3.6	1.6
Poliovirus receptor	1423905_at	3.3	2.0
Dio2	1418937_at	3.1	7.5
Mmp13	1417256_at	3.1	3.9
Csf2	1427429_at	3.4	1.8
Mcpt8	1449965_at	2.6	1.8
Hmga2	1450781_at	2.5	1.7
Il-1rl1	1425145_at	2.5	2.1
Cd44 antigen	1452483_a_at	2.3	2.1
Cebpb	1427844_a_at	2.5	2.4
Ccl17	1419413_at	2.2	1.5
IFrd1	1416067_at	2.2	1.5
Bcl6	1421818_at	2.0	1.6

4.2.10 3P-RNA and non-CpG-DNA trigger proinflammatory cytokines in mesangial cells

The Affymetrix gene array analysis revealed that the genes strongly coinduced by 3P-RNA/CL and non-CpG-DNA/CL included IL-6 as well as multiple proinflammatory CC- and CXC chemokines, i.e. CXCL10, CCL5, CCL2 and CCL17 (Table6).

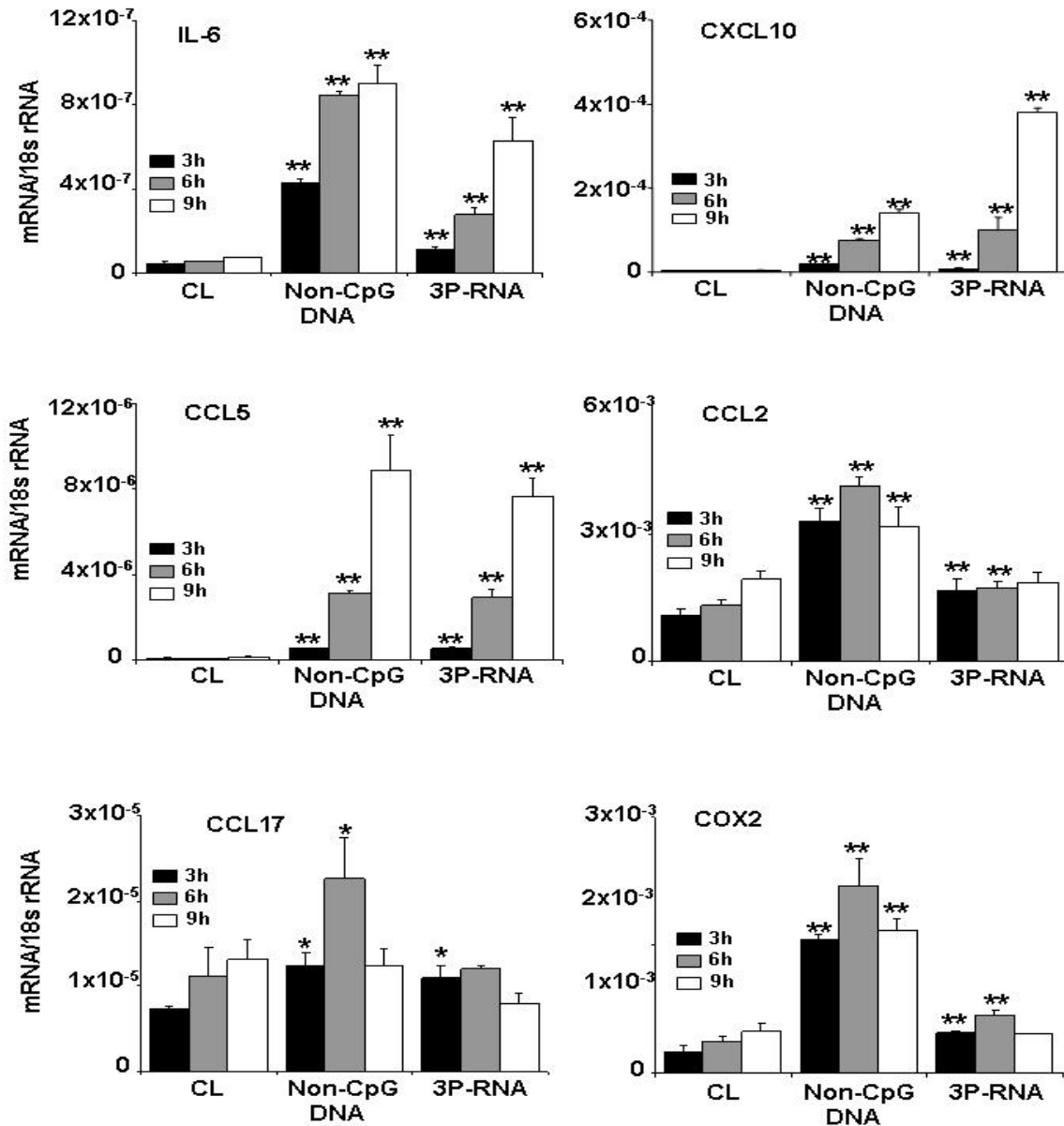


Figure 34. 3P-RNA and non-CpG-DNA trigger proinflammatory cytokines and chemokines in mesangial cells. pMC mRNA was isolated 3, 6, and 9 hours after exposure to 3P-RNA/CL or non-CpG-DNA/CL. Real-time RT-PCR was performed for the indicated targets as described in methods. Data are expressed per respective 18S rRNA expression and represent means \pm SD from three experiments each analyzed in duplicates. * p < 0.05 vs. CL, ** p < 0.01 vs. CL.

We confirmed the induction of these factors as well as that of COX2/Ptgs2 in pMC at 3, 6 and 9 hours of 3P-RNA/CL or non-CpG-DNA/CL stimulation by real time RT-PCR (Figure 34). Real-time PCR also revealed that 3P-RNA and non-CpG-DNA induced these genes to a more similar extent as suggested by the microarray analysis. We also used real-time RT-PCR to confirm that 3P-RNA/CL and non-CpG-DNA/CL did not induce IL-1- β , IL-2, TNF- α , TGF- β , and Hif-1 α in pMC as suggested by the Affymetrix gene array. Do these mRNA expression data translate to the protein level? 3P-RNA/CL and non-CpG-DNA/CL both induced pMC to secrete IL-6, CCL5, and CXCL10 within 24 hours in pMC (Figure 35). Together, these data show that 3P-RNA and non-CpG-DNA stimulate MC to produce multiple proinflammatory cytokines and chemokines.

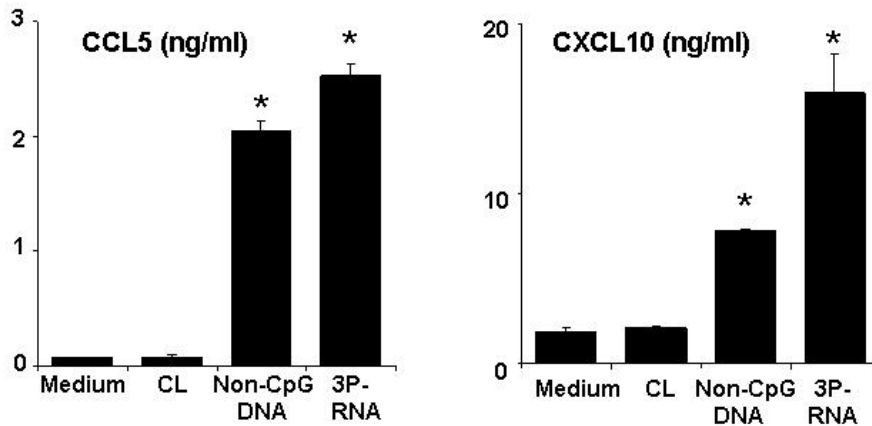


Figure. 35. 3P-RNA and non-CpG DNA trigger CCL5 and CXCL10 mesangial cells. Cell supernatants were harvested from MC after 24 hours of stimulation 3P-RNA and non-CpG-DNA and analyzed by ELISA for Ccl5 and Cxcl10. Data are means \pm SD from three experiments each analyzed in duplicates.* $p < 0.05$ vs. medium.

4.2.11 3P-RNA and non-CpG-DNA trigger type I interferon and interferon-related mediators in mesangial cells

The gene array analysis suggested that many of the genes induced by both 3P-RNA/CL and non-CpG-DNA/CL relate to the type I IFN signaling cascade (Table 6). Real-time RT-PCR was used to confirm the induction for several of these antiviral molecules at 3, 6, and 9 hours of stimulation in pMC. For example, the translation regulator IFN-induced protein with tetratricopeptide repeats (IFIT)-1, the nuclear GTPase myxovirus resistance (MX)-1, and the nuclear RNaseL activator 2',5'-oligoadenylate synthetase-like 2 (OASL2) were all

induced like IFN- β mRNA (Figure 36). Later the production of IFN- α and IFN- β were confirmed by ELISA in pMC supernatants 24 hours after stimulation with 3P-RNA/CL or non-CpG-DNA/CL (Figure 37). Together, these data show that 3P-RNA and non-CpG-DNA stimulate MC to produce IFN- α and IFN- β as well as other IFN-induced genes like MX-1, OASL2, and IFIT1 proteins.

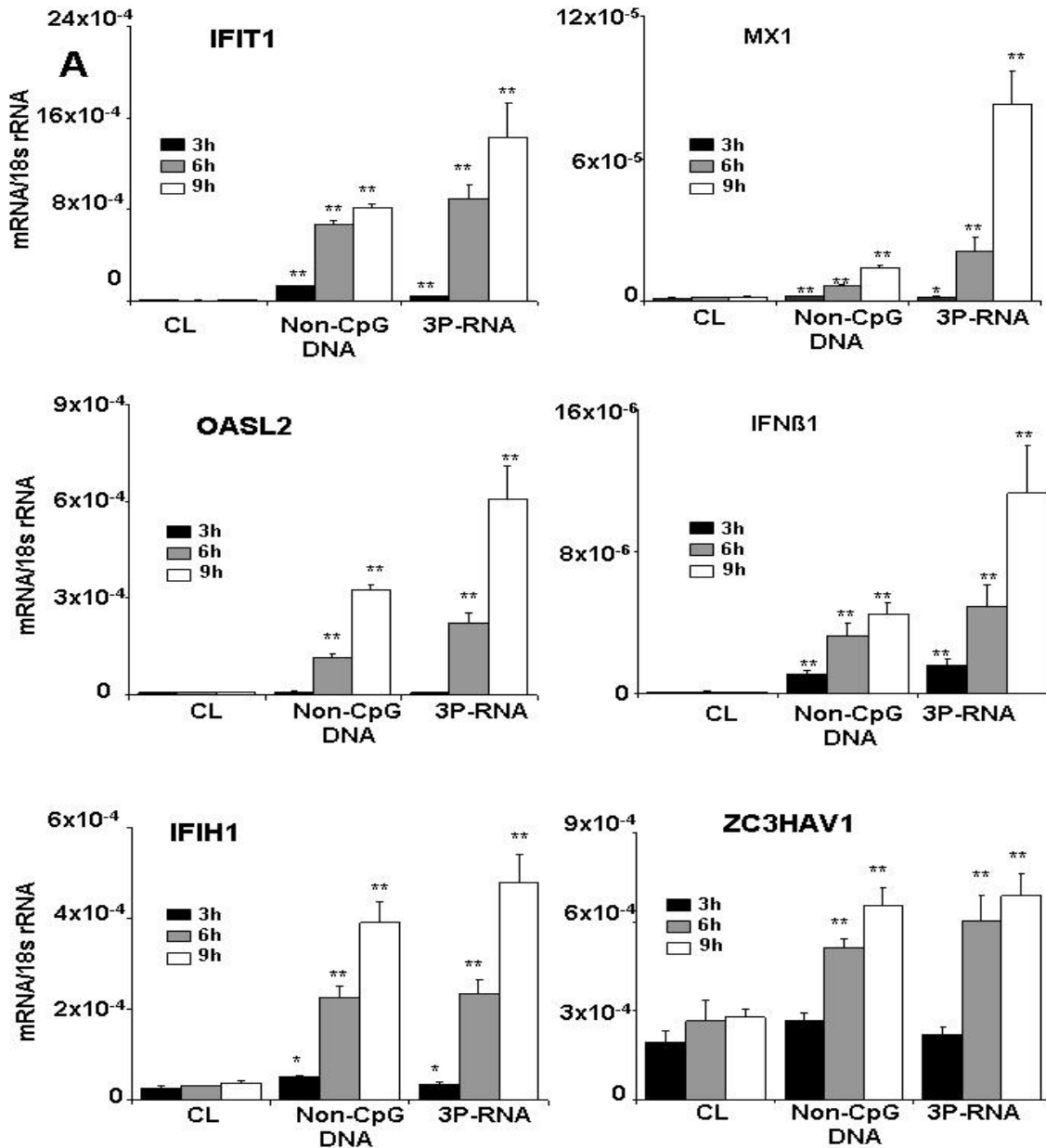


Figure 36. 3P-RNA and non-CpG-DNA trigger IFN-related genes in mesangial cells. Primary MC mRNA was isolated 3, 6, and 9 hours after exposure to 3P-RNA/CL or non-CpG-DNA/CL. Real-time RT-PCR was performed for the indicated targets as described in methods. Data are expressed per respective 18S rRNA expression and represent means \pm SD from three experiments each analyzed in duplicates. * $p < 0.05$ vs. CL, ** $p < 0.01$ vs. CL.

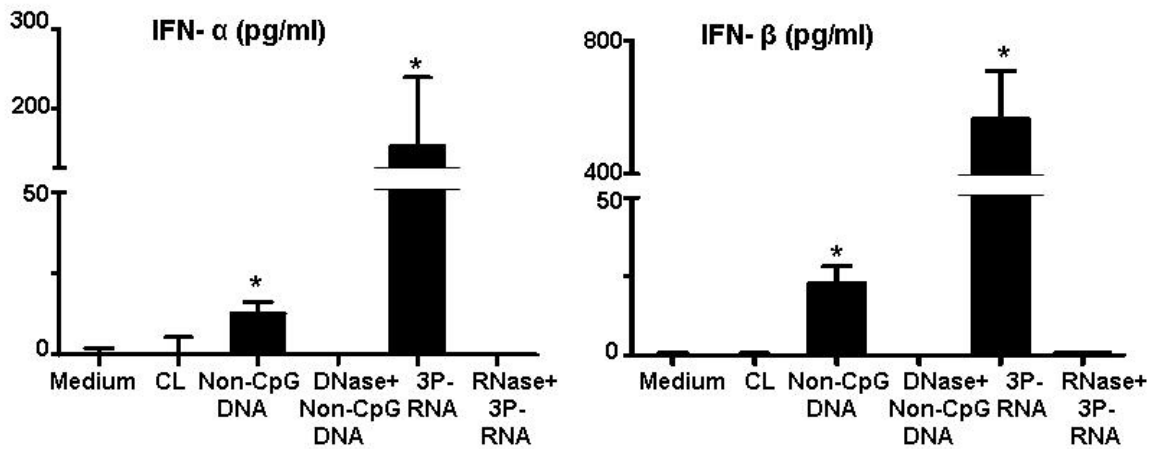


Figure 37. 3P-RNA and non-CpG-DNA trigger IFN-related genes in mesangial cells: Cell supernatants were harvested from MC after 24 hours of stimulation 3P-RNA and non-CpG-DNA and analyzed by ELISA for IFN- α and IFN- β . In similar experiments performed in the presence or absence of RNase or DNase. Data are means \pm SD from three experiments each analyzed in duplicates.* $p < 0.05$ vs+. medium. N.d. = not detected.

4.2.12 3P-RNA and non-CpG-DNA both trigger apoptosis in mesangial cells

Viral recognition commonly triggers apoptotic cell death which is thought to contribute to the control of viral replication and spreading. The gene array analysis suggested that many of the genes induced by both 3P-RNA/CL and non-CpG-DNA/CL relate to cell cycle regulation (Table 5). We therefore analyzed the impact of 3P-RNA/CL and non-CpG-DNA/CL on pMC proliferation. At lower concentrations 3P-RNA/CL and non-CpG-DNA/CL increased the number of pMC cells over a period of 72 hours (Figure 38A). At higher concentrations the number of pMC declined with both nucleic acids in a dose-dependent manner (Figure 38A). Flow cytometry revealed that 3P-RNA/CL and non-CpG-DNA/CL stimulation mainly increased the numbers of propidium iodine and annexin-V double positive MC indicating late apoptotic MC (Figure 38 B and C). Thus, in addition to cytokine and chemokine release and type I IFN signaling 3P-RNA and non-CpG-DNA trigger MC apoptosis, especially at higher concentrations.

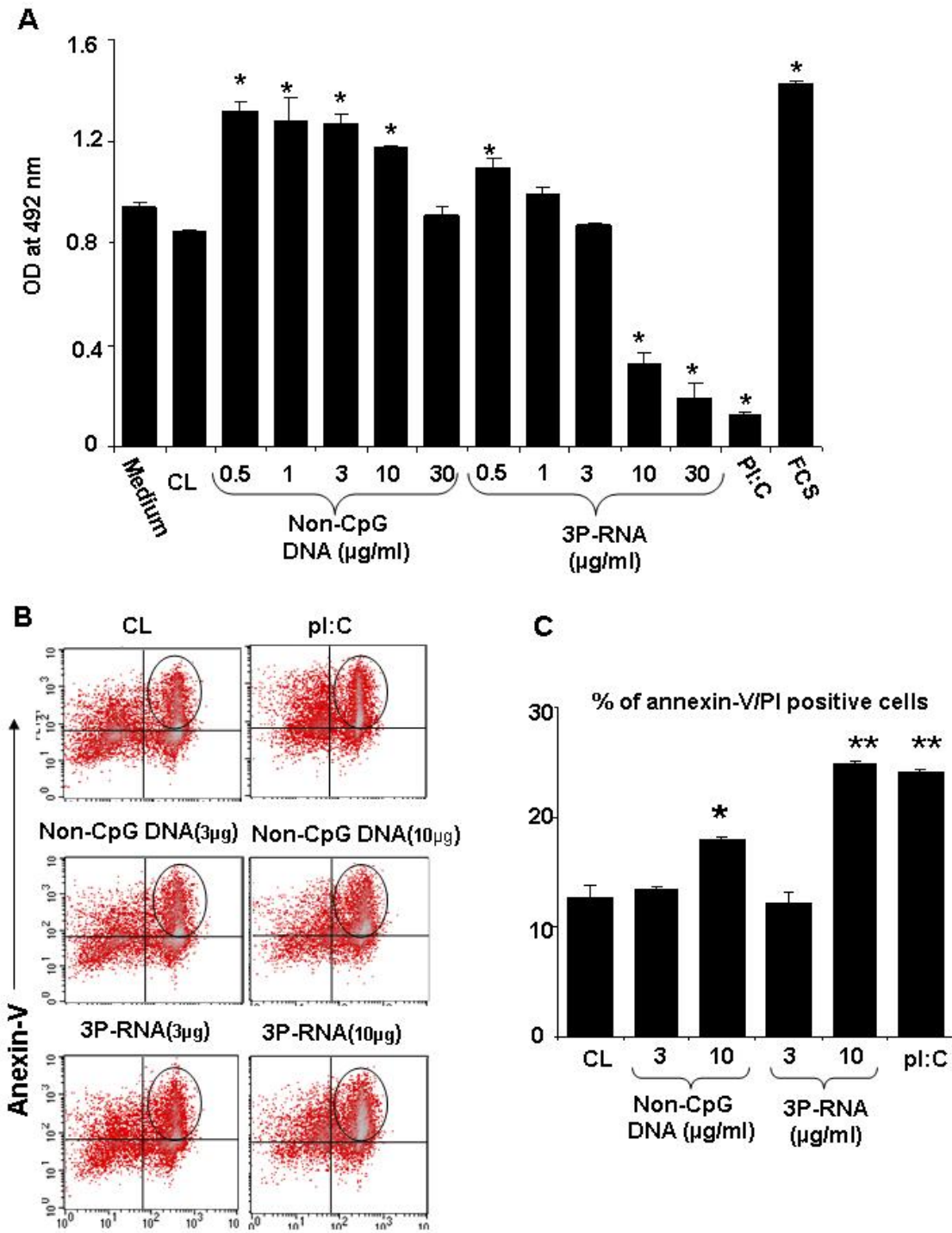


Figure 38. 3P-RNA and non-CpG-DNA trigger apoptosis in mesangial cells. (A) pMC cells were stimulated with increasing doses of 3P-RNA/CL or non-CpG-DNA/CL as indicated. poly I:C RNA (pI:C) 50 µg and fetal calf serum 30%(FCS) were used as controls. After 72 hours the number of proliferating cells was determined by a proliferation assay as described in methods. (B) In similar experiments stimulated MC were stained with propidium iodine (PI) and anti-annexin-V for 24 hours. Flow cytometry analyzed annexin-V/PI double positive cells (encircled). (C): Quantitative analysis of the flow cytometry data shows the percentage either annexin-V/PI double positive cells as means ± SD. * p<0.05 vs. CL.

5. Discussion

Viral infection can aggravate disease activity of autoimmune diseases like SLE but the molecular mechanisms remain unclear. The innate immune system involved in detecting viral ligands through TLRs. Several studies showed that a transient exposure to viral nucleic acids can trigger disease activity in SLE via TLR-dependent pathways [132, 155-157]. The recent discovery of TLR-independent viral nucleic acid recognition raised questions about the role of TLR-independent viral nucleic acid recognition in autoimmunity. In this study we used the model of spontaneous SLE-like autoimmunity in MRLlpr/lpr mice to study the effects of intermittent exposure to 3P-RNA and non-CpG-DNA, synthetic ligands to Rig-1 and recently identified cytosolic dsDNA receptor Dai and AIM2 or yet unknown cytosolic dsDNA receptors, in vivo [87, 88, 99, 101, 105]. 3P-RNA and non-CpG-DNA were reported to elicit immune responses via TLR-independent mechanism. Here we provide first evidence that 3P-RNA and non-CpG-DNA can aggravate both autoimmunity and autoimmune tissue injury in nephritic MRLlpr/lpr mice and that these ligands exacerbate disease through different types of immune responses.

Antiviral host defense requires an activation of innate immunity including the local production of type I interferons. Previous reports showed that a transient exposure to viral dsRNA or imiquimod both aggravates lupus nephritis in MRLlpr/lpr mice in association with enhanced IFN- α signaling and proinflammatory cytokines [155, 156]. While imiquimod triggers endosomal TLR7 signaling via MyD88/IRF-7 [69], viral dsRNA can signal either via endosomal TLR3/TRIF/IRF-3 or by activating both cytosolic RIG-like helicases [158]. 3P-RNA specifically interacts with Rig-1 [87, 88]. In this study we used the immunostimulatory ssRNA triphosphate oligonucleotide to mimic viral 3P-RNA, because its 19 bases were identified to be the minimal length to efficiently induce IFN- α via Rig-1 in monocytes [87]. Repeated injections with 3P-RNA enhanced MX1 mRNA expression in spleens and kidneys of MRLlpr/lpr mice indicating a type I interferon signature but an increase in IFN- α in serum level was not found. This is in line with the observation that autoimmunity in MRLlpr/lpr mice depends on IFN- γ rather than on type I IFNs as compared to autoimmune NZB/NZW mice [159]. In the spleen IFN- α is mainly

produced by plasmacytoid dendritic cells in a TLR-dependent manner [102] but 3P-RNA can activate Rig-1-dependent type I IFN production and also in non-immune cells [85, 99]. Injected 3P-RNA localized to glomerular cells and tubular epithelial cells in kidneys of MRLlpr/lpr mice like cytosolic staining pattern and exposure of 3P-RNA and non-CpG-DNA to C57/BL6 mice induced inflammatory cytokine production in kidney glomeruli. Consistently, Rig-1 expression was reported to localize to mesangial cells in human lupus nephritis [160]. Kidneys of 3P-RNA-injected mice expressed increased levels of CCL2 which was consistent with the moderate increase in glomerular and interstitial macrophage and T cell infiltrates, because the CC-chemokine CCL2 mediates recruitment of these cells to the glomerular and interstitial compartment in MRLlpr/lpr mice [161]. Moreover kidneys of 3P-RNA-injected mice expressed increased levels of IL-6 and TNF α . Both cytokines play a role in the regulation of immune cells, inflammation and apoptosis; further can lead to tissue damage. 3P-RNA also induced the production of dsDNA autoantibodies and subsequent glomerular IgG and complement deposits although 3P-RNA did not trigger plasma cell expansion and hypergammaglobulinaemia. Whether the discrepancy between 3P-RNA-induced autoantibody production and lack of plasma cell proliferation relates to the suppressive effect of 3P-RNA on Foxp3 mRNA expression and the numbers of spleen CD4CD25⁺ T cells or to another yet undefined mechanism remains to be determined. Thus, 3P-RNA aggravates lupus nephritis by enhancing systemic autoimmunity and by aggravating local inflammation. 3P-RNA induces IFN- α signaling, dsDNA autoantibody production and aggravates immune complex disease, renal CCL2 expression, and immune cell infiltrates.

Viral DNA can be recognized by TLR9 and activate immune cells. TLR9 recognizes unmethylated CpG motifs. Recently, it was reported that DNA can initiate immune responses through TLR9-independent pathways in a sequence-independent manner [101]. TLR9-dependent recognition of CpG-DNA causes B cell proliferation and activation of dendritic cells. Repeated injections with CpG-DNA caused significant lymphoproliferation and lymphofollicle destruction in mice [151, 162]. In MRLlpr/lpr mice a transient exposure to CpG-DNA increases the production of DNA autoantibodies and fosters crescentic glomerulonephritis [132]. The role of TLR9 in SLE is still unclear because TLR9 does not

protect from spontaneous anti-DNA autoantibody formation and glomerulonephritis. Furthermore disease induction is aggravated and additional nucleolar antibody specificity develops in autoimmune TLR9-deficient mice. MRLlpr/lpr mice lacking TLR9 developed more severe clinical disease and showed early mortality [137, 139]. Hence, other pathways might be responsible for DNA autoantibody production. DNA autoantibodies are the hallmarks of lupus. In the present study repeated injections of 45 bases long, double-stranded, phosphodiester non-CpG-DNA induced plasma cell expansion, lymphoproliferation, splenomegaly, and dsDNA autoantibodies in MRLlpr/lpr mice similar to CpG-DNA. Stetson and Medzhitov have described overlapping but unique gene expression programs were elicited by CpG- and non-CpG DNA in dendritic cells, e.g. in terms of IL-12 induction [101]. Consistent with these data, CpG-DNA strongly induced serum IL-12, IL-6 and TNF levels. Moreover CpG-DNA reduced spleen GATA3 mRNA expression in MRLlpr/lpr mice but this was not observed in non-CpG-DNA-injected MRLlpr/lpr mice. IL-12 production has been implicated with crescent glomerular lesions in murine glomerulonephritis. In fact, non-CpG-DNA did not induce crescentic glomerulonephritis and did not induce IL-6 and CCL2 mRNA in kidneys as did CpG-DNA. This may explain why non-CpG-DNA was less potent in aggravating lupus nephritis as compared to CpG-DNA. CpG-DNA activated more production of cytokines in comparison to non-CpG-DNA. However; non-CpG-DNA induced hypergammaglobulinaemia, rheumatoid factors, and dsDNA autoantibodies and this was associated with increased glomerular IgG, C3c deposits and glomerular pathology. MyD88-dependent recognition of CpG-DNA and MyD88-independent recognition of non-CpG-DNA share the potential to trigger B cell activation in vivo, however we observed decrease number of B220+CD138 cells with CpG injection, may be this is due lymphofollicle destruction[151]. CpG-DNA and dsDNA differ in terms of shifting T cell function to the Th1-type, which is associated with crescent formation in mice. After intravenous injection with rhodamine-labeled non-CpG-DNA reached kidney glomerular cells. Exposure of non-CpG-DNA to C57/BL6 mice induced inflammatory cytokine in kidney glomeruli. These experiment results and localization experiment results strongly provide evidence that non-CpG-DNA and 3P-RNA can reach to the glomerular compartment and induce local inflammation.

Table 7. PAMPs and their effects on SLE pathology

	Lipo-peptide TLR-2	LPS TLR-4	dsRNA TLR-3	ssRNA TLR-7	CpG-DNA TLR-9	dsDNA DAI and others	3P-RNA RIG-1
Lympho-proliferation	-	+	-	+	+++	+++	-
Regulatory T-Cells	?	?	?	?	?	?	+
dsDNA-antibodies	+	+	-	+	+++	+++	+
Glomerular IG	+	+	-	+	+++	+	+
Mesangio-lysis	-	-	++	-	-	-	-
Proteinuria	+++	+	+	+	+	+	+
Inflammation	++	++	++	++	++	+	+

Altogether the immune responses triggered by 3P-RNA and non-CpG-DNA differently modulate autoimmunity but both aggravate autoimmune tissue injury such as lupus-like nephritis in MRLlpr/lpr mice. These data extend the previous finding that TLR-independent recognition of RNA and DNA initiate overlapping but still different gene expression patterns. Even though 3P-RNA and non-CpG-DNA induced similar gene expression in mesangial cells but in vivo both ligands aggravated the disease in a different fashion. RNA and DNA both enhanced the production of dsDNA autoantibodies, the glomerular deposition of IgG and subsequent complement activation in the glomerulus. However, the immunostimulatory effects of 3P-RNA and non-CpG-DNA differ in terms of type I IFN signaling, Foxp3-mediated regulatory T cells and plasma cell proliferation in MRLlpr/lpr mice. These data suggest that viral 3P-RNA and dsDNA differently modulate autoimmunity but still both aggravate autoimmune tissue injury, e.g. by activating non-immune cells at the tissue level. These data added 3P-RNA and non-CpG-DNA in to pathogen-associated molecules that can aggravate lupus disease (see Table 7). These

pathogen-associated molecules modulate disease progression in different ways (Table 7). Finally, these data support the hypothesis that cytosolic nucleic acid receptors might play a role in autoimmunity.

Viral infections exacerbate disease activity of preexisting glomerular diseases like IgA nephropathy, lupus nephritis or renal vasculitis [163]. Viral infections can induce de novo immune complex glomerulonephritis, e.g. hepatitis C virus-associated glomerulonephritis. Mesangial cells occupy a central position in the glomerulus. The glomerular sieving process exposes MC to all types of circulating micro- and macromolecules including viral particles during extrarenal viral infections. Viral nucleic acids remain partially protected from nuclease digestion when being complexed to immunoglobulins, nucleoproteins or lipid particles, a process that also supports the uptake of such particles into intracellular compartments [123, 164, 165]. Hence, glomerular immune complex deposits are usually taken up and processed by glomerular mesangial cells [166]. Viral nucleic acids activate mesangial cells. It was reported that viral dsRNA activates human and murine MC to produce IL-6 and CCL2 *in vitro* and *in vivo* which is attributed to TLR3, because the only nucleic acid-specific TLR expressed by mesangial cells [155, 167] (mesangial cells won't express TLR7 and 9). TLR3 recognizes dsRNA, but viral nucleic acids occur in formats other than dsRNA, like the 5'-triphosphate RNA, ssRNA, homopolymeric ribonucleotide motifs of hepatitis C virus RNA [89] and various DNA formats. *In vivo* studies on MRL^{lpr/lpr} mice were shown that 3P-RNA and non-CpG-DNA can reach to the glomerular compartment and induce local inflammation. We also demonstrate that 3P-RNA and unmethylated non-CpG-DNA are potent activators of mesangial cells. Consistent with the published literature we confirmed that 3P-RNA and non-CpG-DNA activate mesangial cells via TLR-independent recognition pathways [140]. Both MyD88-deficient and Trif deficient pMC produced CXCL10, IL-6 and CCL5 similar like wild type pMC. 3P-RNA and non-CpG-DNA both induced IL-6 production in dose-dependent manner. RT-PCR data demonstrated that mesangial cells express Rig-1, Mda5 and Dai. Rig-1 and Dai were shown to be involved in the recognition of 3P-RNA and viral non-CpG-DNA, respectively [87, 88, 101]. The role of Rig-1 for the recognition of 3P-RNA has been confirmed with Rig-1-deficient mice by several groups [87, 88]. Consistent with published results, Rig-1 knock

down in mesangial cells significantly reduced 3P-RNA induced CXCL10 and IL-6 expression at mRNA level and protein level. The role of Dai for the recognition of unmethylated dsB-DNA is unclear because cells derived from Dai-deficient mice respond to B-DNA to a similar extent to cells derived from wildtype mice [106]. In a follow up study Wang, et al. admitted that other cytosolic DNA sensors must exist [168]. The data from Dai knockdown experiments demonstrate that Dai (as well as Rig-1) are dispensable for non-CpG-DNA recognition in MC. Still, the recognition of non-CpG-DNA seems to take place inside MC as complex formation with CL was required for dsDNA-induced MC activation. Surprisingly, transfection with Dai-specific siRNA reduced IL-6 and CXCL10 the mRNA expression in MC stimulated with 3P-RNA. The significance of this finding remains doubtful because ELISA-based quantification of the respective proteins in MC supernatants showed significant but only little reduction with the Dai knock down. So far studies have not addressed a potential role of Dai in 3P-RNA-induced cell activation. Recent studies reported a role of Rig-1 in the recognition of dsDNA, however, this mechanism seems to be species specific and dsDNA format-specific [102, 113]. It appears that the role of cytosolic RNA- or DNA-binding proteins for innate pathogen recognition varies between different cell types, and different species. Immunofluorescence data showed that rhodamine-labeled 3P-RNA and non-CpG-DNA both reach the cytoplasm when they have complexed with cationic lipids. So cytoplasmic translocation is important for these ligands to activate cells. 3P-RNA and dsDNA both activate IFNs although 3P-RNA and dsDNA recognition in MC involves different pathways. Both activate the transcription factor IRF3 [101]. This may explain why 3P-RNA and non-CpG-DNA induce almost identical gene expression programs in MC. Transcriptome analysis revealed that 3P-RNA and non-CpG-DNA predominantly induce the expression of four types of genes, i.e. proinflammatory cytokines (IL-6, IFN- α , IFN- β), chemokines (CCL2, CCL5, CCL7, CCL17, CXCL10), a type I IFN-related gene signature (IFIT1, MX1, OASL2, IFN β 1, IFIH1, and ZC3HAV1), and cell growth-related genes. The local expression of cytokines and chemokines is important for antiviral defense as they create a local inflammatory environment and promote the recruitment of antigen-presenting cells and immune effector cells. Among the proinflammatory chemokines CXCL10 is of particular interest because it is specifically induced by IFN and preferentially recruits cytotoxic T cells via the

chemokine receptor CXCR3 [169]. Type I IFNs have multiple other immunoregulatory functions and specifically trigger antiviral effectors. For example, mesangial cells expressed the nuclear GTPase Mx1 that can bind to viral nucleocapsids or other viral components and degrades them [170]. Mesangial cells also induced OASL2 that activates the antiviral endoribonuclease RNase L, a mechanism that initiates the cleavage of viral RNA and that can produce small self-RNA cleavage products which enhance type I signaling via Rig-1, Mda5, and Mavs in a positive amplification loop [170]. This study documented for the first time type I IFN release in mesangial cells. Non-CpG-DNA induced cell proliferation significantly at low concentrations; on the other hand 3P-RNA did not induce cell proliferation. This is may be due to some cell cycle and proliferation related genes which were induced specifically by non-CpG-DNA in arrays. We have addressed this topic in subsequent studies while these results are not mentioned here. Viral infection leads to cell death; to prevent viral replication and spreading. Consistent with these phenomena 3P-RNA and high concentration of non-CpG-DNA induced MC apoptosis. Microarray data showed that 3P-RNA- and non-CpG-DNA induced large number of antiviral genes in mesangial cells. However, the response spectrum remains limited compared to that of professional antigen-presenting cells. In antigen-presenting cells the recognition of viral RNA and DNA also reduces antigen uptake and fosters cell maturation, antigen-presentation as well as costimulation. Non-immune cells like Mesangial cells lack many of these functions because they are functionally and structurally differentiated to serve specialized functions in glomerular microenvironment. Mesangial cells are considered to represent specialized perivascular pericytes that maintain the structure of the glomerular capillary loop, control glomerular hemodynamics and clear macromolecules that cannot pass the glomerular filter membrane [171]. These data suggest a novel and previously unrecognized function of MC to trigger specific antiviral immune responses upon immune recognition of viral 3P-RNA and non-CpG-DNA. These data implicate a novel mechanism for the pathogenesis of viral infection-associated glomerulonephritis. These results were supported the *in vivo* experiments that 3P-RNA and non-CpG-DNA induced antiviral genes in glomeruli of C57BL/6 mice. In these experiments the mRNA expression may also originate from other glomerular cells than MC. In fact, podocytes and glomerular endothelial cells have a similar capacity as MC to

trigger antiviral genes upon immune recognition of viral RNA and DNA [172]. Direct viral infection and replication in glomerular cells has rarely been documented [173]. However, de novo glomerulonephritis or flares of preexisting chronic glomerulonephritis are common during extrarenal viral infections. The activation of antiviral immune responses in glomerular cells, as described here, will always be unable to control the extrarenal viral infection but can induce or aggravate glomerular pathology.

Together the data unravels TLR-independent RNA and DNA recognition in mesangial cells and showed that other formats of nucleic acids can activate these cells. Dai is dispensable for non-CpG-DNA recognition. Rig-1 and Dai are both involved in the recognition of 3P-RNA in glomerular mesangial cells. These data suggest that the role of Rig-1 and Dai for innate pathogen recognition can vary between cell types and species. However, complexed 3P-RNA and dsDNA trigger a common antiviral response program in MC and in the intrarenal glomerular compartment which may explain how extrarenal viral infections can trigger glomerulonephritis. These data support the idea that immune complexes that are associated with nucleic acids can activate glomerular cells, which leads to glomerular inflammation. These data open a new field, i.e. the function of antiviral mechanisms in glomerular cells which was neglected in the past. These mechanism seems to represent another example how functionally inappropriate immune responses trigger immunity-related kidney damage.

6. Summary

Non-CpG-DNA and 3P-RNA activated mesangial cells to produce inflammatory cytokines and type 1 interferons in TLR-independent manner. Both ligands induced similar gene expression patterns in mesangial cells. This data unravelled the existence of TLR-independent pathways and production of type1 interferons in mesangial cells. These results substantiate the idea that, immune complexes that are associated with nucleic acids can activate glomerular cells via TLR-independent manner, which leads to glomerular inflammation. Furthermore, exposure of non-CpG-DNA and 3P-RNA in MRLlpr/lpr mice aggravated the disease pathology in different manner. Even though 3P-RNA and non-CpG-DNA induced similar gene expression in mesangial cells but *in vivo* both ligands aggravated the disease in different fashion. 3P-RNA induced type I IFN signaling and decreased the number of regulatory T cells while non-CpG-DNA induced plasma cell expansion, lymphoproliferation and splenomegaly. However, both ligands induced the production of dsDNA autoantibodies and increased the glomerular deposition of IgG. These data suggest that viral 3P-RNA and non-CpG-DNA differently modulate autoimmunity but still both aggravate autoimmune tissue injury by activating non-immune cells at the tissue level.

7. Zusammenfassung

Stimulation mit Non-CpG-DNA und 3P-RNA führte zu einer Toll-Like-Rezeptor-unabhängigen Ausschüttung proinflammatorischer Zytokine und Typ I Interferone in glomerulären Mesangialzellen. Beide Liganden induzierten vergleichbare Genexpressionsmuster in Mesangialzellen. Damit wurde die Existenz TLR-unabhängiger Signalwege und Produktion von Typ I Interferone in Mesangialzellen aufgedeckt. Dieses Ergebnis unterstützt die These, dass Immunkomplexe, die mit Nukleinsäuren assoziiert sind, glomeruläre Zellen TLR-unabhängig aktivieren und zur Entzündungsreaktion im Glomerulus beitragen können. Des Weiteren veränderte die Exposition von Non-CpG-DNA und 3P-RNA in MRLlpr/lpr-Mäusen die Krankheitsentwicklung der Tiere auf verschiedene Weise. Obwohl 3P-RNA und Non-CpG-DNA ähnliche Genexpression in Mesangialzellen induzierte, wurde die Erkrankung in vivo durch die Injektion beider Liganden unterschiedlich aggraviert. 3P-RNA induzierte Typ I Interferon-Signalwege und verminderte die Anzahl an regulatorischen T-Zellen, während Non-CpG-DNA Plasmazell-Expansion, Lymphproliferation und Splenomegalie induzierte. Hingegen induzierten beide Liganden die Produktion von Autoantikörpern und eine vermehrte Ablagerung von IgG im Glomerulus. Diese Daten lassen vermuten, dass virale 3P-RNA und Non-CpG-DNA unterschiedlich Autoimmunität modulieren, beide Liganden jedoch den autoimmunen Gebeschaden durch aktivierte nicht-Immunezellen verstärken.

8. References

1. D'Cruz, D.P., M.A. Khamashta, and G.R. Hughes, *Systemic lupus erythematosus*. *Lancet*, 2007. **369**(9561): p. 587-96.
2. Johnson, A.E., et al., *The prevalence and incidence of systemic lupus erythematosus in Birmingham, England. Relationship to ethnicity and country of birth*. *Arthritis Rheum*, 1995. **38**(4): p. 551-8.
3. Goldblatt, F. and D.A. Isenberg, *New therapies for systemic lupus erythematosus*. *Clin Exp Immunol*, 2005. **140**(2): p. 205-12.
4. Rahman, A., et al., *Systematic analysis of sequences of anti-DNA antibodies--relevance to theories of origin and pathogenicity*. *Lupus*, 2002. **11**(12): p. 807-23.
5. Okamura, M., et al., *Significance of enzyme linked immunosorbent assay (ELISA) for antibodies to double stranded and single stranded DNA in patients with lupus nephritis: correlation with severity of renal histology*. *Ann Rheum Dis*, 1993. **52**(1): p. 14-20.
6. Cameron, J.S., *Lupus nephritis*. *J Am Soc Nephrol*, 1999. **10**(2): p. 413-24.
7. Hricik, D.E., M. Chung-Park, and J.R. Sedor, *Glomerulonephritis*. *N Engl J Med*, 1998. **339**(13): p. 888-99.
8. Majno, G. and I. Joris, *Apoptosis, oncosis, and necrosis. An overview of cell death*. *Am J Pathol*, 1995. **146**(1): p. 3-15.
9. Rock, K.L. and H. Kono, *The inflammatory response to cell death*. *Annu Rev Pathol*, 2008. **3**: p. 99-126.
10. Huynh, M.L., V.A. Fadok, and P.M. Henson, *Phosphatidylserine-dependent ingestion of apoptotic cells promotes TGF-beta1 secretion and the resolution of inflammation*. *J Clin Invest*, 2002. **109**(1): p. 41-50.
11. Kamradt, T. and N.A. Mitchison, *Tolerance and autoimmunity*. *N Engl J Med*, 2001. **344**(9): p. 655-64.
12. Nagata, S. and T. Suda, *Fas and Fas ligand: lpr and gld mutations*. *Immunol Today*, 1995. **16**(1): p. 39-43.
13. Taylor, P.R., et al., *A hierarchical role for classical pathway complement proteins in the clearance of apoptotic cells in vivo*. *J Exp Med*, 2000. **192**(3): p. 359-66.
14. Licht, R., et al., *Decreased phagocytosis of apoptotic cells in diseased SLE mice*. *J Autoimmun*, 2004. **22**(2): p. 139-45.
15. Herrmann, M., et al., *Impaired phagocytosis of apoptotic cell material by monocyte-derived macrophages from patients with systemic lupus erythematosus*. *Arthritis Rheum*, 1998. **41**(7): p. 1241-50.
16. Baumann, I., et al., *Impaired uptake of apoptotic cells into tingible body macrophages in germinal centers of patients with systemic lupus erythematosus*. *Arthritis Rheum*, 2002. **46**(1): p. 191-201.
17. Monestier, M., *Autoantibodies to nucleosomes and histone-DNA complexes*. *Methods*, 1997. **11**(1): p. 36-43.
18. Tax, W.J., et al., *Apoptosis, nucleosomes, and nephritis in systemic lupus erythematosus*. *Kidney Int*, 1995. **48**(3): p. 666-73.
19. Casciola-Rosen, L. and A. Rosen, *Ultraviolet light-induced keratinocyte apoptosis: a potential mechanism for the induction of skin lesions and autoantibody production in LE*. *Lupus*, 1997. **6**(2): p. 175-80.

20. Mevorach, D., et al., *Systemic exposure to irradiated apoptotic cells induces autoantibody production*. J Exp Med, 1998. **188**(2): p. 387-92.
21. Kalaaji, M., et al., *Glomerular apoptotic nucleosomes are central target structures for nephritogenic antibodies in human SLE nephritis*. Kidney Int, 2007. **71**(7): p. 664-72.
22. Kalaaji, M., et al., *Nephritogenic lupus antibodies recognize glomerular basement membrane-associated chromatin fragments released from apoptotic intraglomerular cells*. Am J Pathol, 2006. **168**(6): p. 1779-92.
23. Sidiropoulos, P.I. and D.T. Boumpas, *Lessons learned from anti-CD40L treatment in systemic lupus erythematosus patients*. Lupus, 2004. **13**(5): p. 391-7.
24. Davidson, A., et al., *Block and tackle: CTLA4Ig takes on lupus*. Lupus, 2005. **14**(3): p. 197-203.
25. Coffman, R.L., D.A. Leberman, and P. Rothman, *Mechanism and regulation of immunoglobulin isotype switching*. Adv Immunol, 1993. **54**: p. 229-70.
26. Shlomchik, M.J., et al., *The role of clonal selection and somatic mutation in autoimmunity*. Nature, 1987. **328**(6133): p. 805-11.
27. Chan, O.T., et al., *A novel mouse with B cells but lacking serum antibody reveals an antibody-independent role for B cells in murine lupus*. J Exp Med, 1999. **189**(10): p. 1639-48.
28. Bagavant, H., et al., *Lupus glomerulonephritis revisited 2004: autoimmunity and end-organ damage*. Scand J Immunol, 2004. **60**(1-2): p. 52-63.
29. Mudd, P.A., B.N. Teague, and A.D. Farris, *Regulatory T cells and systemic lupus erythematosus*. Scand J Immunol, 2006. **64**(3): p. 211-8.
30. Valencia, X., et al., *Deficient CD4+CD25high T regulatory cell function in patients with active systemic lupus erythematosus*. J Immunol, 2007. **178**(4): p. 2579-88.
31. Martin, F. and A.C. Chan, *B cell immunobiology in disease: evolving concepts from the clinic*. Annu Rev Immunol, 2006. **24**: p. 467-96.
32. O'Neill, S.K., et al., *Antigen-specific B cells are required as APCs and autoantibody-producing cells for induction of severe autoimmune arthritis*. J Immunol, 2005. **174**(6): p. 3781-8.
33. Rahman, A. and D.A. Isenberg, *Systemic lupus erythematosus*. N Engl J Med, 2008. **358**(9): p. 929-39.
34. Isenberg, D.A., et al., *Fifty years of anti-ds DNA antibodies: are we approaching journey's end?* Rheumatology (Oxford), 2007. **46**(7): p. 1052-6.
35. Berden, J.H., et al., *Role of nucleosomes for induction and glomerular binding of autoantibodies in lupus nephritis*. Curr Opin Nephrol Hypertens, 1999. **8**(3): p. 299-306.
36. Kramers, C., et al., *Anti-nucleosome antibodies complexed to nucleosomal antigens show anti-DNA reactivity and bind to rat glomerular basement membrane in vivo*. J Clin Invest, 1994. **94**(2): p. 568-77.
37. van Bruggen, M.C., et al., *Antigen specificity of anti-nuclear antibodies complexed to nucleosomes determines glomerular basement membrane binding in vivo*. Eur J Immunol, 1997. **27**(6): p. 1564-9.
38. Grootsholten, C., et al., *Deposition of nucleosomal antigens (histones and DNA) in the epidermal basement membrane in human lupus nephritis*. Arthritis Rheum, 2003. **48**(5): p. 1355-62.

39. Theofilopoulos, A.N., et al., *Type I interferons (alpha/beta) in immunity and autoimmunity*. *Annu Rev Immunol*, 2005. **23**: p. 307-36.
40. Hooks, J.J., et al., *Immune interferon in the circulation of patients with autoimmune disease*. *N Engl J Med*, 1979. **301**(1): p. 5-8.
41. Ronnblom, L. and G.V. Alm, *An etiopathogenic role for the type I IFN system in SLE*. *Trends Immunol*, 2001. **22**(8): p. 427-31.
42. Bengtsson, A.A., et al., *Activation of type I interferon system in systemic lupus erythematosus correlates with disease activity but not with antiretroviral antibodies*. *Lupus*, 2000. **9**(9): p. 664-71.
43. Gota, C. and L. Calabrese, *Induction of clinical autoimmune disease by therapeutic interferon-alpha*. *Autoimmunity*, 2003. **36**(8): p. 511-8.
44. Blanco, P., et al., *Induction of dendritic cell differentiation by IFN-alpha in systemic lupus erythematosus*. *Science*, 2001. **294**(5546): p. 1540-3.
45. Peterson, K.S., et al., *Characterization of heterogeneity in the molecular pathogenesis of lupus nephritis from transcriptional profiles of laser-captured glomeruli*. *J Clin Invest*, 2004. **113**(12): p. 1722-33.
46. Lovgren, T., et al., *Induction of interferon-alpha production in plasmacytoid dendritic cells by immune complexes containing nucleic acid released by necrotic or late apoptotic cells and lupus IgG*. *Arthritis Rheum*, 2004. **50**(6): p. 1861-72.
47. Ronnblom, L., M.L. Eloranta, and G.V. Alm, *Role of natural interferon-alpha producing cells (plasmacytoid dendritic cells) in autoimmunity*. *Autoimmunity*, 2003. **36**(8): p. 463-72.
48. Santiago-Raber, M.L., et al., *Type-I interferon receptor deficiency reduces lupus-like disease in NZB mice*. *J Exp Med*, 2003. **197**(6): p. 777-88.
49. Braun, D., P. Geraldès, and J. Demengeot, *Type I Interferon controls the onset and severity of autoimmune manifestations in lpr mice*. *J Autoimmun*, 2003. **20**(1): p. 15-25.
50. Hron, J.D. and S.L. Peng, *Type I IFN protects against murine lupus*. *J Immunol*, 2004. **173**(3): p. 2134-42.
51. Jacob, C.O. and H.O. McDevitt, *Tumour necrosis factor-alpha in murine autoimmune 'lupus' nephritis*. *Nature*, 1988. **331**(6154): p. 356-8.
52. Charles, P.J., et al., *Assessment of antibodies to double-stranded DNA induced in rheumatoid arthritis patients following treatment with infliximab, a monoclonal antibody to tumor necrosis factor alpha: findings in open-label and randomized placebo-controlled trials*. *Arthritis Rheum*, 2000. **43**(11): p. 2383-90.
53. Mohan, A.K., et al., *Drug-induced systemic lupus erythematosus and TNF-alpha blockers*. *Lancet*, 2002. **360**(9333): p. 646.
54. Naka, T., N. Nishimoto, and T. Kishimoto, *The paradigm of IL-6: from basic science to medicine*. *Arthritis Res*, 2002. **4 Suppl 3**: p. S233-42.
55. Iwano, M., et al., *Intraglomerular expression of transforming growth factor-beta 1 (TGF-beta 1) mRNA in patients with glomerulonephritis: quantitative analysis by competitive polymerase chain reaction*. *Clin Exp Immunol*, 1994. **97**(2): p. 309-14.
56. Raz, E., et al., *Modulation of disease activity in murine systemic lupus erythematosus by cytokine gene delivery*. *Lupus*, 1995. **4**(4): p. 286-92.
57. Hoffmann, J.A., *The immune response of Drosophila*. *Nature*, 2003. **426**(6962): p. 33-8.

58. Akira, S., S. Uematsu, and O. Takeuchi, *Pathogen recognition and innate immunity*. Cell, 2006. **124**(4): p. 783-801.
59. Beutler, B., et al., *Genetic analysis of resistance to viral infection*. Nat Rev Immunol, 2007. **7**(10): p. 753-66.
60. Medzhitov, R., *Recognition of microorganisms and activation of the immune response*. Nature, 2007. **449**(7164): p. 819-26.
61. Janeway, C.A., Jr., *Approaching the asymptote? Evolution and revolution in immunology*. Cold Spring Harb Symp Quant Biol, 1989. **54 Pt 1**: p. 1-13.
62. Akira, S. and K. Takeda, *Toll-like receptor signalling*. Nat Rev Immunol, 2004. **4**(7): p. 499-511.
63. Matsushima, N., et al., *Comparative sequence analysis of leucine-rich repeats (LRRs) within vertebrate toll-like receptors*. BMC Genomics, 2007. **8**: p. 124.
64. O'Neill, L.A. and A.G. Bowie, *The family of five: TIR-domain-containing adaptors in Toll-like receptor signalling*. Nat Rev Immunol, 2007. **7**(5): p. 353-64.
65. Barton, G.M. and J.C. Kagan, *A cell biological view of Toll-like receptor function: regulation through compartmentalization*. Nat Rev Immunol, 2009. **9**(8): p. 535-42.
66. Wang, T., et al., *Toll-like receptor 3 mediates West Nile virus entry into the brain causing lethal encephalitis*. Nat Med, 2004. **10**(12): p. 1366-73.
67. Groskreutz, D.J., et al., *Respiratory syncytial virus induces TLR3 protein and protein kinase R, leading to increased double-stranded RNA responsiveness in airway epithelial cells*. J Immunol, 2006. **176**(3): p. 1733-40.
68. Edelmann, K.H., et al., *Does Toll-like receptor 3 play a biological role in virus infections?* Virology, 2004. **322**(2): p. 231-8.
69. Hemmi, H., et al., *Small anti-viral compounds activate immune cells via the TLR7 MyD88-dependent signaling pathway*. Nat Immunol, 2002. **3**(2): p. 196-200.
70. Peng, G., et al., *Toll-like receptor 8-mediated reversal of CD4+ regulatory T cell function*. Science, 2005. **309**(5739): p. 1380-4.
71. Hemmi, H., et al., *A Toll-like receptor recognizes bacterial DNA*. Nature, 2000. **408**(6813): p. 740-5.
72. Krug, A., et al., *Toll-like receptor expression reveals CpG DNA as a unique microbial stimulus for plasmacytoid dendritic cells which synergizes with CD40 ligand to induce high amounts of IL-12*. Eur J Immunol, 2001. **31**(10): p. 3026-37.
73. Honda, K., et al., *Spatiotemporal regulation of MyD88-IRF-7 signalling for robust type-I interferon induction*. Nature, 2005. **434**(7036): p. 1035-40.
74. West, A.P., A.A. Koblansky, and S. Ghosh, *Recognition and signaling by toll-like receptors*. Annu Rev Cell Dev Biol, 2006. **22**: p. 409-37.
75. Kawagoe, T., et al., *Sequential control of Toll-like receptor-dependent responses by IRAK1 and IRAK2*. Nat Immunol, 2008. **9**(6): p. 684-91.
76. Adhikari, A., M. Xu, and Z.J. Chen, *Ubiquitin-mediated activation of TAK1 and IKK*. Oncogene, 2007. **26**(22): p. 3214-26.
77. Yamamoto, M., et al., *Role of adaptor TRIF in the MyD88-independent toll-like receptor signaling pathway*. Science, 2003. **301**(5633): p. 640-3.
78. Sharma, S., et al., *Triggering the interferon antiviral response through an IKK-related pathway*. Science, 2003. **300**(5622): p. 1148-51.
79. Fitzgerald, K.A., et al., *IKKepsilon and TBK1 are essential components of the IRF3 signaling pathway*. Nat Immunol, 2003. **4**(5): p. 491-6.

80. Kawai, T., et al., *Interferon-alpha induction through Toll-like receptors involves a direct interaction of IRF7 with MyD88 and TRAF6*. Nat Immunol, 2004. **5**(10): p. 1061-8.
81. Uematsu, S., et al., *Interleukin-1 receptor-associated kinase-1 plays an essential role for Toll-like receptor (TLR)7- and TLR9-mediated interferon-{alpha} induction*. J Exp Med, 2005. **201**(6): p. 915-23.
82. Kawai, T. and S. Akira, *Innate immune recognition of viral infection*. Nat Immunol, 2006. **7**(2): p. 131-7.
83. Cui, S., et al., *The C-terminal regulatory domain is the RNA 5'-triphosphate sensor of RIG-I*. Mol Cell, 2008. **29**(2): p. 169-79.
84. Takahashi, K., et al., *Nonsel f RNA-sensing mechanism of RIG-I helicase and activation of antiviral immune responses*. Mol Cell, 2008. **29**(4): p. 428-40.
85. Kato, H., et al., *Cell type-specific involvement of RIG-I in antiviral response*. Immunity, 2005. **23**(1): p. 19-28.
86. Kato, H., et al., *Differential roles of MDA5 and RIG-I helicases in the recognition of RNA viruses*. Nature, 2006. **441**(7089): p. 101-5.
87. Hornung, V., et al., *5'-Triphosphate RNA is the ligand for RIG-I*. Science, 2006. **314**(5801): p. 994-7.
88. Pichlmair, A., et al., *RIG-I-mediated antiviral responses to single-stranded RNA bearing 5'-phosphates*. Science, 2006. **314**(5801): p. 997-1001.
89. Saito, T., et al., *Innate immunity induced by composition-dependent RIG-I recognition of hepatitis C virus RNA*. Nature, 2008. **454**(7203): p. 523-7.
90. Marques, J.T., et al., *A structural basis for discriminating between self and nonself double-stranded RNAs in mammalian cells*. Nat Biotechnol, 2006. **24**(5): p. 559-65.
91. Kato, H., et al., *Length-dependent recognition of double-stranded ribonucleic acids by retinoic acid-inducible gene-1 and melanoma differentiation-associated gene 5*. J Exp Med, 2008. **205**(7): p. 1601-10.
92. Venkataraman, T., et al., *Loss of DExD/H box RNA helicase LGP2 manifests disparate antiviral responses*. J Immunol, 2007. **178**(10): p. 6444-55.
93. Meylan, E., et al., *Cardif is an adaptor protein in the RIG-I antiviral pathway and is targeted by hepatitis C virus*. Nature, 2005. **437**(7062): p. 1167-72.
94. Kawai, T., et al., *IPS-1, an adaptor triggering RIG-I- and Mda5-mediated type I interferon induction*. Nat Immunol, 2005. **6**(10): p. 981-8.
95. Seth, R.B., et al., *Identification and characterization of MAVS, a mitochondrial antiviral signaling protein that activates NF-kappaB and IRF 3*. Cell, 2005. **122**(5): p. 669-82.
96. Xu, L.G., et al., *VISA is an adapter protein required for virus-triggered IFN-beta signaling*. Mol Cell, 2005. **19**(6): p. 727-40.
97. Michallet, M.C., et al., *TRADD protein is an essential component of the RIG-like helicase antiviral pathway*. Immunity, 2008. **28**(5): p. 651-61.
98. Gack, M.U., et al., *TRIM25 RING-finger E3 ubiquitin ligase is essential for RIG-I-mediated antiviral activity*. Nature, 2007. **446**(7138): p. 916-920.
99. Suzuki, K., et al., *Activation of target-tissue immune-recognition molecules by double-stranded polynucleotides*. Proc Natl Acad Sci U S A, 1999. **96**(5): p. 2285-90.

100. Ishii, K.J., et al., *A Toll-like receptor-independent antiviral response induced by double-stranded B-form DNA*. Nat Immunol, 2006. **7**(1): p. 40-8.
101. Stetson, D.B. and R. Medzhitov, *Recognition of cytosolic DNA activates an IRF3-dependent innate immune response*. Immunity, 2006. **24**(1): p. 93-103.
102. Cheng, G., et al., *Double-stranded DNA and double-stranded RNA induce a common antiviral signaling pathway in human cells*. Proc Natl Acad Sci U S A, 2007. **104**(21): p. 9035-40.
103. Kumar, H., et al., *Essential role of IPS-1 in innate immune responses against RNA viruses*. J Exp Med, 2006. **203**(7): p. 1795-803.
104. Sun, Q., et al., *The specific and essential role of MAVS in antiviral innate immune responses*. Immunity, 2006. **24**(5): p. 633-42.
105. Takaoka, A., et al., *DAI (DLM-1/ZBP1) is a cytosolic DNA sensor and an activator of innate immune response*. Nature, 2007. **448**(7152): p. 501-5.
106. Ishii, K.J., et al., *TANK-binding kinase-1 delineates innate and adaptive immune responses to DNA vaccines*. Nature, 2008. **451**(7179): p. 725-9.
107. Ishikawa, H. and G.N. Barber, *STING is an endoplasmic reticulum adaptor that facilitates innate immune signalling*. Nature, 2008. **455**(7213): p. 674-8.
108. Hornung, V., et al., *AIM2 recognizes cytosolic dsDNA and forms a caspase-1-activating inflammasome with ASC*. Nature, 2009. **458**(7237): p. 514-8.
109. Burckstummer, T., et al., *An orthogonal proteomic-genomic screen identifies AIM2 as a cytoplasmic DNA sensor for the inflammasome*. Nat Immunol, 2009. **10**(3): p. 266-72.
110. Fernandes-Alnemri, T., et al., *AIM2 activates the inflammasome and cell death in response to cytoplasmic DNA*. Nature, 2009. **458**(7237): p. 509-13.
111. Roberts, T.L., et al., *HIN-200 proteins regulate caspase activation in response to foreign cytoplasmic DNA*. Science, 2009. **323**(5917): p. 1057-60.
112. Schroder, K., D.A. Muruve, and J. Tschopp, *Innate immunity: cytoplasmic DNA sensing by the AIM2 inflammasome*. Curr Biol, 2009. **19**(6): p. R262-5.
113. Ablasser, A., et al., *RIG-I-dependent sensing of poly(dA:dT) through the induction of an RNA polymerase III-transcribed RNA intermediate*. Nat Immunol, 2009.
114. Kumar, H., T. Kawai, and S. Akira, *Pathogen recognition in the innate immune response*. Biochem J, 2009. **420**(1): p. 1-16.
115. Petrilli, V., et al., *The inflammasome: a danger sensing complex triggering innate immunity*. Curr Opin Immunol, 2007. **19**(6): p. 615-22.
116. Eisenbarth, S.C., et al., *Crucial role for the Nalp3 inflammasome in the immunostimulatory properties of aluminium adjuvants*. Nature, 2008. **453**(7198): p. 1122-6.
117. Hornung, V., et al., *Silica crystals and aluminum salts activate the NALP3 inflammasome through phagosomal destabilization*. Nat Immunol, 2008. **9**(8): p. 847-56.
118. Halle, A., et al., *The NALP3 inflammasome is involved in the innate immune response to amyloid-beta*. Nat Immunol, 2008. **9**(8): p. 857-65.
119. Akira, S., K. Takeda, and T. Kaisho, *Toll-like receptors: critical proteins linking innate and acquired immunity*. Nat Immunol, 2001. **2**(8): p. 675-80.
120. Schnare, M., et al., *Toll-like receptors control activation of adaptive immune responses*. Nat Immunol, 2001. **2**(10): p. 947-50.

121. Lang, K.S., et al., *Toll-like receptor engagement converts T-cell autoreactivity into overt autoimmune disease*. Nat Med, 2005. **11**(2): p. 138-45.
122. Barrat, F.J., et al., *Nucleic acids of mammalian origin can act as endogenous ligands for Toll-like receptors and may promote systemic lupus erythematosus*. J Exp Med, 2005. **202**(8): p. 1131-9.
123. Lau, C.M., et al., *RNA-associated autoantigens activate B cells by combined B cell antigen receptor/Toll-like receptor 7 engagement*. J Exp Med, 2005. **202**(9): p. 1171-7.
124. Vollmer, J., et al., *Immune stimulation mediated by autoantigen binding sites within small nuclear RNAs involves Toll-like receptors 7 and 8*. J Exp Med, 2005. **202**(11): p. 1575-85.
125. Pisitkun, P., et al., *Autoreactive B cell responses to RNA-related antigens due to TLR7 gene duplication*. Science, 2006. **312**(5780): p. 1669-72.
126. Subramanian, S., et al., *A Tlr7 translocation accelerates systemic autoimmunity in murine lupus*. Proc Natl Acad Sci U S A, 2006. **103**(26): p. 9970-5.
127. Marshak-Rothstein, A., *Toll-like receptors in systemic autoimmune disease*. Nat Rev Immunol, 2006. **6**(11): p. 823-35.
128. Leadbetter, E.A., et al., *Chromatin-IgG complexes activate B cells by dual engagement of IgM and Toll-like receptors*. Nature, 2002. **416**(6881): p. 603-7.
129. Waldner, H., M. Collins, and V.K. Kuchroo, *Activation of antigen-presenting cells by microbial products breaks self tolerance and induces autoimmune disease*. J Clin Invest, 2004. **113**(7): p. 990-7.
130. Tsunoda, I., et al., *Exacerbation of viral and autoimmune animal models for multiple sclerosis by bacterial DNA*. Brain Pathol, 1999. **9**(3): p. 481-93.
131. Miyata, M., et al., *Unmethylated oligo-DNA containing CpG motifs aggravates collagen-induced arthritis in mice*. Arthritis Rheum, 2000. **43**(11): p. 2578-82.
132. Anders, H.J., et al., *Activation of toll-like receptor-9 induces progression of renal disease in MRL-Fas(lpr) mice*. Faseb J, 2004. **18**(3): p. 534-6.
133. Anders, H.J., et al., *Bacterial CpG-DNA aggravates immune complex glomerulonephritis: role of TLR9-mediated expression of chemokines and chemokine receptors*. J Am Soc Nephrol, 2003. **14**(2): p. 317-26.
134. Stacey, K.J., et al., *The molecular basis for the lack of immunostimulatory activity of vertebrate DNA*. J Immunol, 2003. **170**(7): p. 3614-20.
135. Stunz, L.L., et al., *Inhibitory oligonucleotides specifically block effects of stimulatory CpG oligonucleotides in B cells*. Eur J Immunol, 2002. **32**(5): p. 1212-22.
136. Pawar, R.D., et al., *Inhibition of Toll-like receptor-7 (TLR-7) or TLR-7 plus TLR-9 attenuates glomerulonephritis and lung injury in experimental lupus*. J Am Soc Nephrol, 2007. **18**(6): p. 1721-31.
137. Christensen, S.R., et al., *Toll-like receptor 9 controls anti-DNA autoantibody production in murine lupus*. J Exp Med, 2005. **202**(2): p. 321-31.
138. Christensen, S.R., et al., *Toll-like receptor 7 and TLR9 dictate autoantibody specificity and have opposing inflammatory and regulatory roles in a murine model of lupus*. Immunity, 2006. **25**(3): p. 417-28.
139. Yu, P., P. Musette, and S.L. Peng, *Toll-like receptor 9 in murine lupus: more friend than foe!* Immunobiology, 2008. **213**(2): p. 151-7.

140. Baccala, R., et al., *TLR-dependent and TLR-independent pathways of type I interferon induction in systemic autoimmunity*. Nat Med, 2007. **13**(5): p. 543-51.
141. Decker, P., et al., *Nucleosome, the main autoantigen in systemic lupus erythematosus, induces direct dendritic cell activation via a MyD88-independent pathway: consequences on inflammation*. J Immunol, 2005. **174**(6): p. 3326-34.
142. Napirei, M., et al., *Features of systemic lupus erythematosus in Dnase1-deficient mice*. Nat Genet, 2000. **25**(2): p. 177-81.
143. Tsukumo, S. and K. Yasutomo, *DNaseI in pathogenesis of systemic lupus erythematosus*. Clin Immunol, 2004. **113**(1): p. 14-8.
144. Cohen, P.L. and R.A. Eisenberg, *Lpr and gld: single gene models of systemic autoimmunity and lymphoproliferative disease*. Annu Rev Immunol, 1991. **9**: p. 243-69.
145. Wolf, G., U. Haberstroh, and E.G. Neilson, *Angiotensin II stimulates the proliferation and biosynthesis of type I collagen in cultured murine mesangial cells*. Am J Pathol, 1992. **140**(1): p. 95-107.
146. Schmid, H., et al., *Modular activation of nuclear factor-kappaB transcriptional programs in human diabetic nephropathy*. Diabetes, 2006. **55**(11): p. 2993-3003.
147. Tusher, V.G., R. Tibshirani, and G. Chu, *Significance analysis of microarrays applied to the ionizing radiation response*. Proc Natl Acad Sci U S A, 2001. **98**(9): p. 5116-21.
148. Pisetsky, D.S. and C.F. Reich, 3rd, *The binding of anti-DNA antibodies to phosphorothioate oligonucleotides in a solid phase immunoassay*. Mol Immunol, 1998. **35**(18): p. 1161-70.
149. Adachi, O., et al., *Targeted disruption of the MyD88 gene results in loss of IL-1- and IL-18-mediated function*. Immunity, 1998. **9**(1): p. 143-50.
150. Austin, H.A., 3rd, et al., *Diffuse proliferative lupus nephritis: identification of specific pathologic features affecting renal outcome*. Kidney Int, 1984. **25**(4): p. 689-95.
151. Heikenwalder, M., et al., *Lymphoid follicle destruction and immunosuppression after repeated CpG oligodeoxynucleotide administration*. Nat Med, 2004. **10**(2): p. 187-92.
152. Zheng, Y. and A.Y. Rudensky, *Foxp3 in control of the regulatory T cell lineage*. Nat Immunol, 2007. **8**(5): p. 457-62.
153. Marshak-Rothstein, A. and I.R. Rifkin, *Immunologically active autoantigens: the role of toll-like receptors in the development of chronic inflammatory disease*. Annu Rev Immunol, 2007. **25**: p. 419-41.
154. Tamura, T., et al., *The IRF family transcription factors in immunity and oncogenesis*. Annu Rev Immunol, 2008. **26**: p. 535-84.
155. Patole, P.S., et al., *Viral double-stranded RNA aggravates lupus nephritis through Toll-like receptor 3 on glomerular mesangial cells and antigen-presenting cells*. J Am Soc Nephrol, 2005. **16**(5): p. 1326-38.
156. Pawar, R.D., et al., *Toll-like receptor-7 modulates immune complex glomerulonephritis*. J Am Soc Nephrol, 2006. **17**(1): p. 141-9.
157. Pawar, R.D., et al., *Bacterial lipopeptide triggers massive albuminuria in murine lupus nephritis by activating Toll-like receptor 2 at the glomerular filtration barrier*. Immunology, 2008.

158. Yoneyama, M., et al., *Shared and unique functions of the DExD/H-box helicases RIG-I, MDA5, and LGP2 in antiviral innate immunity*. J Immunol, 2005. **175**(5): p. 2851-8.
159. Balomenos, D., R. Rumold, and A.N. Theofilopoulos, *Interferon-gamma is required for lupus-like disease and lymphoaccumulation in MRL-lpr mice*. J Clin Invest, 1998. **101**(2): p. 364-71.
160. Suzuki, K., et al., *Expression of retinoic acid-inducible gene-I in lupus nephritis*. Nephrol Dial Transplant, 2007. **22**(8): p. 2407-9.
161. Kulkarni, O., et al., *Spiegelmer inhibition of CCL2/MCP-1 ameliorates lupus nephritis in MRL-(Fas)lpr mice*. J Am Soc Nephrol, 2007. **18**(8): p. 2350-8.
162. Krieg, A.M., et al., *CpG motifs in bacterial DNA trigger direct B-cell activation*. Nature, 1995. **374**(6522): p. 546-9.
163. Lai, A.S. and K.N. Lai, *Viral nephropathy*. Nat Clin Pract Nephrol, 2006. **2**(5): p. 254-62.
164. Savarese, E., et al., *UI small nuclear ribonucleoprotein immune complexes induce type I interferon in plasmacytoid dendritic cells through TLR7*. Blood, 2006. **107**(8): p. 3229-34.
165. Yasuda, K., et al., *Murine dendritic cell type I IFN production induced by human IgG-RNA immune complexes is IFN regulatory factor (IRF)5 and IRF7 dependent and is required for IL-6 production*. J Immunol, 2007. **178**(11): p. 6876-85.
166. Gomez-Guerrero, C., et al., *Soluble IgA and IgG aggregates are catabolized by cultured rat mesangial cells and induce production of TNF-alpha and IL-6, and proliferation*. J Immunol, 1994. **153**(11): p. 5247-55.
167. Wornle, M., et al., *Novel role of toll-like receptor 3 in hepatitis C-associated glomerulonephritis*. Am J Pathol, 2006. **168**(2): p. 370-85.
168. Wang, Z., et al., *Regulation of innate immune responses by DAI (DLM-1/ZBP1) and other DNA-sensing molecules*. Proc Natl Acad Sci U S A, 2008. **105**(14): p. 5477-82.
169. Hsieh, M.F., et al., *Both CXCR3 and CXCL10/IFN-inducible protein 10 are required for resistance to primary infection by dengue virus*. J Immunol, 2006. **177**(3): p. 1855-63.
170. Sadler, A.J. and B.R. Williams, *Interferon-inducible antiviral effectors*. Nat Rev Immunol, 2008. **8**(7): p. 559-68.
171. Schlondorff, D., *The glomerular mesangial cell: an expanding role for a specialized pericyte*. Faseb J, 1987. **1**(4): p. 272-81.
172. Hagele, H., et al., *Double-stranded RNA activates type I interferon secretion in glomerular endothelial cells via retinoic acid-inducible gene (RIG)-I*. Nephrol Dial Transplant, 2009.
173. Winston, J.A., et al., *Nephropathy and establishment of a renal reservoir of HIV type 1 during primary infection*. N Engl J Med, 2001. **344**(26): p. 1979-84.

9. Abbreviations

AIM2	Member absent in melanoma 2
ANA	Antinuclear antibodies
AP-1	Activator protein 1
APC	Antigen presenting cell
ATF	Activating transcription factor
BCR	B cell receptor
BMDC	Bone marrow dendritic cell
BSA	Bovine serum albumin
CAM	Cell adhesion molecule
CARD	Caspase recruitment domain
cDNA	Complementary DNA
DC	Dendritic cell
DEPC	Diethyl pyrocarbonate
DMEM	Dulbecco's modified Eagle's medium
DNA	Deoxyribonucleic acid
DNTPs	Deoxynucleotide triphosphates
ELISA	Enzyme-linked immuno sorbent assay
FCS	Fetal calf serum
FITC	Fluorescein isothiocyanate
Flt3L	FMS-like tyrosine kinase 3 ligand
GMCSF	Granulocyte-macrophage colony-stimulating factor
HMGB1	High mobility group box protein 1
IC	Immune complex
IFN	Interferon
Ig	Immunoglobulin
IKK	Ikappa B kinase
IL-1R	Interleukin 1 receptor
IRAK	Interleukin-1 receptor associated kinase
IPS-1	IFN β promoter stimulator 1
IRF	Interferon regulatory factor
ITS	Insulin/transferrine/selenium
JNK	C-jun N-terminal protein kinase
LGP2	Laboratory of genetics and physiology 2
LPR	Lymphoproliferative
LPS	Lipopolysaccharide
MCP-1 (CCL2)	Monocyte chemoattractant protein-1
MDA5	Melanoma differentiation associated protein 5
MHC	Major histocompatibility complex
MIP-2 (CXCL2)	Macrophage inflammatory protein 2
MyD88	Myeloid differentiation protein 88
MSU	Monosodium urate
NALP3	NACHT-LRR-PYD-containing protein 3
NADH	Nicotinamidadenindinukleotid
NF-kB	Nuclear factor k B

NOD	Nucleotide-binding oligomerization domain
ODN	Oligodeoxynucleotide
PAMPs	Pathogen-associated molecular patterns
PBS	Phosphate-buffered saline
PCR	Polymerase chain reaction
PE	Phycoerythrin
PI3K	Phosphoinositide 3-kinase
PRR	Pattern recognition receptors
PS	Penicillin/streptomycin
RIG-1	Retinoic acid-inducible gene 1
RNA	Ribonucleic acid
RT	Reverse transcriptase
SLE	Systemic lupus erythematosus
Sm	Smith antigen
SNP	Single nucleotide polymorphism
snRNP	Small nuclear ribonucleoproteins
ssRNA	Single stranded RNA
STING	Stimulator of IFN genes
TBK1	TANK binding kinase 1
TIR	Toll interleukin like receptor domain
TLR	Toll-like receptor
TMB	3,3',5,5'-tetramethylbenzidine
TNF	Tumour necrosis factor
TRAF	TNF receptor associated factor
TRAM	TRIF-related adaptor molecule
TRIF	TNF receptor-inhibitory factor
WT	Wild type

Appendix

1. FACS buffer:

Sterile DPBS 500 ml
Sodium azide 500 mg (0.1 %)
BSA 1 g (0.2 %)

2. 10X HBSS (Hank's Balanced Saline Solution) with Ca, Mg:

For 1000 ml
KCl 4 g
KH₂PO₄ 0.6 g
NaCl 80 g
Na₂HPO₄·2H₂O 0.621 g
NaHCO₃ 3.5 g
CaCl₂ 1.4 g (or CaCl₂·2H₂O 1.854 g)
MgCl₂·6H₂O 1 g
MgSO₄·7H₂O 1 g
D-Glucose 10 g

Dissolve in 900 ml of distilled water and adjust to pH 7.4 with 1N HCl or 1N NaOH. Make up the volume with distilled water to 1000 ml.

3. 10X HBSS (Hank's Balanced Saline Solution) without Ca, Mg:

For 1000 ml
KCl 4 g
KH₂PO₄ 0.6 g
NaCl 80 g
Na₂HPO₄·2H₂O 0.621 g

Dissolve in 1000 ml and autoclave.

4. 50 % Glycerol in 20 mM Tris-HCl (pH 7.5), 1 mM MgCl₂:

a). 0.48 g of Tris-HCl in 100 ml of distilled water, adjust pH to 7.4 (= 40 mM)

- b). 50 ml of Glycerol 100 % + 50 ml of 40 mM Tris-HCl (20 mM)
- c). Add 100 ul of 1M MgCl₂ solution.

5. EDTA 2 mM:

EDTA 7.44 mg in 10 ml HBSS (without Ca, Mg)

To be preheated in 37 °C water bath before use.

6. Anesthesia mixture:

10 ml Midazolam (1 mg/ml)

2 ml Fentanyl (0.05 mg/ml)

1 ml Dormitor (1 mg/ml)

7. Antagonist mixture:

5 ml Anexate (0.1mg/ml)

0.5 ml Antisedan (5 mg/ml)

3 ml Naloxon (0.4 mg/ml)

8. MACS buffer:

PBS pH 7.2 0.5% BSA, 2 mM EDTA

9. Citrate buffer:

10X 110 mM Sodiumcitrate in ddH₂O with 2N NaOH to pH 6

10. PBS:

2.74 M NaCl 54 mM KCl 30 mM KH₂PO₄ 130 mM Na₂HPO₄ in ddH₂O with HCl to pH

7.5

Curriculum Vitae

Personal details

Surname: Allam
First name: Ramanjaneyulu
Date of birth: 14th may 1979
Place of birth: Vempalli
Nationality: Indian

Academic profile

Ph.D fellow in Human Biology (2006-in progress)

University of Munich, Munich, Germany.

M. Sc. in Biochemistry (2000 - 2002)

Sri Venkateswara University, Tirupati, Andhra Pradesh, India.

B. Sc. in Biology and Chemistry (1997-2000)

Sri Venkateswara University, Tirupati, Andhra Pradesh, India.

Publications

- 1) Fluor K, **Allam R**, Zecher D, Kulkarni O, Lichtnekert J, Schwarz M, Beutler B, Vielhauer V, Anders HJ. Viral RNA induces type I interferon-dependent cytokine release and cell death in mesangial cells via melanoma-differentiation-associated gene-5. Implications for viral infection-associated glomerulonephritis. *Am J Pathol.* 2009
- 2) Hägele H, **Allam R**, Pawar RD, Reichel C, Krombach F, Anders HJ. Double-stranded DNA activates glomerular endothelial cells and enhances albumin permeability via a Toll-like receptor-independent cytosolic DNA recognition pathway. *Am J Pathol.* 2009
- 3) **Allam R**, Lichtnekert J, Moll AG, Taubitz A, Vielhauer V, Anders HJ. Viral RNA and DNA Trigger Common Antiviral Responses in Mesangial Cells. *J Am Soc Nephrol.* 2009; 20(9):1986-96.
- 4) Lech M, Avila-Ferruffino A, **Allam R**, Segerer S, Khandoga A, Krombach F, Garlanda C, Mantovani A, Anders HJ. Resident Dendritic Cells Prevent Postischemic Acute Renal Failure by Help of Single Ig IL-1 Receptor-Related Protein. *J Immunol.* 2009; 183(6):4109-18.
- 5) Hägele H, **Allam R**, Pawar RD, Anders HJ. Double-stranded RNA activates type I interferon secretion in glomerular endothelial cells via retinoic acid-inducible gene (RIG)-1. *Nephrol Dial Transplant.* 2009; 24(11):3312-8.

6) Vielhauer V, **Allam R**, Lindenmeyer MT, Cohen CD, Draganovici D, Mandelbaum J, Eltrich N, Nelson PJ, Anders HJ, Pruenster M, Rot A, Schlöndorff D, Segerer S. Efficient renal recruitment of macrophages and T cells in mice lacking the duffy antigen/receptor for chemokines. *Am J Pathol.* 2009; 175(1):119-31.

7) Sharma A, **Ramanjaneyulu A**, Ray R, Rajeswari MR. Involvement of high mobility group B proteins in cisplatin-induced cytotoxicity in squamous cell carcinoma of skin. *DNA Cell Biol.* 2009; 28(7):311-8.

8) Pawar RD, Castrezana-Lopez L, **Allam R**, Kulkarni OP, Segerer S, Radomska E, Meyer TN, Schwesinger CM, Akis N, Gröne HJ, Anders HJ. Bacterial lipopeptide triggers massive albuminuria in murine lupus nephritis by activating Toll-like receptor 2 at the glomerular filtration barrier. *Immunology.* 2009;128(1 Suppl):e206-21

9) **Allam R**, Pawar RD, Kulkarni OP, Hornung V, Hartmann G, Segerer S, Akira S, Endres S, Anders HJ. Viral 5'-triphosphate RNA and non-CpG DNA aggravate autoimmunity and lupus nephritis via distinct TLR-independent immune responses. *Eur J Immunol.* 2008; 38(12):3487-98.

10) Kulkarni O, Eulberg D, Selve N, Zöllner S, **Allam R**, Pawar RD, Pfeiffer S, Segerer S, Klussmann S, Anders HJ. Anti-Ccl2 Spiegelmer permits 75% dose reduction of cyclophosphamide to control diffuse proliferative lupus nephritis and pneumonitis in MRL-Fas (lpr) mice. *J Pharmacol Exp Ther.* 2009; 328(2):371-7.

11) **Allam R**, Anders HJ. The role of innate immunity in autoimmune tissue injury. *Curr Opin Rheumatol.* 2008; 20(5):538-44.

12) Patole PS, Pawar RD, Lichtnekert J, Lech M, Kulkarni OP, **Ramanjaneyulu A**, Segerer S, Anders HJ. Coactivation of Toll-like receptor-3 and -7 in immune complex glomerulonephritis. *J Autoimmun.* 2007; 29 (1):52-9.

13) Pawar RD, **Ramanjaneyulu A**, Kulkarni OP, Lech M, Segerer S, Anders HJ. Inhibition of Toll-like receptor-7 (TLR-7) or TLR-7 plus TLR-9 attenuates glomerulonephritis and lung injury in experimental lupus. *J Am Soc Nephrol.* 2007; 18(6):1721-31.

Poster presentations and Symposiums

“Interferon- α and β . Neglected mediators of viral infection-triggered glomerulonephritis?”
Poster presented at. American Society of Nephrology conference. San Diego, U.S.A,
November 2009.

“5'-Triphosphate RNA and Non-CpG-DNA Induce A Common Immune Response Program in Glomerular Mesangial Cells”. Poster presented at Recent Advances in Pattern Recognition | Toll 2008 International Meeting, Lisbon, Portugal, 24-27 September 2008.

“TLR independent recognition of viral nucleic acids in Mesangial cells” poster presented at Pattern-recognition receptors in human disease conference, Queens' College, University of Cambridge, UK, September 2007.

Fellowships and Awards

Since June 2008, receiving fellowship from “GRK 1202 Oligonucleotides in Cell Biology and Therapy”. LMU, Munich, Germany.

Research Fellowship awarded by the Indian Council of Medical Research (ICMR), New Delhi, India in 2002.

Qualified Graduate Aptitude Test in Engineering (GATE) conducted by Indian Institute of science in 2002.